Master Thesis

A Thermal Analysis of Engine Components Performed on a Turbocharger

accomplished at

CAMPUS 02 - University of Applied Sciences

Master Degree Programme
for Automation Technology - Economy

by

Andreas Diemath
1510322014

supervised and reviewed by
Dipl.-Ing. Johannes Fritz, BSc

Graz, February 2017

....
Signature

AUTHOR'S DECLARATION

Unless otherwise indicated in the text or references, or acknowledged above, this thesis is entirely the product of my own scholarly work. Any inaccuracies of fact or faults in reasoning are my own and accordingly I take full responsibility. This is to certify that the printed version is equivalent to the submitted electronic one.

Ich erkläre ehrenwörtlich, dass ich die vorliegende Arbeit selbstständig und ohne fremde Hilfe verfasst, andere als die angegebenen Quellen nicht benützt und die benutzten Quellen wörtlich zitiert sowie inhaltlich entnommene Stellen als solche kenntlich gemacht habe. Die vorliegende Fassung entspricht der eingereichten elektronischen Version.

Graz, am 28. February 2017

....

(Andreas Diemath)

ACKNOWLEDGEMENTS

I wish to thank Mr. Johannes Fritz from the University of Applied Sciences, CAMPUS 02, for supervising my master-thesis. Special thanks to Mr. Thomas Resch, Manager of Customer Services at AVL-AST and to my team leader Mr. Wolfgang Baier, for giving me the possibility to attend the master program.
Furthermore, I want to thank also Mr. Andreas Ennemoser, Manager for CFD Analysis of Power Train Engineering and his team members, who participated in the survey.

Very special thanks to my girlfriend, Marina Thelliez, for supporting me during my entire studies, the bachelor and the master program.

ABSTRACT

In the early stages of the conceptual and the design phases of a new product simulation is involved in the decision making process, even before any prototyping is done. This concept is so-called front loading. Designing a new turbocharger for example requires better understanding of the rotor-dynamics. Multi-body dynamics simulation (MBD) is a suitable tool to investigate phenomena, e.g. rotor imbalance, which has a vast impact on the durability of bushing bearings. Combining multi-body dynamics simulation and computational fluid dynamics (CFD), the CFD supplies important boundary conditions for MBD, which is a new simulation methodology investigated in this thesis. The simulation tool AVL FIRE M with its multi-material capability is being used for this investigation. One of the most important fields related to this objective is the heat transfer analysis with special focus on the thermal dynamics of the heat flow within the turbocharger. Since CFD simulation is already a well established tool in product development and especially in the component design phase, this novel simulation approach is offering an alternative method to the conventional fluid-solid coupling which is usually used to calculate temperature distribution in solid structure and stress analysis. This proposed approach represents the simulation of heat transfer within the turbocharger structure and its parts by considering the solid and fluid parts of the turbocharger as a multi-domain and multi-material simulation model. The theoretical part builds up the fundamentals to the engineering background and the physical modelling. Furthermore, the basic essentials of workflow and the general evaluation process are introduced, which should form a transition between engineering outcome, usablity and user's acceptance of the novel simulation approach. In the evaluation part of the thesis the gathered results are presented and summarized. The engineering outcome as well as the workflow and methodology of such kind of simulations are discussed. Finally, the summary presents all pillars of the evaluation process and an additional outlook is given as a reflection of the presented workflow. It provides recommendations for further improvement and gives suggestions for future investigations. The presented methodology proves to be a next level approach in prediction of turbocharger simulation in the product development process.

KURZFASSUNG

In der frühen Konzept- oder Konstruktionsphase eines neuen Produktes wird die Simulation und Analyse in die Entwicklung mit einbezogen, um wichtige Produktentscheidungen durch virtuelle Versuche abzusichern. Dieser Vorgang ist auch unter dem Begriff Frontloading bekannt. Die neuesten Anforderungen in der Auslegung von Turboladern erfordern tiefere Einblicke in die Bewertung der Rotordynamik. Dabei sind Mehrkörperberechnungsprogramme ein geeignetes Werkzeug zur Modellierung von Phänomenen wie z.B der Rotorunwucht und deren Auswirkung auf die Lebensdauer der Gleitlager. In Kombination mit der numerische Strömungssimulation, die dabei als Randbedingungslieferant für die Mehrkörperdynamikberechnung dient, soll eine neue Berechnungsmethodik untersucht werden. In dieser Arbeit wird primär die Berechnungsmethodik für das Zusammenwirken zwischen Gasströmung, Festkörper- und Mehrkörperdynamik untersucht und bewertet. Zum Einsatz kommt dabei das multimaterialfähige Simulationstool AVL FIRE M. Technische Schwerpunkte der Untersuchung sind die Gebiete Gasströmung und Festkörper, im Speziellen die thermische Dynamik der Wärmeleitung zwischen den Berechnungsgebieten. Zielsetzung ist die Etablierung einer neuen Berechnungsmethodik, sowie die Untersuchung des Zusammenspiels von Festkörper und Gasströmung. Diese Berechnungsmethodik soll erweiterte Einblicke in die Wärmeübertragung, speziell im Bereich der Gleitlager ermöglichen, welche wiederum der Bewertung der Rotordynamik dienlich sind. Der Schwerpunkt der Arbeit liegt in der Untersuchung der Berechnungsmethodik mit Bewertung dieser hinsichtlich Anwendbarkeit im Berechnungsalltag sowie der Vergleichbarkeit von Simulationsergebnissen in Bezug auf Prüfstandsergebnisse. Im theoretischen Teil wird die neue Berechnungsmethode sowie die Grundlagen dazu erarbeitet. Des Weiteren wird auch eine Einführung in das Thema der modellgestützten Entwicklung gegeben und der Bogen zu bereits existierende Berechnungsmethodiken gespannt. Die Kriterien zur Bewertung der Methodik werden auch in diesem Teil der Arbeit behandelt. Die wichtigsten beschreibenden Gleichungen zur Abbildung der physikalischen Problemstellung sollen ebenfalls kurz beschrieben werden. Im praktischen Teil der Arbeit wird die neue Berechnungsmethode einerseits in Bezug auf Anwendbarkeit im Simulations- bzw. Berechnungsalltag durch Anwender im Unternehmen und andererseits hinsichtlich der bereits erwähnten Belastbarkeit in Bezug auf Prüfstandsergebnisse bewertet. Zu diesem Zweck werden einzelne Betriebspunkte gewählt und zur Bewertung herangezogen.

Table of contents

1. Introduction

In the early stages of the conceptual and the design phases of a new product simulation is involved in the decision making process, even before any protoyping is done. This concept is so-called front loading. Designing a new turbocharger requires a very good understanding of any kind of physical phenomenon, such as fluid dynamics, heat transfer, structural mechanics and the interaction between those.
One of the most important fields related to this objective is the heat transfer analysis with special focus on the thermal dynamics of the heat and fluid flow within the turbocharger. Since the computational fluid dynamics (CFD) simulation is already a well-established tool in product development and especially in the component design phase a novel simulation approach is being investigated. This offers an alternative method to the conventional fluid-solid coupling which is usually used to calculate temperature distribution in solid structure on the one hand and stress analysis on the other hand.
The multi-body dynamics simulation (MBD) is a suitable tool to investigate phenomena having a vast impact on the durability of bushing bearings, e.g. rotor imbalance. Combining the CFD and multi-body dynamics, where the CFD delivers important boundary conditions for the MBD, a new simulation methodology is investigated in the present work with focus to the fluid dynamical phenomena and heat transfer. The simulation tool AVL FIRE M with its multi-material capability is being used for this kind of investigation and the workflow of the CFD part is presented and evaluated in the present work.

1.1. Motivation

This thesis was accomplished while studying towards the master program *Automation Technology at CAMPUS 02 – University of Applied Sciences* together with *AVL List GmbH*, the world largest independent company for the development of powertrain systems, with internal combustion engines as well as instrumentation and test systems. The work was performed in the skill area Customer Services (CC) and was supervised in the department for fluid mechanics (CCAF) in the headquarter in Graz (Austria).

1.2. Scope

Considering the bearing bushings of a turbocharger, little changes of bearing surface temperature will have effect on clearance and bearing profile, and furthermore can change bearing stiffness and damping characteristics. This may influence the dynamics and especially the rotor radial deflection. Durability issues like the collision of the rotor with the housing may occur as a consequence. Thus, the typical targets for CFD simulation within the turbo charger development process are investigating flow and thermal as well as providing accurate thermal boundary condition for Thermo-Mechanical Fatigue (TMF) analysis. The CFD analysis uses a fully coupled fluid-structure interaction where both domains are modelled within the same tool, by using the same CFD model to provide the required boundary conditions for dynamic analysis. In the framework of this thesis the fully coupled fluid-structure interaction, implemented in the commercial CFD code *AVL FIRE M*, is assessed with performance data gathered from the measurement performed on the turbo charger *S410 Euro4* of the automotive supplier Borg Warner Turbo Systems (BWTS).
In many publications in the past mainly the contribution to the engineering result of a simulation was

considered worth to be investigated.[1] Only very little attention was payed to look also into the acceptance and usability of a simulation workflow from the perspective of a simulation engineer.[2] Thus, a second pillar of this evaluation process is dedicated to the workflow itself seen from user's and simulation management's point of view.

1.3. Thesis outline

This work is divided into three main parts resulting into five chapters distributed as follows:

Theoretical part

The theoretical part consists of two main chapters providing a solid base of being able to follow the content of this thesis. The chapter *Background* builds up the fundamentals about the engineering background and the physical modelling. The second chapter *Simulation approach* introduces into the basic essentials about the workflow and the general evaluation process, which should form a transition between engineering outcome, usablity and user's acceptance of the novel simulation approach.

Evaluation part

This part consists of one main chapter and presents the gathered results. It discusses the engineering outcome as well as the workflow and method.

Summary and outlook

Summary and outlook are split into two dedicated chapters. The summary presents all pillars of the evaluation process in a compressed form, and the outlook shall be seen as a reflection of the presented workflow. It provides recommendations for further improvement and gives also suggestions for additional investigations which were not scope of this thesis.

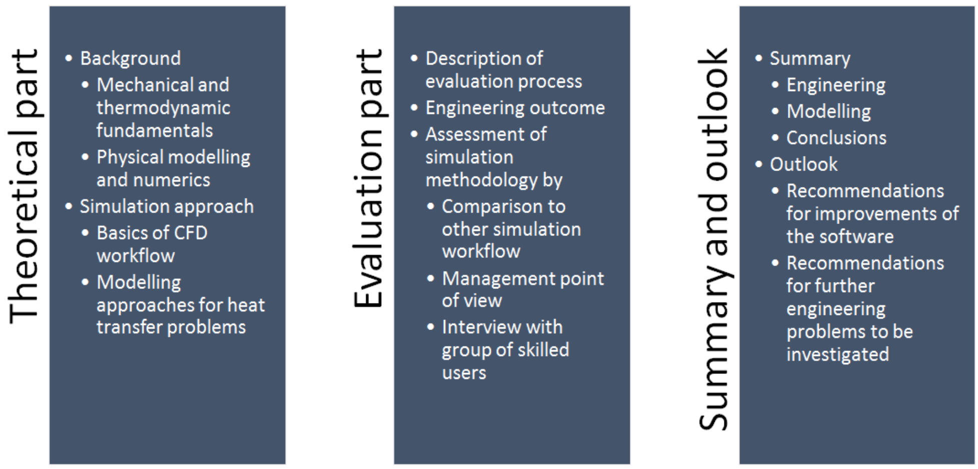

Figure 1.1.: Thesis outline, Source: own chart

[1] Cf. Bergqvist S. (2014)
[2] Cf. Barth P. (2011)

2. Background

In the recent years turbocharging has become more important in the engine technology. The turbocharger has a big contribution to the success of diesel engines. Nowadays, almost every diesel engine is equipped with a turbocharger and also the usage of charged gasoline engines is constantly growing.[3]
There are also other concepts of charging a piston engine available, but this work does not attempt to discuss all possiblities. Fur further interest, please refer to following reference[4].

In order to get a better understanding about the purpose of a turbocharger and its interaction with an internal combustion engine (ICE), the present chapter provides the required fundamentals. It also builds up the thermodynamic fundamentals. Furthermore the concept of modelling in CFD of such an application in terms of fluid flow and thermal analysis is described in detail, as this is the main scope of this thesis.

2.1. Introduction to turbocharger

A turbocharger is a rotating machinery that raises an internal combustion engine's efficiency and power output by increasing the mean effective pressure (MEP) of the ICE. In contrast to a naturally aspirated (NA) engine, an additional amount of air is forced into the combustion chamber thanks to a higher pressure level in the intake duct.[5]
Applying a turbocharger has many advantages for an ICE.[6] The most important ones are adressed here:

- Turbocharging results in same power output while having a better efficiency and thus a lower fuel consumption for a more compact engine (downsizing of engine)
- Downsizing is the prerequisite for reduction of dimensions, weight and manufacturing costs

Thus, this downsizing requires enhanced simulation methods in the development of turbocharger components. Considering this kind of machinery from a thermal perspective, the heat transfer plays an important role as the heat fluxes inside the turbocharger have to be limited and controlled in order to avoid damage in the structure of the turbocharger housing and rotating parts, such as turbine and compressor (T/C). Furthermore the knowledge of the correct temperatures of the turbocharger components is also crucial as they impact performance maps when operating on the engine.[7]

2.2. Fundamentals

The turbocharger uses a thermodynamic working principle and is thermodynamically coupled to the ICE. Hot exhaust gas, the so-called exhaust gas residual (EGR), is coming from the combustion chamber and expands through a turbine that powers a compressor. Turbine and compressor are mechanically linked though a rotating shaft. In passenger cars rotational speeds beyond 200000 revolutions per minute (RPM)

[3]Braess, H. H., Seiffert, U. (2013) p. 366
[4]Cf. Merker G. P. , Teichmann R. (2014) p. 408
[5]Merker G. P. , Teichmann R. (2014) p. 407
[6]Braess, H. H., Seiffert, U. (2013) p. 350
[7]Cf. Aghaali, H. (2013) p. 15

are common nowadays and the temperature of EGR can exceed 1000°C at the inlet of the turbine.[8]
The airflow through the turbocharger and the engine is shown schematically in Figure 2.1 (for graphical representation):

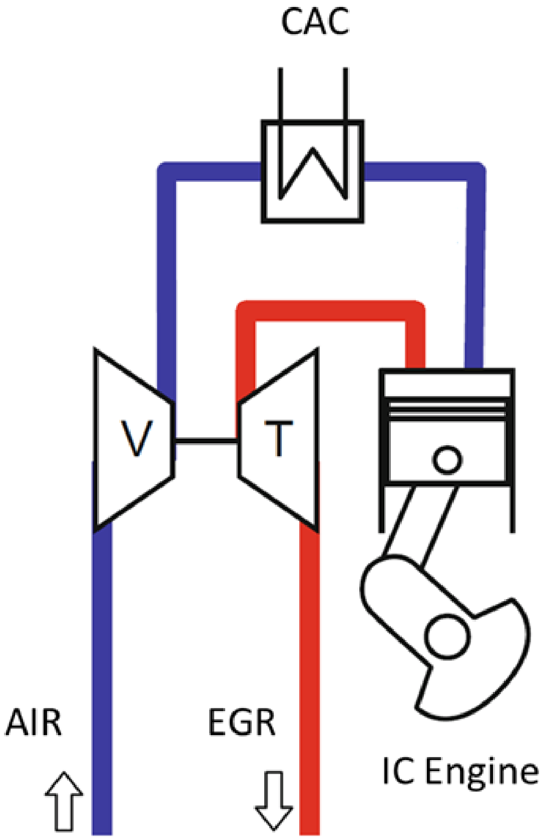

Figure 2.1.: Turbocharger flow scheme, Source: based on external source[9] and modified

The charge air enters the compressor in axial direction and is accelerated by the compressor wheel, leaving the compressor through the volute whilst experiencing a further pressure increase in the diffusive volute. Since a charger aggregate always causes an increase in the temperature of the fresh gas, the charge air has to be cooled down in the Charge Air Cooler (CAC) in order to increase the charge air mass and with that the performance of the engine.

[8] van Basshuysen, R. ; Schaeffer, F. (2014) p. 334
[9] Merker G. P. , Teichmann R. (2014) p. 408

2.2.1. Mechanical turbocharger fundamentals

Since the main mechanical components of a turbocharger for diesel as well as for gasoline engines are very similar, the following graphical representation (Figure 2.2) is used to provide a suitable overview of the relevant parts.

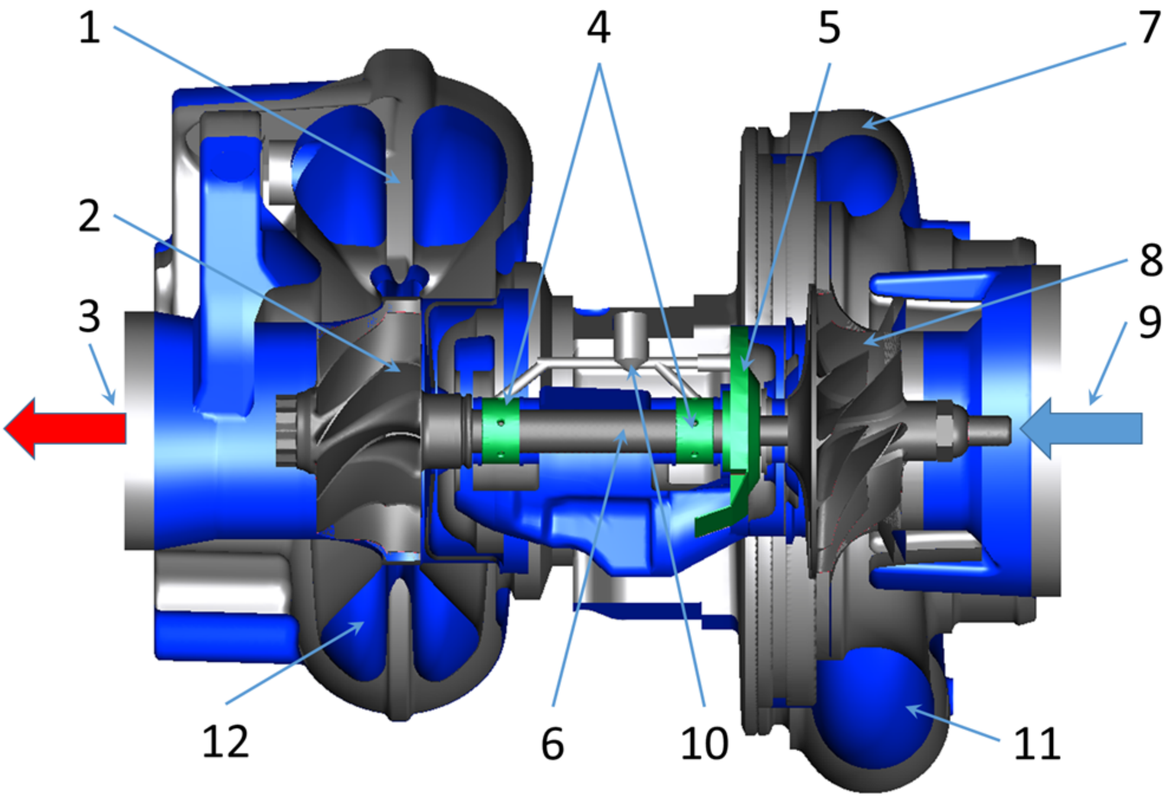

Figure 2.2.: Mechanical components of a turbocharger, Source: own model

Legend to Figure 2.2:

1 ...Turbine housing	4 ...Bushing bearings	7 ...Compressor housing	10 ...Oil line
2 ...Turbine blades	5 ...Axial bearing	8 ...Compressor blades	11 ...Air path (out)
3 ...Turbine outlet	6 ...Shaft	9 ...Compressor inlet	12 ...EGR path (in)

As stated above, the major housing are the turbine housing, bearing housing and the compressor housing. In terms of thermodynamics those components inside the housing, such as turbine blades (turbine impeller), compressor blades (compressor impeller) and shaft duild the backbone of a turbocharger. They are responsible for transforming the energy from the exhaust gas into rotational energy and powering the compressor, which creates the forced induction of the ICE.

The turbine blades and the shaft are usually connected via a welding rod, and the compressor blades and the shaft are typically connected through a screw. All three components form the so-called rotor.

It is very common to mount the rotor on hydrodynamic bearing bushings as the rotational speed is above 200000 rpm. Therefore the oil supply is connected to the engine lubrication system. Radial bearings and the axial thrust bearing are separated from each other. The axial thrust bearing compensates the aerodynamic forces from the turbine and compressor blades.

A turbocharger in engine operation runs often under critical conditions in terms of resonance, hence the radial bearings have to provide also sufficient damping to the rotor. Due to acoustic issues, durability and higher costs, only a few turbochargers are equipped with roller bearings, even if applying roller bearings is seen as beneficial in terms of efficiency and dynamical behavior of the rotor.[10]

Separating the bearing housing from the turbine housing thermically is crucial in order to avoid overheating and coking of the lubrication oil. This thermal insulation is performed by using a heat shield between the turbine housing and the bearing housing. This heat shield is mounted directly behind the turbine impeller as shown in Figure 2.3.
Also the bearing housing has to be sealed from the environment as the lubricant oil must not exceed strict tolerances in terms of leackage. Additionally, the contamination of the bearing housing by exhaust gas must be avoided and this is accomplished by piston rings forming a labyrinth.
The turbine and compressor impellers of modern turbochargers are shaped in a way, that the main flow

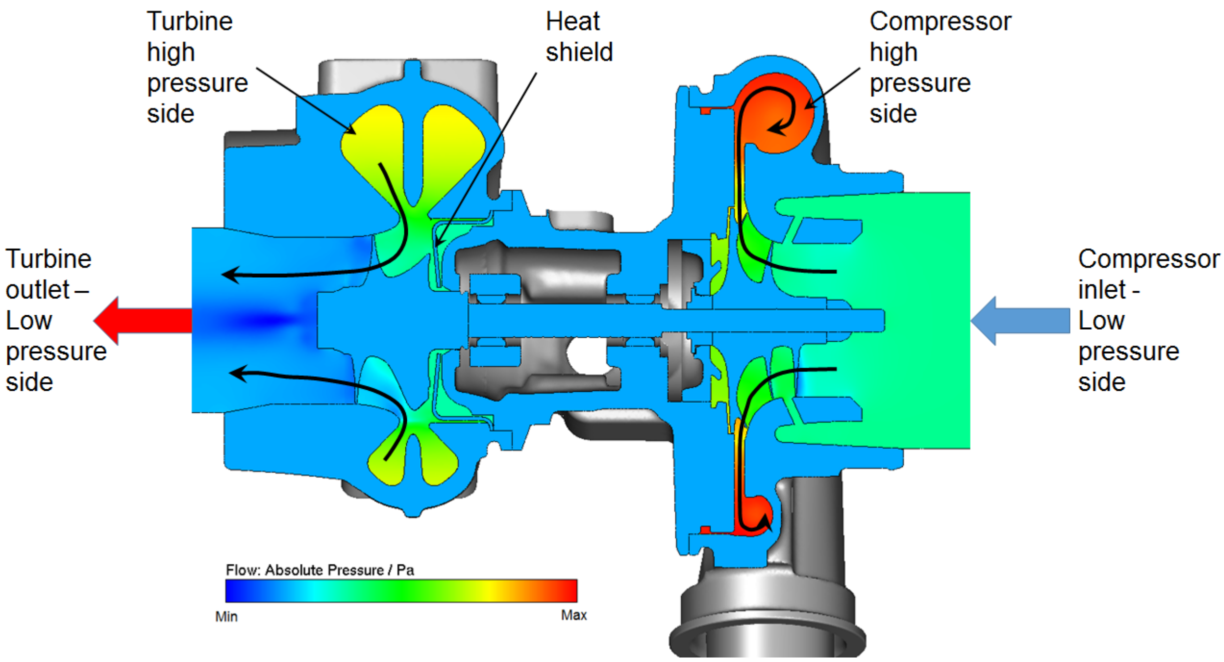

Figure 2.3.: Cross Section - Flow through turbocharger, Source: own screenshot

direction on the high-pressure side of either parts (turbine inlet and compressor outlet) is oriented in radial direction. The main flow on the low-pressure side is oriented in axial direction in order to allow a more compact design. Nowadays the impellers are manufactured by milling, as it is seen as beneficial in terms of acoustics and mechanical fatigue.

The flow domain around turbine and compressor is formed by a volute. Compressor impeller and housing material is usually an aluminium alloy, and for high rotational speeds sometimes titanium-based alloys are used. As the temperature of the exhaust gas exceeds 1000°C the turbine impeller is manufacured of nickel-based alloys.

A turbocharger is typically equipped with a control unit, that allows regulating the intake pressure (boost pressure) of the fresh gas. There are mainly two different types of devices to control the charge air motion:

[10] Eissler, W. (2011)

- The first possiblity is to apply a bypass valve in the exhaust gas flow to bypass the flow through the turbine as shown in Figure 2.4 (left part of the figure). This valve is usually opened at high load conditions with the effect of decreasing the exhaust gas flow through the turbine. This steering device is so-called *Wastegate*. This method is quite robust and therefore often used in ICE for passenger cars. It is also used in truck engines as these engines require a high expectancy in terms of operational lifetime.[11]
- From the energetic point of view a more elegant possibility to control the exaust gas flow is a device called *VTG-turbocharger*. VTG stands for Variable Turbine Geometry and this kind of controlling is accomplished by adjustable vanes directly integrated in the turbine housing in front of the turbine wheel as shown in Figure 2.4 (right part of the figure). This vanes are actuated by a ring mechanism which influence the flow conditions at the entrance of the turbine by guiding the flow to the turbine blades.[12]

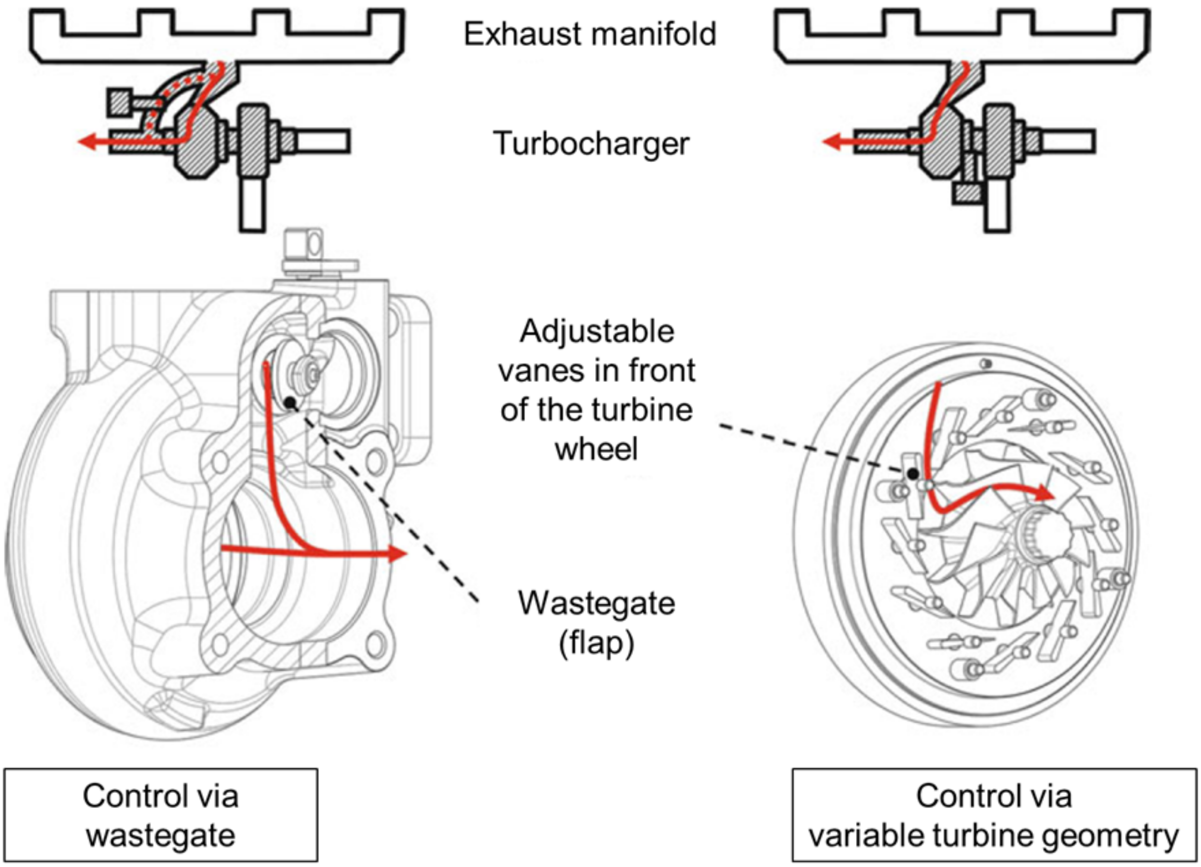

Figure 2.4.: Turbocharger steering, Source: based on external source[11] and modified

[11]Merker G. P. , Teichmann R. (2014) p. 424
[12]Merker G. P. , Teichmann R. (2014) p. 425

2.2.2. Thermodynamic turbocharger fundamentals

In order to develop an understanding for the turbocharger and its interaction with the ICE, some basic essential have to be discussed. Information about the turbocharger performance are typically extracted from the so-called turbocharger maps, These maps contain important information for the engine development process and provide the required input for the engine performance calculation. The turbocharger performance maps are gathered from measurements on a test bench, which is shown in Figure 2.5. It is especially designed for turbocharger.[13]

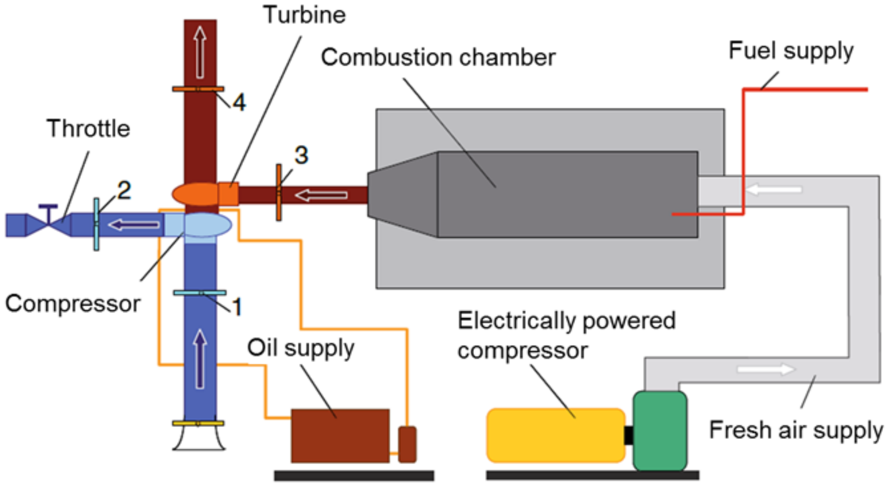

Figure 2.5.: Turbocharger test bench, Source: external reference[13] and modified

Legend to Figure 2.5 (Measurement points):

1 ...Compressor inlet	2 ...Compressor outlet	3 ...Turbine inlet	4 ...Turbine outlet

The main components of a turbocharger test bench are the combustion chamber, the throttle after the compressor, the oil supply, in certain cases also water supply for cooling (which is not displayed in Figure 2.3) and measurement devices. The interaction of the most important components shall be briefly described in the following:

Combustion chamber
The purpose of the combustion chamber is to create the hot exhaust gas and supply the turbine. This is typically accomplished by burning Diesel or natural gas. An electrically powered compressor delivers the required fresh air directly into the chamber.

Throttle after the compressor outlet
The throttle is responsible for prescribing the required load to the compressor. Depending on the applied load a certain speed of the turbocharger rotor is resulting from the fact, that turbine and compressor wheel are mechanically connected via a shaft. The throttle is usually actuated electrically.

Oil supply
In order to provide sufficient lubrication to the bearings, the test bench has to be equipped with an oil supply. The oil circuit contains further components such as oil filter, oil pump and a conditioning system, as for certain testcycles the oil has to be cooled or heated.s

[13] van Basshuysen, R. ; Schaeffer, F. (2014) p. 555

2.2.2.1. Energy transformation and equations

The hot exhaust gas coming from the combustion engine is expanding through the turbine and transforms the kinetic and mostly thermal energy into mechanical power which is denoted as:[14]

$$P_T = \eta_T \, \dot{m}_T \, (h_3 - h_4) \tag{2.1}$$

P_T / W	Effective turbine power
$\dot{m}_T$ / kg s^{-1}	Turbine mass flow (EGR mass flow)
h_3 / J kg^{-1}	Specific enthalpy at the turbine inlet
h_4 / J kg^{-1}	Specific enthalpy at the turbine outlet
η_T / Dimensionless	Turbine efficiency

The expansion of the exhaust gas in the turbine stage is a polytropic process from state *3* (turbine inlet) to state *4* (turbine outlet) and is shown in Figure 2.6[15]:

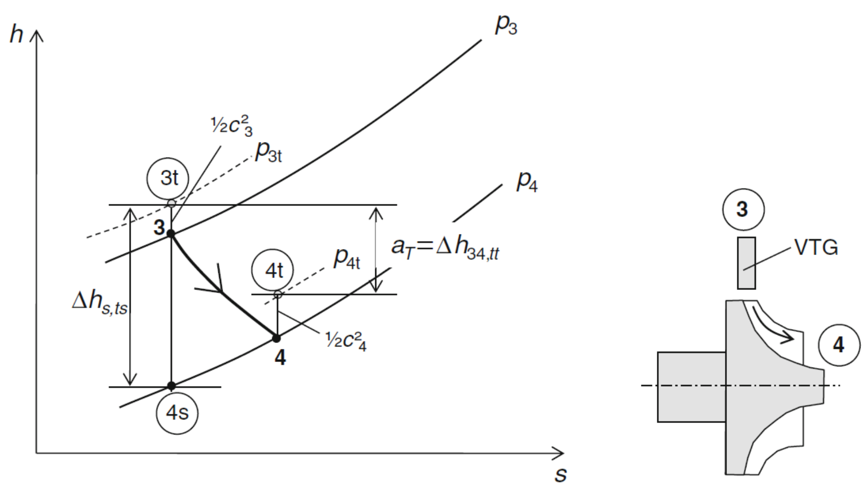

Figure 2.6.: Polytropic expansion in the turbine stage, Source: external reference[15]

With the help of the graphical representation of Figure 2.6 the interpretation of the specific enthalpy drop $h_3 - h_4$ and the turbine efficiency η_T is made easier.

Applying fundamental thermodynamics the isentropic enthalpy drop is given in Equation (2.2), where the subscript *g* refers to the exhaust gas as a working fluid of the turbine:

$$h_3 - h_4 = c_{p,g} \, T_3 \left[1 - \left(\frac{p_4}{p_3} \right)^{\left(\frac{\kappa-1}{\kappa}\right)_g} \right] \tag{2.2}$$

[14]Nguyen-Schäfer (2015) p. 24
[15]Nguyen-Schäfer (2015) p. 23

$c_{p,g}$ / J kg$^{-1}K^{-1}$	Specific heat capacity of exhaust gas at constant pressure
T_3 / K	Temperature at turbine inlet
p_3 / Pa	Static pressure at turbine inlet
p_4 / Pa	Static pressure at turbine outlet
κ / Dimensionless	Isentropic exponent of exhaust gas

The turbine efficiency η_T is defined as the ratio of the polytropic total enthalpy drop between state *3t* and state *4t* to the isentropic total enthalpy drop between state *3t* and *4s*.[16]
Applying also here thermodynamic fundamentals, an enthalpy drop can be also expressed by their related temperature differences which leads then to the Equation (2.3):

$$\eta_T = \frac{\Delta h_{34,tt}}{\Delta h_{s,ts}} = \frac{T_{4t} - T_{3t}}{T_{4s} - T_{3t}} \tag{2.3}$$

$\Delta h_{34,tt}$ / J kg^{-1}	Polytropic total enthalpy drop between state *3t* and *4t*
$\Delta h_{s,ts}$ / J kg^{-1}	Polytropic total enthalpy drop between state *3t* and *4t*
ΔT_{3t} / K	Temperature at state *3t*
ΔT_{4t} / K	Temperature at state *4t*
ΔT_{4s} / K	Temperature at state *4s*

In other words, due to friction and losses in the polytropic expansion process the turbine delivers less energy output compared to the ideal isentropic expansion process.
The effective turbine power P_T is then obtained by inserting Equation (2.2) into Equation (2.1):

$$P_T = \eta_T \; P_{T,ideal} = \eta_T \; \dot{m}_T \; c_{p,g} \; T_3 \left[1 - \left(\frac{p_4}{p_3} \right)^{\left(\frac{\kappa-1}{\kappa}\right)_g} \right] \tag{2.4}$$

$P_{T,ideal}$ / W	Isentropic turbine power

As the turbine and the compressor are mechanically coupled by the shaft, the resulting compressor power can be derived from the turbine power by considering the friction losses in the bearings by applying the mechanical efficiency η_m to the turbine power P_T, which leads to the Equation (2.5):

$$P_C = \eta_m \; P_T = \eta_m \; \eta_T \; \dot{m}_T \; c_{p,g} \; T_3 \left[1 - \left(\frac{p_4}{p_3} \right)^{\left(\frac{\kappa-1}{\kappa}\right)_g} \right] \tag{2.5}$$

η_m / Dimensionless	Mechanical efficiency
P_C / W	Compressor power

Typical values for η_m are found in following external references and allow in the early conception phase a rough estimation of the required compressor power P_C.

A more comprehensive way to derive the compressor power is to apply the fundamentals of thermodynamics in an analog way to Equation (2.2). With the usage of the compressor efficiency η_c the ideal isentropic

[16]Nguyen-Schäfer (2015) p. 24

compression leads to:

$$P_C = \frac{1}{\eta_C} P_{C,ideal} = \frac{1}{\eta_C} \dot{m}_C \, c_{p,a} \, T_1 \left[\left(\frac{p_2}{p_1} \right)^{\left(\frac{\kappa-1}{\kappa}\right)_a} - 1 \right] \tag{2.6}$$

$P_{C,ideal}$ / W	Isentropic compressor power
η_C / Dimensionless	Compressor efficiency
$c_{p,a}$ / J kg$^{-1}K^{-1}$	Specific heat capacity of air at constant pressure
T_1 / K	Temperature at compressor inlet
p_1 / Pa	Static pressure at compressor inlet
p_2 / Pa	Static pressure at compressor outlet
κ / Dimensionless	Isentropic exponent of air

The subscript *a* denotes the air as a working fluid of the compressor. In order to develop a better understanding for the polytropic compression process, please refer to Figure (2.7) for graphical representation.

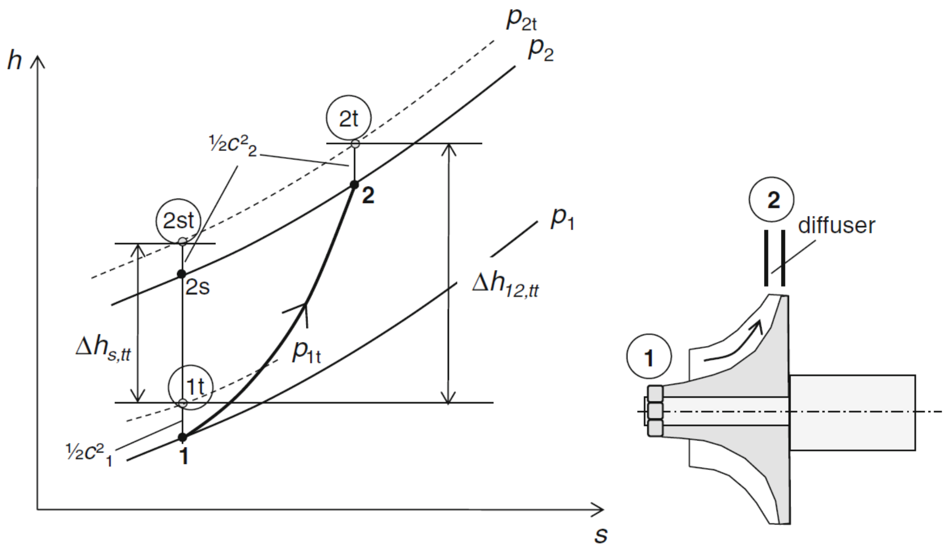

Figure 2.7.: Polytropic compression in the compressor stage, Source: external reference[17]

The compressor efficiency η_C is then defined as the ratio of the polytropic total enthalpy increase between state *1t* and state *2st* to the isentropic total enthalpy increase between state *1t* and *2t*.[18]
The enthalpy increase can be also expressed by their related temperature differences which leads then to the Equation (2.7):

$$\eta_C = \frac{\Delta h_{s,tt}}{\Delta h_{12,tt}} = \frac{T_{2st} - T_{1t}}{T_{2t} - T_{1t}} \tag{2.7}$$

[17]Nguyen-Schäfer (2015) p. 22
[18]Nguyen-Schäfer (2015) p. 22

$\Delta h_{s,tt}$ / J kg^{-1}	Polytropic total enthalpy raise between state *1t* and *2st*
$\Delta h_{12,tt}$ / J kg^{-1}	Polytropic total enthalpy raise between state *1t* and *2t*
ΔT_{2st} / K	Temperature at state *2st*
ΔT_{2t} / K	Temperature at state *2t*
ΔT_{1t} / K	Temperature at state *1t*

An finally the mechanical efficiency η_m is then expressed as:

$$\eta_m = \frac{P_C}{P_T} \tag{2.8}$$

If one substitutes Equations (2.4) and (2.6), the result is the *first turbocharger equation*:

$$\frac{p_2}{p_1} = \left(1 + \frac{c_{p,g}}{c_{p,a}} \left\langle \frac{\dot{m}_T}{\dot{m}_C}\frac{T_3}{T_1}\eta_m\eta_T\eta_C \right\rangle \left[1 - \left(\frac{p_4}{p_3}\right)^{-\left(\frac{\kappa-1}{\kappa}\right)_g}\right]\right)^{\left(\frac{\kappa-1}{\kappa}\right)_a} \tag{2.9}$$

using following expressions:

$$\pi_C = \frac{p_2}{P_1} \tag{2.10}$$

π_C / Dimensionless Pressure ratio of compressor

$$\pi_T = \frac{p_3}{P_4} \tag{2.11}$$

π_T / Dimensionless Pressure ratio of turbine or turbine expansion ratio

$$\eta_{TC} = \eta_m\eta_T\eta_C \tag{2.12}$$

η_{TC} / Dimensionless Overall efficieny of the turbocharger

$$\delta = \frac{\dot{m}_T}{\dot{m}_C}\frac{T_3}{T_1}\eta_{TC} \tag{2.13}$$

δ / Dimensionless Auxilary parameter to connect pressure ratios of compressor and turbine

The first turbocharger equation shows the relation between the compressor's pressure ratio π_C over the turbine's pressure ratio π_T. At full load conditions, the dimensionless parameter δ in the Equation (2.13) can be nearly treated as constant in the compressor performance map (refer to Figure (2.11)) which allows then to consider the behavior of the relevant pressure ratios of turbine and compressor at different values of δ as shown in Figure (2.8).

According to Equation (2.9) a high boost pressure level p_2 can be achieved, if the compressor ratio π_C is

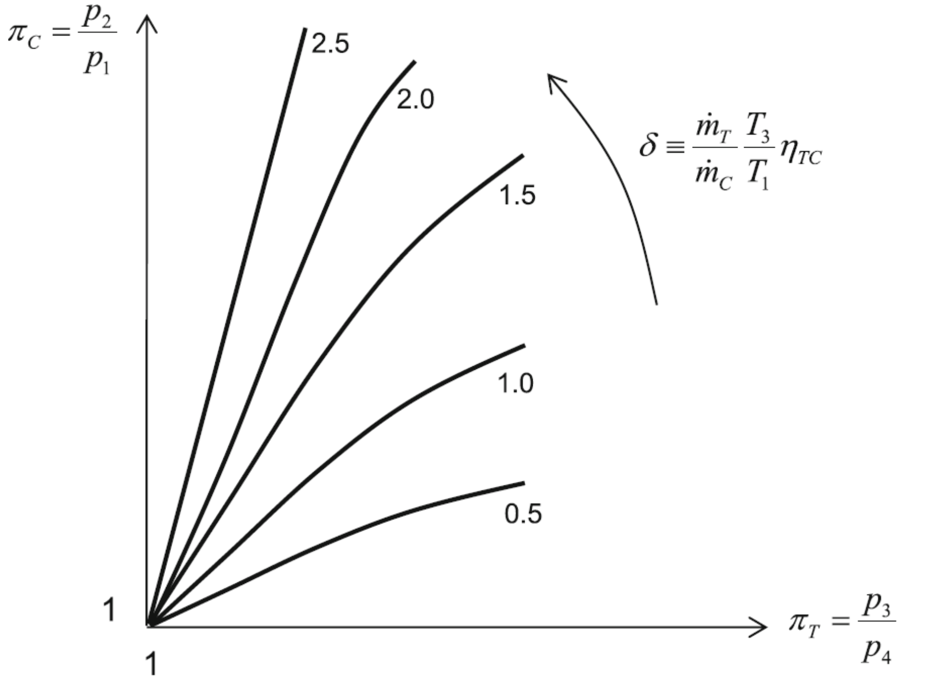

Figure 2.8.: Trend of pressure ratios for turbine and compressor, Source: External reference[19]

high. This is the case, if

- η_{TC} is large, which is related to a large η_m of the bearing system under low-end torque conditions,
- the exhaust gas temperature T_3 is high due to a high level of enthalpy at the turbine inlet, which generates more turbine power,
- the turbine expansion ratio π_T is as high as possible,
- the temperature at compressor inlet T_1 is as low as possible; hence, the temperature of the charge-air T_2 will be also low and this is leading to a high density of the charge-air,
- an optimal level of the exhaust gas temperature T_3 is chosen to compromise between the turbine power the specific fuel consumption,
- the mass flow rate through the turbine is high.

The level of the turbine inlet pressure depends only on the exhaust gas mass flow and the pressure resistance of the turbine. Hence, the flow in the turbocharger is treated as compressible flow in a nozzle and can be modelled as such. This leads to the *second turbocharger equation*. It describes the mass flow rate through the turbine as a function of pressure and temperature at turbine inlet and the expansion ratio in the turbine.

$$\dot{m}_T = \mu \; A_T \; p_{3t} \sqrt{\frac{2}{R_g \; T_{3t}}} \sqrt{\left(\frac{\kappa}{\kappa - 1}\right)_g \left(\left(\frac{p_{3t}}{p_4}\right)^{\left(\frac{-2}{\kappa_g}\right)} - \left(\frac{p_{3t}}{p_4}\right)^{-\left(\frac{\kappa+1}{\kappa}\right)_g} \right)} \tag{2.14}$$

[19]Nguyen-Schäfer (2015) p. 26

μ / Dimensionless	Flow coefficient due to friction and contraction at the nozzle outlet
A_T / m^2	Reference cross-sectional area in the turbine impeller
R_g / J kg$^{-1}K^{-1}$	Specific gas constant of exhaust gas

For engineering purpose it is more convenient to eliminate p_{3t} and T_{3t} from equation (2.14) and make the mass flow independent from the inlet conditions. A reduced mass flow is introduced as the so-called corrected mass flow:

$$\dot{m}_{T,corr} = \frac{\dot{m}_T\sqrt{T_{3t}}}{p_{3t}} = \mu\ A_T\sqrt{\frac{2}{R_g}\sqrt{\left(\frac{\kappa}{\kappa-1}\right)_g\left(\left(\frac{p_{3t}}{p_4}\right)^{\left(\frac{-2}{\kappa_g}\right)} - \left(\frac{p_{3t}}{p_4}\right)^{-\left(\frac{\kappa+1}{\kappa}\right)_g}\right)}} \tag{2.15}$$

$\dot{m}_{T,corr}$ / kg s$^{-1}K^{0.5}bar^{-1}$ Corrected mass flow rate of the turbine

The graphical representation in Figure 2.9 outlines the corrected mass flow rate of the turbine over the turbine expansion ratio $\pi_{T,ts}$ for various rotor speeds $N_{T,C}$ and is called turbine performance map[20].

The fundamental meaning of Figure 2.9 is that the mass flow rate can only be increased upto a certain

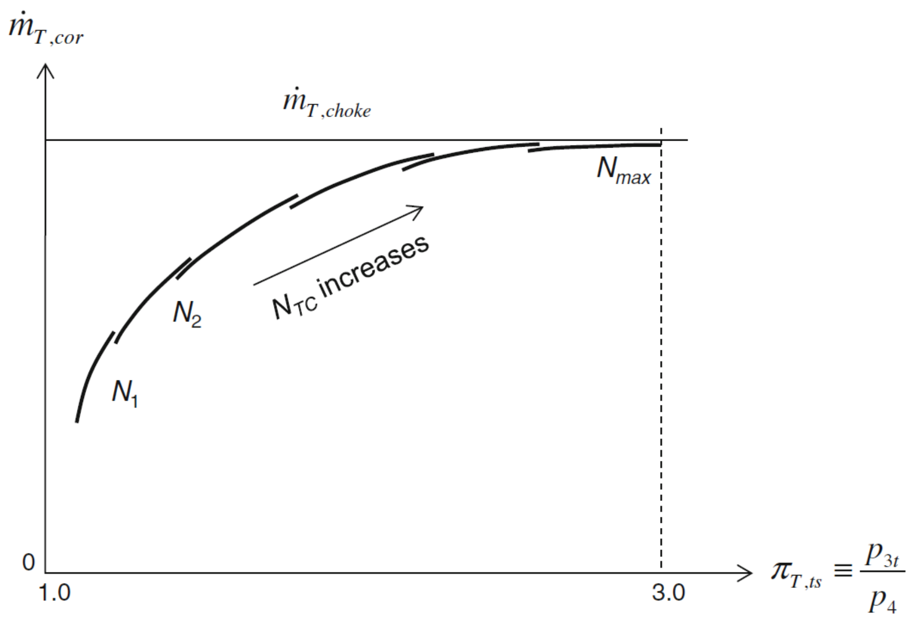

Figure 2.9.: Performance map of the turbine, Source: External reference[20]

level. Even by further increasing the rotor speed, the mass flow rate approaches asymptotically to the so-called *choke line*. The exhaust gas reaches sonic speed conditions at Mach number Ma = 1. Under choked flow conditions the isentropic turbine efficiency is very low and unusable for automotive turbocharger application[20].

With the help of Figure 2.10. the optimal point for the maximal efficiency of $\eta_m\eta_T$ depending on the turbine expansion ratio $\pi_{T,ts}$ can be found. This graph is derived by measuring of the thermodynamic characteristics which are required to calculate $\eta_m\eta_T$ based on the equations derived in this section. It shows that the optimal point is in the middle of the rotational speed range which corresponds to an expansion ratio of approximatelly

[20] Nguyen-Schäfer (2015) p. 27

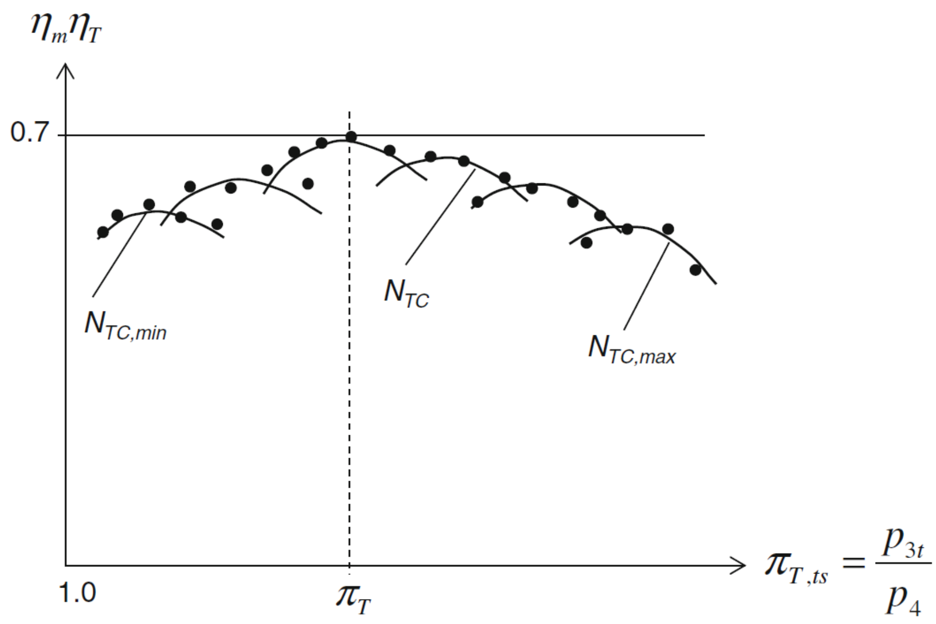

Figure 2.10.: Efficiency $\eta_m\eta_T$ over $\pi_{T,ts}$ for various $N_{T,C}$, Source: External reference[21]

$\pi_{T,ts}$ = 1.5 [21].

The compressor performance map as shown in Figure 2.11 is derived in an analog way to the turbine performance map. It shows the relation between the compressor ratio $\pi_{C,tt}$ and the corrected compressor mass flow $\dot{m}_{C,corr}$[22].

Following exemplary the full load curve according to the *first turbocharger equation* and starting on the left side of the compressor performance map with low rotational speed, one can see immediately an increase of the compression ratio $\pi_{C,tt}$ with increasing the mass flow $\dot{m}_{C,corr}$. This behavior is seen as beneficial for the dynamic behavior of the turbocharger in terms of response time at low-end torque. A further increase of the rotor speed to approximately 70 % of the maximal speed, the compressor ratio increases to nearly 2.5 and the engine reaches the maximal torque point T_1. The design point T_{DP} is the one with the best overall efficiency. At higher rotor speeds the turbine efficiency is reduced and therefore the overall efficiency of the turbocharger is also decreasing. Thus, this leads to a further decrease of the compressor pressure ratio to the point P_{nom} marking the nominal engine power.

As also shown in Figure 2.11, the compressor map is bounded at part load conditions by the so-called *surge line*. At this line a stall, which is a flow separation at the leading edges of the compressor impeller, creates periodic recirculations. Similar to the characteristics of the turbine, the compressor has also a choke line representing the maximum speed of the turbocharger.

[21] Nguyen-Schäfer (2015) p. 28
[22] Nguyen-Schäfer (2015) p. 30

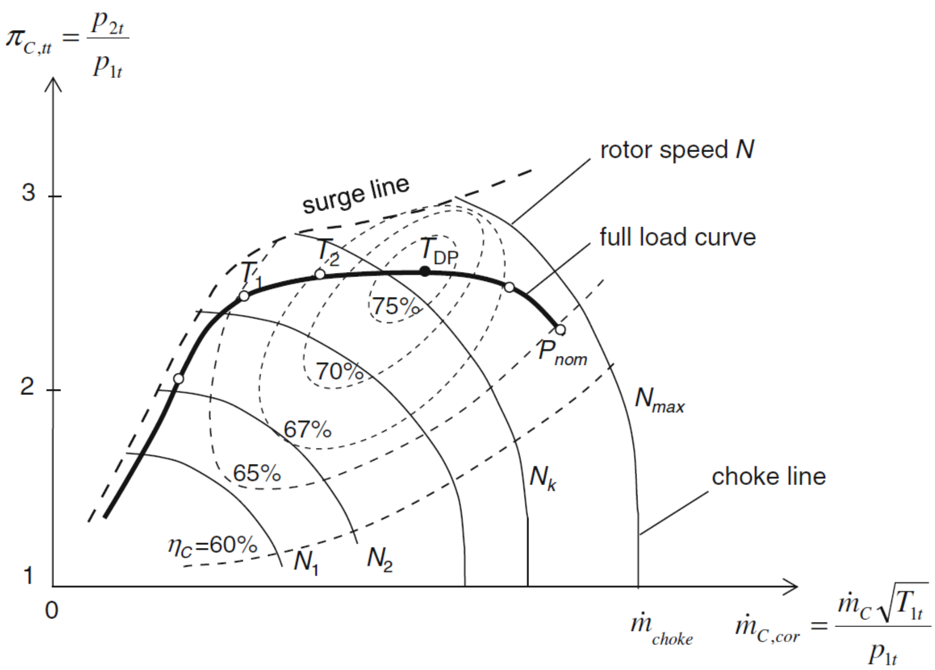

Figure 2.11.: Compressor performance map, Source: External reference[22]

2.2.2.2. Matching the turbocharger with the ICE

In this subsection the matching procedure of the turbocharger with the ICE is briefly described.[23]

The operation conditions for the component is defined by the engine characteristics in the first place. Therefore, different engine load conditions such as *rated power* and *rated torque* are analyzed. Then the corresponding data to the chosen load points are determined, hence, charge air mass flow $\dot{m}_C$ and compressor ratio π_C have to be prepared. Figure 2.12 outlines the matching procedure.

In the next step, based on $\dot{m}_C$ and π_C the relevant points in the compressor performance map can be determined and the auxilary parameter δ, which connects the pressure ratios of compressor and turbine can be calculated. Using the diagram of the first turbocharger equation, the corresponding turbine pressure ratio π_T can be determined.

And finally, the turbine performance map provides the turbine operating point using the given exhaust gas mass flow $\dot{m}_T$ delivered by the ICE.

Using this input from aboves procedure, the actual dimensions from the T/C, such as inflow and outflow diameter, can be determined in an iterative process based on the turbomachinery theory.[24]

[23]Cf. Nguyen-Schäfer (2015) pp. 33-35
[24]Nguyen-Schäfer (2015) p. 32

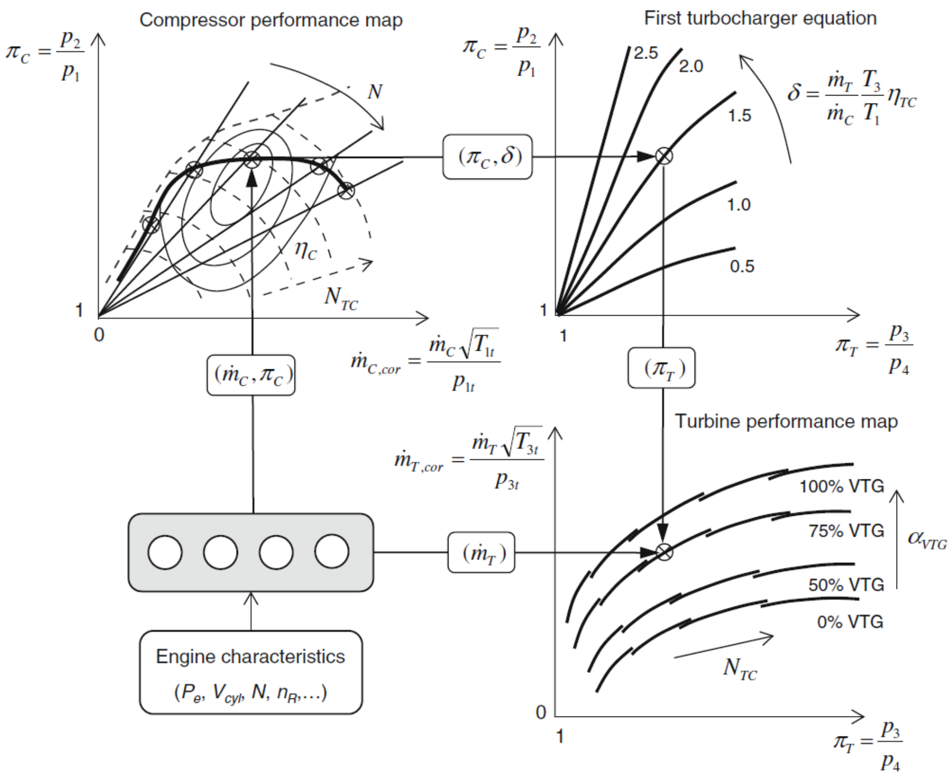

Figure 2.12.: T/C Matching with ICE, Source: External reference[23]

2.3. Physical modelling

This chapter introduces the theory of the models on the mathematical basis that have been considered in the work. CFD modelling in thermal flow problems is a multi-domain or multi-material task that involves fluid-flow and conjugate heat transfer problems. In general, the gas phase is treated in an Eulerian[25] approach, calculating the property of a fluid in each computational cell.
The most common methodology to solve fluid flow problems is based on modelling of the *Navier-Stokes equations*.[26] In fluid flow it is much more convenient to consider a certain spatial region, the so-called *control volume*. Applying this methodology, the continuity equation, *Navier-Stokes* equations of momentum and the energy equation are discretized to solve a specific fluid problem delimited in space and divided into a vast number of computational cells.

2.3.1. Conservation principles

The physics of fluid motion is represented by a set of governing equations stating the following dynamic and thermodynamic properties:[27]

- The *mass conservation*, where the mass of a fluid parcel is conserved and can neither be created nor destroyed.
- *Newton's second law*, which states that the rate of change of momentum is equal to the sum of the external forces acting.
- *First law of thermodynamic*, where the rate of change of energy per time unit equals the sum of the rate of heat addition to the particle and the rate of work done on the fluid particle.

In general, the fluid is treated as a continuum. With respect to the formulation of the conservation laws applied on the control volume it is very often denoted as particle or parcel. Furthermore, the molecular structure and the molecular motions are also neglected. Only macroscopic properties, such as velocity, pressure, density and temperature are used to describe the fluid.[28]

2.3.1.1. Conservation laws for a control volume

Fundamental physical conservation laws, such as mass, momentum, energy and enthalpy in their original forms are defined for a control volume and can be formulated in a unique form stating that the rate of change of an extensive property $\hat{\Phi}$ is a consequence of the interaction of this system with its environment. Introducing the property as:

$$\hat{\Phi} = \int_V \hat{\rho}\hat{\phi} dV \tag{2.16}$$

[25] Ansorge (2003) p. 13
[26] Versteeg H. K. (1995) p. 21
[27] Cf. Versteeg H. K. (1995) p. 10
[28] Cf. White F. M. (1979) p. 4

$\hat{\Phi}$ / Quantity of matter	Extensive transferable property
$\hat{\phi}$ / per unit mass	Intensive transferable property
$\hat{\rho}$ / kg m^{-3}	Fluid density
V / m^3	Volume (control volume)

Applying equation (2.16) to the control volume V which is bounded by a surface A is defined in the following equation, the so-called *Reynolds Transport Theorem*[29]:

$$\left(\frac{d\hat{\Phi}}{dt}\right)_m = \int_A \hat{\hat{\gamma}}_A dA + \int_V \hat{\rho}\hat{\hat{\gamma}}_m dV \tag{2.17}$$

A / m^2	Surface (control boundary) which is bounding the control volume V
$\hat{\hat{\gamma}}_A$ / per unit time	Local diffusion flag of $\hat{\phi}$ at the control boundary A
$\hat{\hat{\gamma}}_m$ / per unit mass per unit time	Source or sink of $\hat{\phi}$
t / s	Time

A direct application of the *Reynolds Transport Theorem* leads to a general form[30] (strong conservative form) of the differential conservation law for an intensive property $\hat{\phi}$ written in index notation for cartesian coordinates:

$$\frac{D\left(\hat{\rho}\hat{\phi}\right)}{Dt} = \frac{\partial\left(\hat{\rho}\hat{\phi}\right)}{dt} + \frac{\partial\left(\hat{\rho}\hat{\phi}\left[\hat{U}_j - \hat{U}b_j\right]\right)}{\partial x_j} = \frac{\partial\hat{\hat{\gamma}}_A}{\partial x_j} + \rho\hat{\hat{\gamma}}_m \tag{2.18}$$

$\hat{U}b_j$ / m s^{-1}	Local velocity of the moving boundary of the control volume
$\hat{U}_j$ / m s^{-1}	Local absolute flow velocity
x_j / m	Cartesian coordinates with $j = (1,2,3)$ corresponding to the directions (x,y,z)

Equation (2.18) describes the total or substantive derivative of a property with respect to time and per unit volume.[31] Note also, that a *strong conservative form* can be easily recognized by the density being lumped together with the extensive property $\hat{\Phi}$ under all differentiation operators.
For convenience, in the following procedure it is assumed that the control surface is fixed in a coordinate system, hence $\hat{U}b_j = 0$.

In order to obtain the continuity equation in differential form, the following expressions $\hat{\phi} = \hat{\Phi}/m = 1$ and $\hat{\hat{\gamma}}_m = \hat{\hat{\gamma}}_A = 0$ are applied to equation (2.18):

$$\frac{\partial\hat{\rho}}{\partial t} = -\frac{\partial}{\partial x_j}\left(\hat{\rho}\hat{U}_j\right) \tag{2.19}$$

Using the continuity equation (2.19), the differential conservation law can be transformed into the weak conservative form by applying a chain differentiation. This form is more convenient in handling equations, but

[29] Cf. Peric M., Ferziger J. H. (2002) p. 3
[30] Cf. Peric M., Ferziger J. H. (2002) pp. 7-8
[31] Cf. Versteeg H. K. (1995) p. 13

less convenient for considering variable-density flows in the Finite Volume (FV) formulation. It is given by:

$$\hat{\phi}\underbrace{\left[\frac{\partial\hat{\rho}}{\partial t}+\frac{\partial\left(\hat{\rho}\hat{U}_j\right)}{\partial x_j}\right]}_{=0}+\hat{\rho}\frac{\partial\hat{\phi}}{\partial t}+\hat{\rho}\left(\hat{U}_j\frac{\partial\hat{\phi}}{\partial x_j}\right)=\hat{\dot{\gamma}} \tag{2.20}$$

$\hat{\dot{\gamma}}$ / s^{-1} Total source term

The total source term $\hat{\dot{\gamma}}$ can be associated with the mass of the system, split into the two briefly introduced components $\hat{\dot{\gamma}}_A$ and $\hat{\dot{\gamma}}_m$ from equation (2.17). Additional description for the two sources is given as follows:

- The local diffusion flag of $\hat{\dot{\gamma}}_A$ at the control boundary A denotes a force on the control surface due to pressure and viscous stresses in the momentum equation and the diffusion flux of heat through the control boundary in the energy equation.
- $\hat{\dot{\gamma}}_m$ represents the source per unit mass of heat due to chemical reactions, combustion, electric or magnetic heating in the energy equation and the gravitational, Coriolis, centrifugal or electromagnetic forces in the momentum equation.

The local diffusion flags (surface flux) for the major conservation laws which are used in this thesis are summarized as follows:

For the conduction flux based on *Fourier's law*:

$$\hat{\dot{\gamma}}_A=-\vec{q}=\lambda\nabla\hat{T}\quad or,\qquad -q_i=\lambda\frac{\partial\hat{T}}{\partial x_i} \tag{2.21}$$

$\vec{q},\ q_i$ / W m^{-2}	Heat flux
$\hat{T}$ / K	Temperature
λ / W m^{-1} K^{-1}	Thermal conductivity

For the mass molecular diffusion flux based on *Fick's law*:

$$\hat{\dot{\gamma}}_A=-\vec{m}''=D\nabla\hat{C}\quad or,\qquad -m_i^{''}=D\frac{\partial\hat{C}}{\partial x_i} \tag{2.22}$$

$\vec{m}'',\ m_i$ / kg m$^{-2}s^{-1}$	Mass flux of a species
$\hat{C}$ / kg m^{-3}	Concentration of species
D / m$^2s^{-1}$	Mass diffusivity

For the momentum flux (for instance the viscous stress) based on the *Newton-Poisson law*:

$$\hat{\sigma}_{ij}=-\hat{p}\delta_{ij}+\mu\left(\frac{\partial\hat{U}_i}{\partial x_j}+\frac{\partial\hat{U}_j}{\partial x_i}-\frac{2}{3}\frac{\partial\hat{U}_k}{\partial x_k}\delta_{ij}\right) \tag{2.23}$$

$\hat{p}$ / N m^{-2}	Local pressure
$\hat{\sigma}_{ij}$ / N m^{-2}	Stress tensor
δ_{ij} / Dimensionless	Kronecker delta
μ / kg m$^{-1}s^{-1}$	Dynamic molar viscosity
$\hat{U}_i, \hat{U}_j, \hat{U}_k$ / m s^{-1}	Local absolute velocities

The expression in the square bracket of equation (2.20) equals zero, as it is the continuity equation (2.19). Hence, the weak conservative form is denoted as:

$$\hat{\rho}\frac{D\hat{\phi}}{Dt} = \hat{\rho}\frac{\partial\hat{\phi}}{\partial t} + \hat{\rho}\hat{U}_j\frac{\partial\hat{\phi}}{\partial x_j} = \hat{\dot{\gamma}} \tag{2.24}$$

2.3.1.2. Conservation laws in common form

The common differential form of the conservation law can now be written:

$$\hat{\rho}\frac{D\hat{\phi}}{Dt} = \hat{\rho}\frac{\partial\hat{\phi}}{\partial t} + \hat{\rho}\hat{U}_j\frac{\partial\hat{\phi}}{\partial x_j} = \hat{\rho}\hat{\dot{\gamma}}_m + \frac{\partial\hat{\dot{\gamma}}_A}{\partial x_j} \tag{2.25}$$

Replacing the intensive transferable property $\hat{\phi}$ from equation (2.25) by the appropriate quantity and applying in addition the corresponding source term leads to the common conservation equations.[32]

The momentum (Navier-Stokes) equation[33] can be derived by replacing $\hat{\phi} = \hat{U}_i$:

$$\begin{aligned}\hat{\rho}\frac{D\hat{U}_i}{Dt} &= \hat{\rho}\frac{\partial\hat{U}_i}{\partial t} + \hat{\rho}\hat{U}_j\frac{\partial\hat{U}_i}{\partial x_j} = \hat{\rho}g_i + \frac{\partial\hat{\sigma}_{ij}}{\partial x_j} \\ &= \hat{\rho}g_i - \frac{\partial\hat{p}}{\partial x_i} + \frac{\partial}{\partial x_j}\left[\mu\left(\frac{\partial\hat{U}_i}{\partial x_j} + \frac{\partial\hat{U}_j}{\partial x_i} - \frac{2}{3}\frac{\partial\hat{U}_k}{\partial x_k}\delta_{ij}\right)\right]\end{aligned} \tag{2.26}$$

g_i / m s^{-2}	Gravity of earth

The energy equation is derived by introducing the specific stagnation or specific total enthalpy and replacing $\hat{\phi} = \hat{H} = \hat{h} + \hat{U}^2/2$:

$$\hat{\rho}\frac{D\hat{H}}{Dt} = \hat{\rho}\left(\frac{\partial\hat{H}}{\partial t} + \hat{U}_j\frac{\partial\hat{H}}{\partial x_j}\right) = \hat{\rho}\dot{q}_g + \frac{\partial\hat{p}}{\partial t} + \frac{\partial\left(\hat{\tau}_{ij}\hat{U}_j\right)}{\partial x_i} + \frac{\partial}{\partial x_j}\left(\lambda\frac{\partial\hat{T}}{\partial x_j}\right) \tag{2.27}$$

$\hat{H}$ / m$^2s^{-2}$	Stagnation (total) enthalpy
$\hat{h}$ / m$^2s^{-2}$	Static enthalpy
$\dot{q}_g$ / W kg^{-1}	Internal heat source
τ_{ij} / N m^{-2}	Turbulent strain tensor, refer also to subsection 2.3.1.3

[32] Cf. Peric M., Ferziger J. H. (2002) pp. 5-10
[33] Cf. AVL List GmbH. (2014) Feb. 28

Note, by using the expression *total or static enthalpy* the *specific total or specific static enthalpy*[34] is meant. Since in fluid mechanics the mass is conserved, it is common practice to use the shorter expressions of *total or static enthalpy*[35].

Finally, the concentration equation for a species is given by exchanging $\hat{\phi} = \hat{C}$:

$$\hat{\rho}\frac{D\hat{C}}{Dt} = \hat{\rho}\left(\frac{\partial \hat{C}}{\partial t} + \hat{U}_j\frac{\partial \hat{C}}{\partial x_j}\right) = \hat{\rho}\hat{\dot{r}} + \frac{\partial}{\partial x_j}\left(D\frac{\partial \hat{C}}{\partial x_j}\right) \tag{2.28}$$

$\dot{r}$ / kg$^{-1}s^{-1}$ Internal source per unit time

2.3.1.3. The closure problem

Since the Navier-Stokes equations are non-linear partial differential equations of second order, only for some special cases the exact solution exists. For engineering purposes it is sufficient to consider averaged results and their fluctuations. Hence the mathematical formulation of the turbulence can be also described in a simpler way. A suitable method, called the *Reynolds decomposition*, was developed by Osborne Reynolds to deal with this problem of averaging by deriving statistically averaged equations. Further exhaustive information about the Reynolds decomposition can be found in following reference[36].

Applying the Reynolds averaging to the differential form of conservation equations for the instantaneous variable $\hat{\phi}$, one can get the Reynolds-averaged Navier-Stokes equations (RANS) as follows:

$$\rho\frac{DU_i}{Dt} = \rho g_i - \frac{\partial P}{\partial x_i} + \frac{\partial}{\partial x_j}\left[\mu\left(\frac{\partial U_i}{\partial x_j} + \frac{\partial U_j}{\partial x_i} - \frac{2}{3}\frac{\partial U_k}{\partial x_k}\delta_{ij}\right) - \rho\overline{u_i u_j}\right] \tag{2.29}$$

and the Reynolds-averaged energy equation:

$$\rho\frac{DH}{Dt} = \rho\left(\frac{\partial H}{\partial t} + U_j\frac{\partial H}{\partial x_j}\right) = \rho\dot{q}_g + \frac{\partial P}{\partial t} + \frac{\partial(U_j\tau_{ij})}{\partial x_i} + \frac{\partial}{\partial x_j}\left(\lambda\frac{\partial T}{\partial x_j}\right) \tag{2.30}$$

as well as the Reynolds-averaged concentration equation:

$$\rho\frac{DC}{Dt} = \rho\left(\frac{\partial C}{\partial t} + U_j\frac{\partial C}{\partial x_j}\right) = \rho\dot{r} + \frac{\partial}{\partial x_j}\left(D\frac{\partial C}{\partial x_j} - \rho\overline{cu_i}\right) \tag{2.31}$$

where

$\rho\overline{u_i u_j} = \tau^t_{ij}$ / N m^{-2} turbulent stress (or strain) tensor
$\rho\overline{cu_i} = m''^t_i$ / kg m$^{-3}s^{-1}$ turb. mass flux (of a species per unit volume ρc, by velocity fluctuation u_j)

The previous lines illustrating that the Reynolds averaged transport equations contain unknown variables,

[34]Cf. Versteeg H. K. (1995) p. 20
[35]Cf. Peric M., Ferziger J. H. (2002) p. 10
[36]Cf. AVL List GmbH. (2014) Feb. 28, section 4.2.1.2

so-called second moments $\overline{\phi u_j}$ as a consequence of averaging. In order to close this set of equations these variables have to be added before any solution can be obtained. This problem is known as the *Turbulence Closure Problem*[37].
Therefore additional algebraic or differential relations are required. A set of mathematical equations, which provide these unknown variables, is called Turbulence Closure Model. It has to be noted, that these second moments are always vectors of higher order than the basic variables, for instance if ϕ is a scalar, $\overline{\phi u_j}$ is a vector. In case ϕ is a vector then $\overline{\phi u_j}$ becomes a second order tensor. And this makes the closure problem more complicated as one needs to solve more equations than e.g. for a laminar flow of the same complexity. The type of *algebraic* or *differential* and the number of auxiliary equations define the level of closure.[38]

There are two basic levels of modelling currently used in computational fluid dynamics and transport processes:[39]

- Eddy Viscosity/Diffusivity Models (EVM), known also as the first-order models
- Second-Moment Closure Models (SMC), known under the name Reynolds/stress/flux models or second order models

Each category has several variants. The EVM are based on the assumption that the turbulent flux of momentum, heat and species is directly related to the mean flow field, i.e. mean velocity, mean temperature, and mean concentrations, respectively. The second-order models obtain the turbulent flux by solving separate differential transport equations for each flux component $\overline{\phi u_j}$.[40]
Nowadays, it is common practice to use unstructured grids. With the reduction of meshing time, even the *poor quality* meshes are used in calculations. This undoubtedly leads to a negative impact to the convergence behavior and therefore to the numerical stability of a simulation. The results obtained by Basara show that the second-moment closure can be efficiently applied on unstructured grids (particular for polyhedral cells) used in engineering CFD applications.[41]
One of the greater challenges in turbulence closure problem is the modelling of the non-linear convective acceleration term, the turbulent stress tensor (refer to equation (2.29)). The target of the modelling is to find an expression for the stress tensor as a function of the mean flow, independent of the velocity. The state of the art approach is briefly outlined in the next subsection.

2.3.1.4. Turbulence modelling

The state of the art turbulence model in AVL FIRE is the so-called $k - \zeta - f$ turbulence model. It is based on the original model $\overline{v^2} - f$ which was developed by Hanjalic, Popovac and Hadziabdic.[42]
The $k - \zeta - f$ RANS model used in the present work relies on the elliptic relaxation concept providing a continuous modification of the homogeneous pressure-strain process as the wall is approached to satisfy the wall conditions, and therefore avoiding the need for any wall topology parameter.[43]
In other words, the $k - \zeta - f$ shows anisotropic behavior of the turbulence especially near the wall and close to stagnation points which is beneficial for heat transfer problems, as this determines the heat and mass transfer up to a certain extend. From the numerical stand point the aim of the new model is to improve

[37] Cf. Lesieur M. (1996), p 105
[38] Hanjalic K., Launder B. (2011), p. 60
[39] Cf. AVL List GmbH. (2014) Feb. 28, section 4.2.1.4.1
[40] AVL List GmbH. (2014) Feb. 28, section 4.2.1.4.1
[41] Cf. Basara B. (2004), pp. 377-407
[42] Cf. Hanjalic, K., Popovac, M., Hadziabdic, M. (2004), pp. 1047-1051
[43] Cf. AVL List GmbH. (2014) Feb. 28, section 4.2.1.4.9

numerical stability of the original $\overline{v^2} - f$ model by solving a transport equation for the velocity scale ratio $\zeta = \overline{v^2}/k$ instead of velocity scale $\overline{v^2}$. Hanjalic et al. also demonstrated that the model is numerically more robust and more accurate compared to the simpler two-equation eddy viscosity models.

The set of necessary equations is stated based on following reference[44], starting with the eddy-viscosity, which is obtained from:

$$\nu_t = C_\mu \zeta \frac{k^2}{\varepsilon} \tag{2.32}$$

ν_t / Pa s	Eddy viscosity or turbulence eddy viscosity
C_μ / Dimensionless	Model specific constant, refer to Table 2.1
ζ / Dimensionless	Velocity scale ratio, $\zeta = \overline{v^2}/k$
k / m$^2 s^{-2}$	Turbulence kinectic energy
ϵ / m$^2 s^{-3}$	Turbulence dissipation rate

The remaining variables are derived from the following set of model equation starting with the turbulence kinetic energy k:

$$\rho \frac{Dk}{Dt} = \rho(P_k - \varepsilon) + \frac{\partial}{\partial x_j}\left[\left(\mu + \frac{\mu_t}{\sigma_k}\right)\frac{\partial k}{\partial x_j}\right] \tag{2.33}$$

P_k / W	Production of turbulence kinetic energy
σ_k / Dimensionless	Model specific constant, refer to Table 2.1

Continuing with the turbulence dissipation rate ϵ:

$$\rho \frac{D\varepsilon}{Dt} = \rho \frac{C_{\varepsilon 1}^{*} P_k - C_{\varepsilon 2}\varepsilon}{T} + \frac{\partial}{\partial x_j}\left[\left(\mu + \frac{\mu_t}{\sigma_\varepsilon}\right)\frac{\partial \varepsilon}{\partial x_j}\right] \tag{2.34}$$

$C_{\varepsilon 1}^{*}, C_{\varepsilon 2}, \sigma_\varepsilon$ / Dimensionless	Model specific constants, refer to Table 2.1

And finally the ζ function is given by:

$$\rho \frac{D\zeta}{Dt} = \rho f - \rho \frac{\zeta}{k} P_k + \frac{\partial}{\partial x_j}\left[\left(\mu + \frac{\mu_t}{\sigma_\zeta}\right)\frac{\partial \zeta}{\partial x_j}\right] \tag{2.35}$$

σ_ζ / Dimensionless	Model specific constant, refer to Table 2.1

The following form of the f equations as adopted:

$$f - L^2 \frac{\partial^2 f}{\partial x_j \partial x_j} = \left(C_1 + C_2 \frac{P_k}{\zeta}\right)\frac{(2/3 - \zeta)}{T} \tag{2.36}$$

[44] Cf. AVL List GmbH. (2014) Feb. 28, section 4.2.1.4.9

f / Dimensionless Elliptic relaxation function
C_1, C_2 / Dimensionless Model specific constants, refer to Table 2.1

The turbulent time scale T and length scale L are given by:

$$T = \max\left(\min\left(\frac{k}{\varepsilon}, \frac{a}{\sqrt{6}C_\mu\,|S|\,\zeta}\right), C_T\left(\frac{\nu}{\varepsilon}\right)^{1/2}\right) \tag{2.37}$$

$$L = C_L \max\left(\min\left(\frac{k^{3/2}}{\varepsilon}, \frac{k^{1/2}}{\sqrt{6}C_\mu\,|S|\,\zeta}\right), C_\eta\frac{\nu^{3/4}}{\varepsilon^{1/4}}\right) \tag{2.38}$$

C_μ, C_T, C_η / Dimensionless Model specific constants, refer to Table 2.1

An additional modification to the ε equation (equation 2.34) is that the constant $C_{\varepsilon 1}$ is dampened close to the wall:

$$C^*_{\varepsilon 1} = C_{\varepsilon 1}\left(1 + 0.045\sqrt{1/\zeta}\right) \tag{2.39}$$

According to Hanjalic et al.[45] this formulation is computationally more robust than the original model $\overline{v^2} - f$. All latest dimensionless used in this section are based on following reference[46] and summarized below in Table 2.1.

C_1	C_2	$C_{\varepsilon 1}$	$C_{\varepsilon 2}$	C_μ	
0.4	0.65	1.4	1.9	0.22	
σ_k	σ_ε	σ_ζ	C_T	C_L	C_η
1.0	1.3	1.2	6.0	0.36	85

Table 2.1.: Model specific constants for turbulence modelling

2.3.1.5. Heat transfer and wall modelling

As the turbocharger uses a thermodynamic working principle and is thermodynamically coupled to the ICE, the hot exhaust gas is coming from the combustion chamber and expands through a turbine that powers a compressor. In passenger cars the temperature of EGR can exceed 1000°C at the inlet of the turbine and on the compressor side inlet temperatures between 20°C to 40°C are not unusual. The solid components of a turbocharger assembly are all in physical contact with each other, hence a resulting heatflow is established driven by different temperature levels of the relevant component. For instance the turbine housing has a significant higher temperature than the bearing housing. This results in a mainly conductive heat transfer through the entire assembly until thermal equilibrium is reached.

[45] Cf. Hanjalic, K., Popovac, M., Hadziabdic, M. (2004), pp. 1047-1051
[46] Šaric S., Basara B., Žunic Z. (2016), p. 2

Since the turbine side of the turbocharger is in contact with the hot EGR, the energy transfer to the housing and rotor is mainly based on forced convection. The inherent dynamics of the hot gas flow is enhancing the heat transfer and therefore the local heat transfer coefficient is also increasing. On the compressor side the rather cold intake air is cooling the intake flange of the compressor housing whereas the compressed air provides additional heat input to the compressor outlet volute.
The third mechanism of heat transfer is considering radiative effects as the structural temperatures especially on the exhaust side can reach very high temperatures. Radiative phenomena inside the turbine stage are not considered, hence the radiation boundary conditions are applied to all external faces to the environment.

A physical and mathematical description of the three considered heat transfer mechanism shall briefly be given in the following lines in order to develop a better understanding.

Conduction: The mechanism of conduction shall be seen as a physical phenomenon from an energetic point of view acting on the atomic or molecular level. It may be seen as the transfer of energy from more energetic to less energetic particles of a substance due to interactions among them. This random molecular motion is also named *diffusion*. The thermal conduction is characterized by the heat flow in the direction of decreasing temperature. On a macroscopic scale, the conduction is independent of *bulk* motion and therefore, it appears in solids, liquids as well as gases.[47]
A quantification of the process in terms of appropriate rate equations is based on Fourier's law:

$$\dot{q}_\lambda = -\lambda \frac{\Delta T}{\Delta x} \tag{2.40}$$

$\dot{q}_\lambda$ / W m^{-2}	Heat flux, here in a single direction for instance represented by Δx
ΔT / K	Temperature gradient
λ / W m$^{-1}K^{-1}$	Thermal conductivity, a transport property as a characteristic of the wall material

The minus sign is a consequence of the fact that heat is transferred into the direction of lower temperature, means driven by the temperature gradient. Furthermore, it has to be mentioned that the heat flux is a vector quantity as already indicated in equation (2.21).

Convection: The convection heat transfer consists two mechanisms. Beside the energy transfer due to diffusion, energy is also transferred by macroscopic (bulk) motion of the fluid. The term *convection* in fact refers to this cumulative motion, whereas the term *advection* refers only to the phenomenon of macroscopic bulk motion. In engineering tasks special attention is paid to convection between fluid in motion and a bounding surface (wall) when each of them are at different temperature levels. The flow profile close to the wall develops a nonlinear shape, varying from zero directly at the wall to a finite value inside the fully developed flow field.[48]
Figure 2.13. outlines the development of the *hydrodynamic* or *velocity boundary layer* (left part) and the *thermal boundary layer* (right part). The temperature distribution has a nonlinear profile starting from the wall with T_W to T_∞ in the inner flow region.
The thermal and the hydrodynamic boundary layer are usually different in position looking downstream the flow path, but have significant influence to the convective heat transfer. Close to the wall the molecular diffusion is the dominating mechanism due to very low velocities. In fact, at the wall the heat transfer is due to pure conduction. In the outer flow regime with higher velocities the heat transfer is mainly governed by the macroscopic motion of the fluid.

[47] Bergman T. L., Incopera F. P. (2011), p. 3
[48] Bergman T. L., Incopera F. P. (2011), p. 6

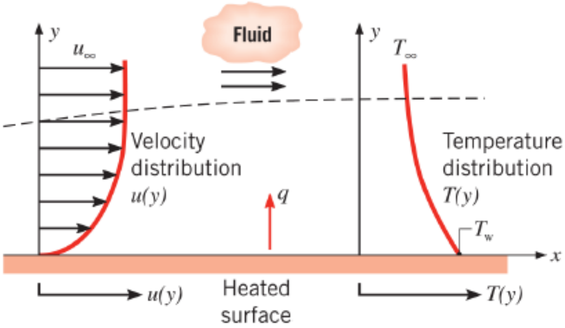

Figure 2.13.: Wall boundary in convective heat transfer, Source: external reference according to Bergman et al.[48]

The mathematical description of the convection is known as *Newtons law of cooling* and is expressed by the following rate equation:

$$\dot{q}_\alpha = \alpha(T_W - T_\infty) \tag{2.41}$$

$\dot{q}_\alpha$ / W m^{-2}	Convective heat flux
α / W m$^{-2}K^{-1}$	Convective heat transfer coefficient
$(T_W - T_\infty)$ / K	Temperature difference at the wall boundary, refer to Figure 2.13.

The convective heat transfer coefficient (HTC) depends on temperature dependent fluid properties, process parameters of the flow (such as velocity, turbulence etc.) and on the wall geometry and surface roughness.[49]

Radiation: This type of heat transfer is based on the emission of energy in form of electromagnetic waves. Compared to conduction and convection, radiation does not require any type of media to transport the heat. In fact it has its best efficiency in vacuum and all matter with a temperature greater than absolute zero emits thermal radiation.[50]
The radiation heat flux from a surface, derived from the *Stefan-Boltzmann law*, is given by:

$$\dot{q}_{rad} = \varepsilon_{rad}\sigma T^4 \tag{2.42}$$

$\dot{q}_{rad}$ / W m^{-2}	Radiation heat flux
ε_{rad} / Dimensionless	Emissivity, a material property of the radiative surface
σ / W m$^{-2}K^{-4}$	Stephan-Boltzmann constant, $\sigma = 5.67E-08$ / $W\ m^{-2}K^{-4}$

The emissivity ε_{rad} depends on the material properties such as surface morphology, direction of radiation and the temperature.[51]

The dominating mechanism for the heat transfer in a turbocharger is the convective one. Hence it is necessary to have a closer look at that modelling. One has to distinguish between laminar and the turbulent boundary layers as displayed in Figure 2.14.[52]

[49]Cf. VDI-Heat Atlas (2010), p. A6
[50]Cf. VDI-Heat Atlas (2010), p. Ka1
[51]Cf. VDI-Heat Atlas (2010), pp. Ka4-Ka6
[52]Bergman T. L., Incopera F. P. (2011), p. 359

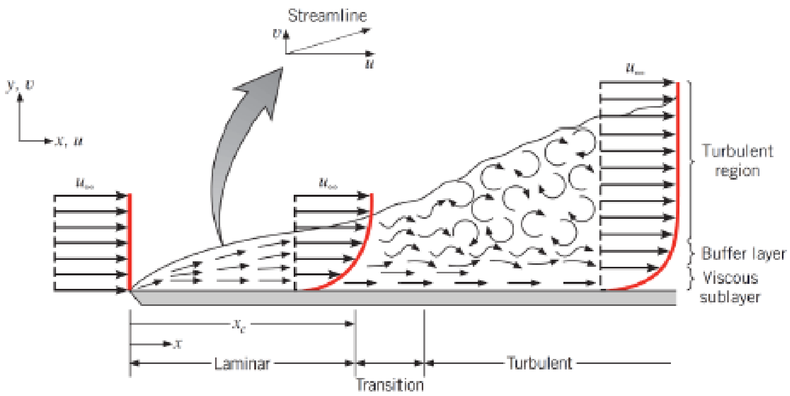

Figure 2.14.: Laminar and turbulent velocity boundary layer, Source: external reference according to Bergman et al.[52]

Nowadays, commercial CFD packages offer wall treatment models to approximate the near wall velocity and temperature distribution.[53]

2.3.2. Numerical solution method

Once the mathematical model has been selected, one has to choose a suitable discretization method approximating the differential equations by a system of algebraic equations for the variables at each set of discrete locations in space and time[54].
Nowadays, commercial CFD codes provide a complete package to solve a general fluid flow problem. In this thesis the software package AVL FIRE in the version R2017 is used for that purpose, applying the finite volume method with following main features:

- The governing equations are used in integral form.
- The solution domain is subdivided into a finite number of contiguous control volumes.
- The conservation equation is applied to each control volume (computational cell).
- The computational node is located at the centroid of each computational cell.
- Solution procedure can be applied to any type of grids, especially complex geometries.

The mathematical modelling of fluid flow phenomena such as momentum, energy, mass and turbulence transport has been introduced in the previous Chapter. The numerical solution method, here denoted as the SIMPLE[55] algorithm, is outlined for a finite volume methode as follows:

- Assumption of the pressure field,
- Solving the momentum equations to obtain velocity field,
- Solving the pressure correction equation,
- Updating the velocity field based on corrected pressure,

[53]Cf.AVL List GmbH. (2014) Feb. 28, section 3.1.4.14
[54]Ferziger, J. H. (2002), p. 25
[55]Cf. AVL List GmbH. (2014) Feb. 28, section 3.2

- Solving all other transport equations.

This procedure runs in an iterative loop as long as the convergence is not reached.

2.3.3. Mesh generation techniques

In this subsection a short introduction in state of the art meshing techniques is provided. In particular, in this subsection the expression *grid* is used for description and explanation purpose. It is mentioned here that within this thesis there is no difference made between grid and mesh. Hence, both expressions are treated as equal.[56]

The reason, why it is required to build a mesh, is found in the way how the governing equations are discretized (refer to subsection 2.3.2.). Using the finite volume method the partial differential equations are solved in the cell-centers and the fluxes are computed via faces of these volumes. Since every flow problem contains a variety of flow features, such as vortices or high velocity gradients, the mesh has to be adapted to meet certain criteria to ensure a well defined flow problem. In such critical areas usually the mesh resolution has to be increased. In order to fulfil this demand several type of grid topologies have been established. Those will be briefly described in the following subsubsection.

Structured grids :

A structured grid consists of a set of coordinates and connectivities that are mapped into the elements of the describing mathematical (mesh) matrix. The adjacent points of a grid in the physical space are also the adjacent elements in the mesh matrix.[57] Structured grids are represented by a regular repeating pattern of quadrilateral elements.[58] Usually this type of meshes require a lot of user interaction in creating them, but it enables the user a high degree of freedom in controlling the quality of the generated grid. It is also possible to create a flow aligned grid which reduces the numerical diffussivity caused by the grid. Three major topological structures[59] for structured grids have been established as shown in Figure 2.15.

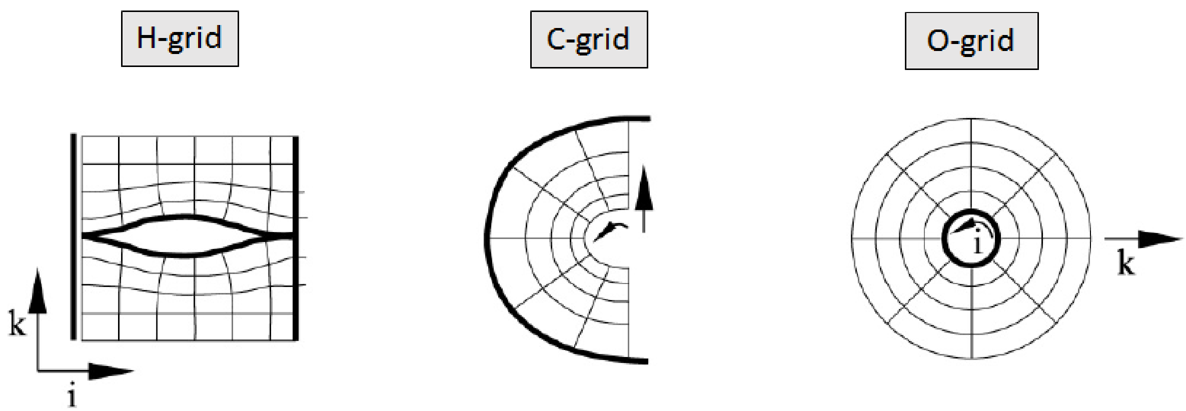

Figure 2.15.: Grid topologies for structured meshes, Source: external reference[59]

A certain type of structured grid is the so-called block-structured grid. It is a combination of several

[56] Cf. Thompson J. F., Soni B. K., Weatherill N. P. (1999) p. 8
[57] Cf. Thompson J. F., Soni B. K., Weatherill N. P. (1999) p. 20
[58] Cf. Schaefer M. (1999) p. 54
[59] Laurien E., Oertel H. (2013) p. 102

blocks of structured grids, such as H-grid, C-grid and O-grid, and it is used for rather complex geometries. The example of an exhaust manifold[60] geometry displayed in Figure 2.16. may give an idea about the possible complexity this grid type can handle. The highlighted lines mark the boundaries of each individual block. Due to the higher demand of user interaction to build these type of meshes they

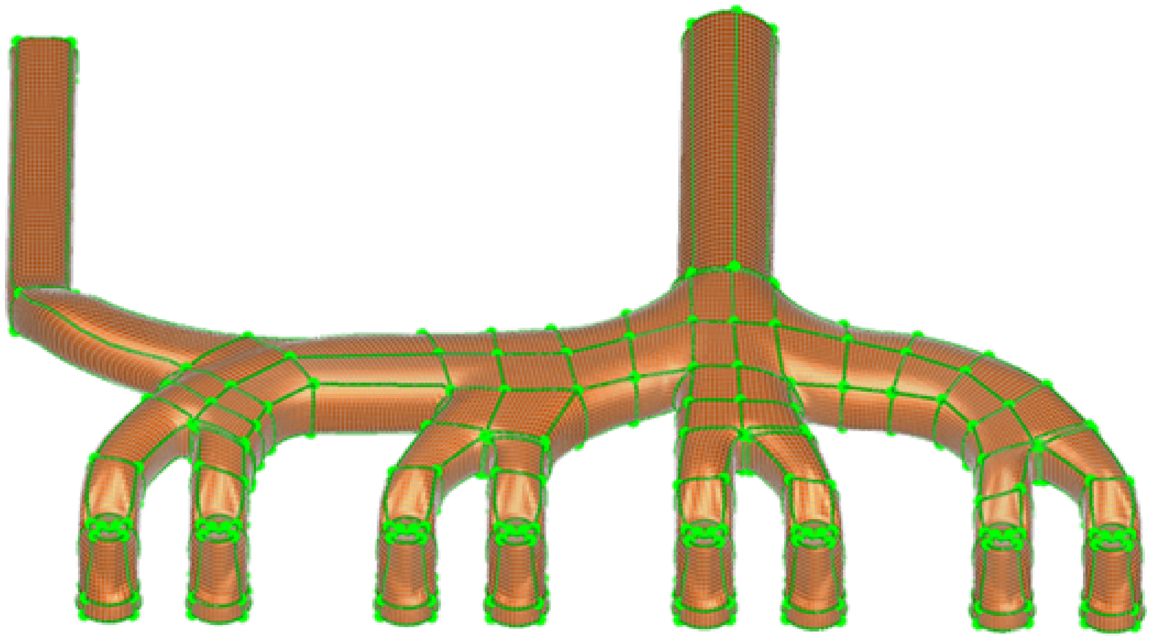

Figure 2.16.: Example of block structured mesh, Source: external reference[60]

are not further discussed in this thesis.

Unstructured grids :

The major difference between structured and unstructured grids is the form of the data structure that describes the grid, meaning the way the mesh matrix is written. For an unstructured grid the points cannot be represented in the same way like it is done in a structured grid. It is not possible that the adjacent points of a grid in the physical space are also the adjacent elements in the mesh matrix. Hence, additional information is required. For any particular grid point, also the connectivity to other points has to be defined explicitly in a so-called connectivity matrix.[61]

For better understanding a graphical represention is given in the following Figure 2.17. showing a cooling water jacket of a single cylinder research engine[62]. The tesselation, which means here tiling a surface by geometrical shapes, consists of triangulated elements with an irregular pattern. Triangles are the simplest way to describe volumetric elements, forming a tetrahedron volumetric cell. These elements are able to discretize any geometry of complex shape, and the most popular mesh technique is the *Delauny*[63] approach. This meshing technique produces almost equilateral triangles. Compared to structured grids, simulation results produced by unstructured grids and especially grids based on tetrahedron elements are less accurate. The numerical induced diffusion caused by these type of meshes is higher compared to other grid types. Comparable results are achievable, but usually by applying appropriate discretization resulting in higher computational effort.[64]

[60]Gsenger C. (2015) p. 25
[61]Cf. Thompson J. F., Soni B. K., Weatherill N. P. (1999) p. 21
[62]Cf. AVL List GmbH. (2010)
[63]Cf. Thompson J. F., Soni B. K., Weatherill N. P. (1999) p. 22
[64]Cf. Charlesworth D. J. (2003) p. 184

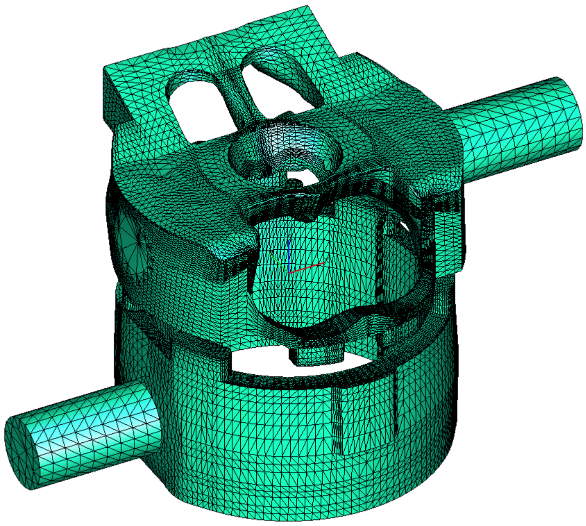

Figure 2.17.: Unstructured grid example, Source: own model, geometry from external reference[62]

Therefore, an alternative methode for meshing is that the tetrahedron based meshes can be extended to a so-called polyhedral mesh, an example is given in Figure 2.18. A common method to create

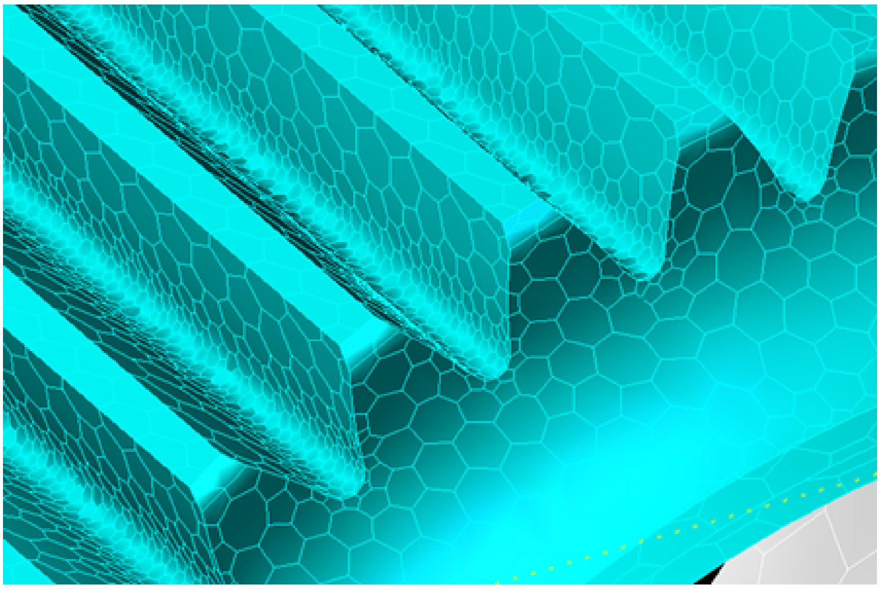

Figure 2.18.: Polyhedral grid example, Source: own model

polyhedral meshes is based on the Delauney-Voronoi dualism[65]. The procedure itself is based on the *principle of duality transform*, which shall be described briefly in the following sentences.
In this principle the input mesh, here referred as the *primal mesh*, will be transformed into a modified mesh, here referred as the *dual mesh*. The rule for this transformation[66] states that the vertices of the dual mesh have to coincide with those from the primal cell centers. The vertices of the tetrahedron mesh are defining a circumsphere that does not contain any other nodes of a tetrahedral mesh stated by the Delauney criterion (equilateral triangles).
The duality as shown Figure 2.19. and an edge of the Voronoi polygon is equidistant from the two points that separates it. This results in an perpendicular position to the connecting line of the two

[65]Cf. Thompson J. F., Soni B. K., Weatherill N. P. (1999) pp. 462-467
[66]Garimella R. V., Kim J., Berndt M. (2013)

points[67].

The great advantage of polyhedral cells is that they are surrounded by many neighboring cells.

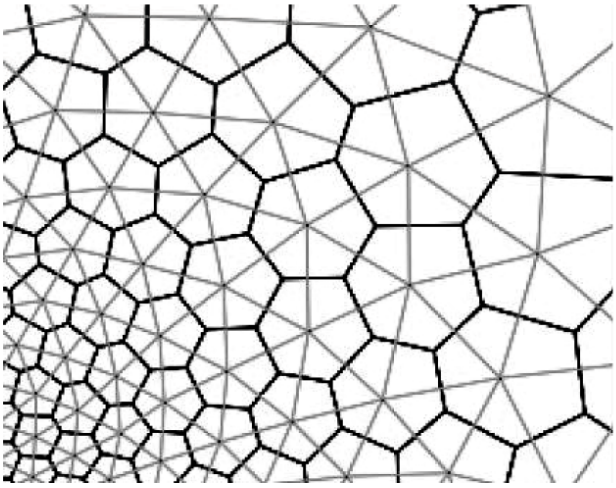

Figure 2.19.: Voronoi Diagram, Delaunay Triangulation and their Duality, Source: external reference[67]

Gradient approximation is therefore performed much better than with tetrahedral cells. Furthermore, polyhedral cells allow the same benefits in automatic meshing as tetrahedras, but overcoming their numerical disadvantages related to numerical diffusivity.[68] And regarding the proper wall treatment which has to be applied it is also possible to create any types and numbers of boundary layer on a polyhedral mesh.

2.4. Summary

In the present chapter the required background was built up in order to develop a better understanding for the actual engineering problem to be solved in this thesis. Furthermore, the physical fundamentals as well as the basics for the numerical implementation of the models into the CFD code AVL FIRE were provided. State of the art modelling and meshing techniques were also discussed and especially the importance of correct wall boundary modelling to obtain most accurate results from the simulation of heat transfer problems was outlined.

[67] Otero C., Díaz J. A., Togores R., Manchado C. (2006), p 251
[68] Cf. Peric M. (2004), p. 219

3. Simulation approach

This chapter outlines the selected approach for a CFD simulation workflow in general but especially for the thermal analysis using CFD in particular. The intention of the section *Introduction* is seen as additional information to describe the role of a turbocharger as an engine component in an entire engine development process. All other sections in the present chapter are dealing with the actual fundamentals related to the scope within this thesis.

3.1. Introduction

Due to increasing global competition it is important to reduce the product development lead time. In the past years the concept of so-called front-loading has become more and more visible in the automotive industry. The definition of front-loading states:

"Front-loading is defined as a strategy that seeks to improve development performance by shifting the identification and solving of problems to earlier phases of a product development process[69]".

If one applies this definition to the CAE world it means, that in the early stages of the conceptual and the design phases of a new product simulation is involved in the decision making process, even before any protoyping is done. The idea of front-loading in particular is fairly intuitive, as the sooner one is able to identify a problem, it can be isolated, assessed and solved more efficently and effectively.
To deal with the complexity of these systems some guidance is required, which is within the scope of systems engineering[70]. A well known methodical approach nowadays in systems engineering is the V-model[71]. Originally developed for the software development then adopted for complex mechatronic defense systems, the term V-model can be used in a broader sense and is already successfully applied as state of the art in other application fields[72].
The V-model is an expression applied to a range of models, starting from a conceptual model used to develop a simplified understanding of the complexity associated with systems development to a more detailled development of lifecycle models and project management models. It is seen as a macro-cyle which describes the necessary and logical sub-steps in the development of mechatronic systems. Starting at the system level with the system specifications on the top left and following a top-to-down methodology each part has to be finished before the next phase can start in the product development cycle.
The left hand-side of the V-model lists the system specifications and represents the decomposition of the requirements. The right-hand side represents the integration of the components and their validation.
It is not within the scope of this thesis to give a detailed explanation about the V-model, but a compressed explanation shall be outlined with the aid of Figure 3.1[73].

[69] Thomke S. , Fujimoto T. (2000)
[70] Kossiakoff A., Sweet W. N., Seymour S. J., Biemer S. M. (2011)
[71] VDI 2206. (2004)
[72] Cf. Potinecke T. W. (2009)
[73] Fritz J. (2013), p. 45

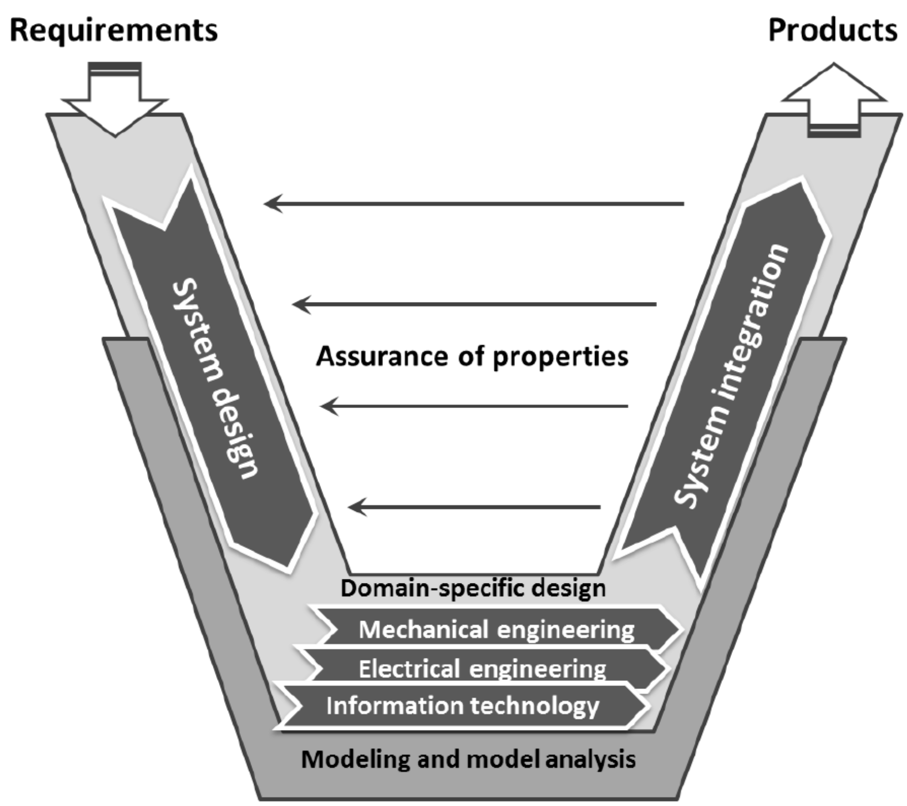

Figure 3.1.: The V-model, Source: external source according to Fritz[73]

According to VDI 2206[74] the V-model consists of the following main procedures:

Requirements: The starting point is set by an actual development order. The target has to be defined more precisely and described in form of requirements. These requirements are used as measure the final product is assessed against.

System design: Target is a cross-domain concept, describing the logical and physical properties of the designated product. The overall functionality of the product is split into sub-systems, including the classical task distribution between mechanical, electrical and electronic components, and the creation of synergies among other technical disciplines involved in this process. The performance of the individual sub-system is checked in the context of the entire system forming a solid basis for the domain specific design[75].

Domain specific design: In this part a more detailled analysis in the relevant domain takes place in order to ensure a reliable functionality of critical items. Each domain uses its typical tools and methodes to accomplish this target.

System integration: The results gathered from the domain specific design are combined and form the overall system in order to investigate the interactions among them.

Assurance of properties: The progress made within the process has to be checked continuously within the specified requirements. It has to be guaranteed, that the actual system properties meet the expecations of the desired system properties.

[74]Cf. VDI 2206 (2004), pp. 29-30
[75]Gausemaier J. (2008)

Modelling and model analysis: During all these previously mentioned phases analysis and simulation tools are involved supporting the investigation process of the system propierties.

Product: Usually a complex product is generated in several cycles, depending on the level of maturity of the product after each cycle.

Relevance for a CFD simulation workflow

As stated above, simulation in general and CFD simulation in particular has a vital contribution in design and optimization of dedicated components. Therefore, another model introduced by Bender[76] is used to specify briefly the role of the CFD simulation more precisely.
According to Bender a modfied V-model is used in the framework of a three layer model, introducing a system level, a sub-system level and a component level.

It has to be highlighted that the original three layer model from Bender, as shown in Figure 3.2, exists in a detailled and exhaustive explanation in german language. A very much compressed explanation shall be used here and is seen as sufficient in order to explain the contribution of CFD simulation at the component level. Similar to the V-model, the three layer model is starting at the system level with the specification of

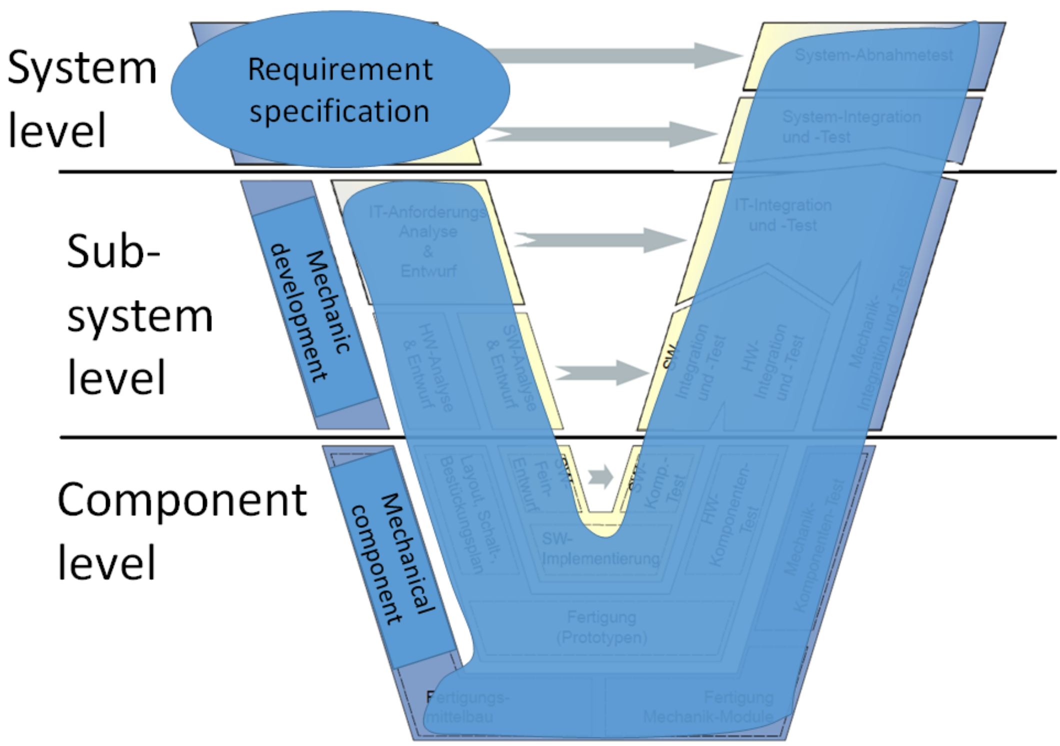

Figure 3.2.: The three layer model, Source: according to Bender[77] and modified

requirements for the development of the desired product. This includes also the product's main functionality as well as the interactions among the involved technical disciplines.
The next step is the separation into sub-systems and the assignment of the relevant disciplines such as mechanic development or information technology. The requirements have to be also transfered accordingly to the disciplines. Since the mechanic development is already able to act quite autonomously compared to the other disciplines in the sub-system level, only software and electronics (hardware) have to be further

[76]Bender, K. (2005), pp. 44-47.
[77]Bender, K. (2005), p. 45

separated.
Since software, electronics and other related disciplines are not within the scope of this thesis, they are not further considered here. The focus stays here on the component level and especially on the mechanical side as the turbocharger represents a classical mechanical component.
Virtual Functional Tests (VFT), in order to ensure that the actual component properties meet the expecations of the desired component properties, are required as the real component does not exist in hardware at this stage of development[78]. The VFT even states, that the existence of the component in hardware is not required[79], which means in the early stage of the development process simulation is a vital tool to ensure the prescribed requirements.
In other words, it allows to stay as long as possible on the left-hand side of the V-model to achieve the virtual approval for a component, as the technical maturity of the prototype is higher, resulting in less testing effort.

3.2. Basics of the CFD simulation workflow

Based on the fundamentals for the modelling of a fluid and heat transfer problem which were derived in section 3.2 in particular the CFD simulation workflow can be described as a series of steps. The basic classification of a CFD simulation workflow into

- Preprocessing - CAD data preparation, mesh generation and model setup.
- Simulation - The actual solution process.
- Postprocessing - Analysis and assessment of results.

is extended by a more detailled description in this chapter and is outlined in Figure 3.3.

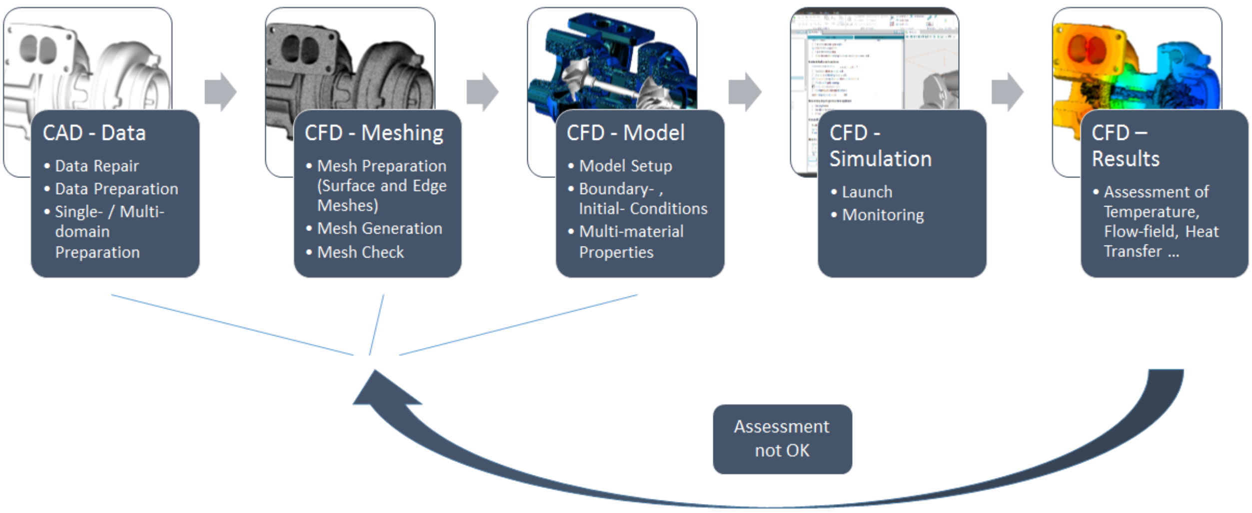

Figure 3.3.: General CFD Workflow, Source: own chart

[78]Bender, K. (2005), p. 55
[79]Bender, K. (2005), p. 56

The investigation is done on the turbocharger *S410 Euro4* of the automotive supplier Borg Warner Turbo Systems (BWTS). This type of turbocharger was chosen as it is the reference turbo charger for the engine category of commercial vehicles in AVL and is used for the charging of heavy-duty engines.

3.2.1. CAD - data

As a prerequisite for the automatic meshing process, it is crucial to provide a well prepared representation of the simulation domain, the so-called surface mesh. A very common file format for this kind of input data is the Standard Tessellation Language (STL), representing the surface data by triangular surface patches, which is also used in *Rapid Prototyping*[80]. An example is given in Figure (3.4).

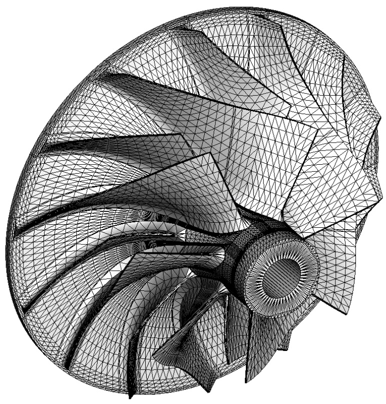

Figure 3.4.: Example surface in STL format, Source: own screenshot

An important request to this kind of input data is that the input surface must not contain any open regions, in other words the surface has to be *watertight*. Since the STL format can be generated by most of the CAD and CAE software packages available on the market, the preparatory work and surface repair is typically done already in the CAD software.
Under certain circumstances it may be required to perform the surface repair directly on the STL geometry, therefore in section 3.4.1 a possible tool is briefly described with special focus on the preparation of surfaces for multi-material and multi-domain simulation tasks.
This part of the workflow may not consist only of the repair works to be done on surface data, depending on the flow problem it is also necessary to consider simplifications in certain areas of the simulation domain. In advance knowledge about the expected solution of the flow problem is beneficial, because it allows already at the beginning of the workflow to set actions which can increase the efficiency and accuracy of the simulation and therefore reduce the lead time of a simulation task.[81]

3.2.2. CFD - meshing

Creating the CFD mesh is a set of activities starting already prior to the actual meshing process with preparation of regions on the input surface, for instance to apply local mesh refinement during the meshing process. An automated mesh generation process requires auxiliary data, such as edge meshes, in order

[80] Cf. Schulze G., Fritz A. H. (2008), p. 105
[81] Cf. Laurien et al (2013), p. 99

to provide sufficient information to the mesh generator of being able to create sharp edges and generate a suitable mesh for the simulation. The meshing process is briefly outlined in Figure 3.5:

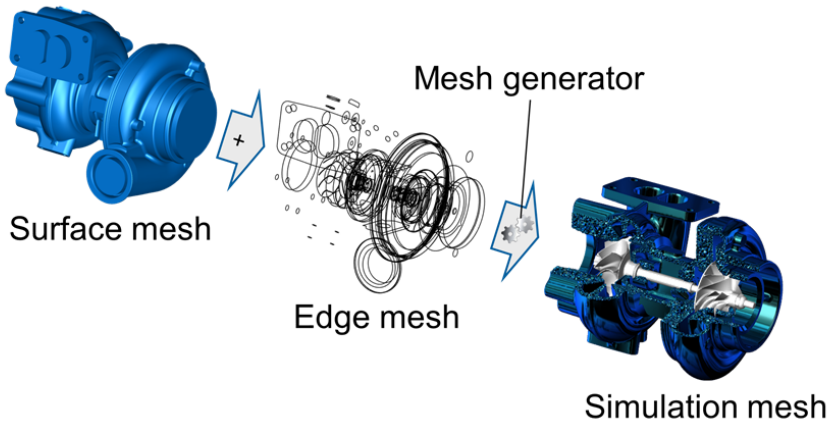

Figure 3.5.: Meshing process, Source: own chart

The actual preparatory work for meshing starts with the creation of so-called selections. A selection is a predefined area on the surface mesh, which is used for following purposes:

Local refinement: Applying local mesh refinement allows to resolve geometrical details in a proper manner. For instance small gaps in the simulation domain require a reduction of the overall cell-size locally. Marking such particular region of interest by creating a selection ensures that the local refinement is only applied in this specific location and the total number of cells is kept on a suitable level.

Boundary conditions: Boundary conditions in CFD problems are typically applied on outer surface patches. In order to reduce the effort in the model generation an advance knowledge of the location of the boundary conditon prior to the meshing process is beneficial but not crucial.

Initial conditions: It is recommended to create the regions for initial conditions also prior to the meshing process. Initial conditions in CFD problems are applied on the volumetric computational cell elements. State of the art meshing techniques ensure a proper transfer of the marked regions from the surface mesh to the volume mesh.

Material domains: A prerequisite for the meshing of a multi-material problem is to define the material domains already on the surface data. During the automatic mesh generation process the interfaces between the domains will be established automatically.

Rotating domains: Rotational domains, for instance the rotating impellers, require also their geometrical definition prior to meshing. Interfaces between rotating and steady parts of the geometry are created then automatically during the meshing procedure.

In the following Figure 3.6. an overview of some selections is given for graphical representation. Furthermore an auxiliary mesh is created, it is called edge mesh. The edge mesh is used to specify regions for the meshing process were in particular flow separation is expected or sharp edges need to be modelled. Figure 3.7 demonstrates on an example whether an edge is created or not.

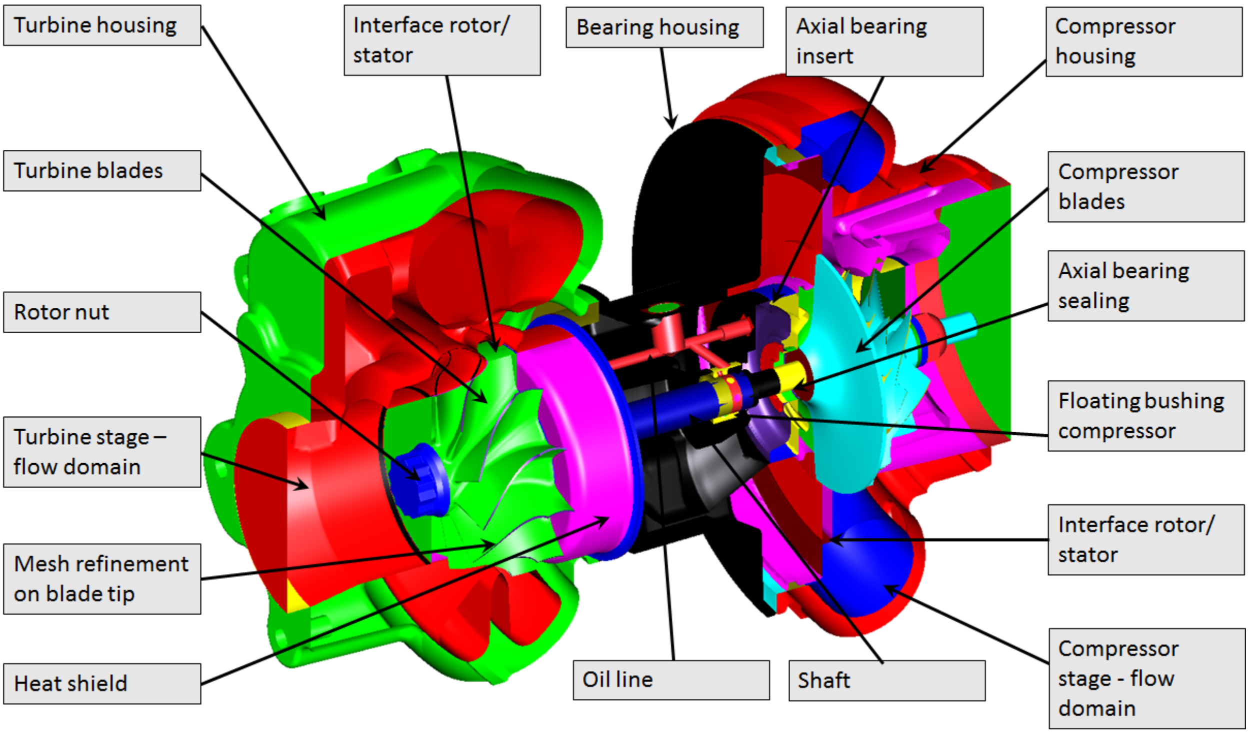

Figure 3.6.: Selections on Surface Mesh, Source: own model

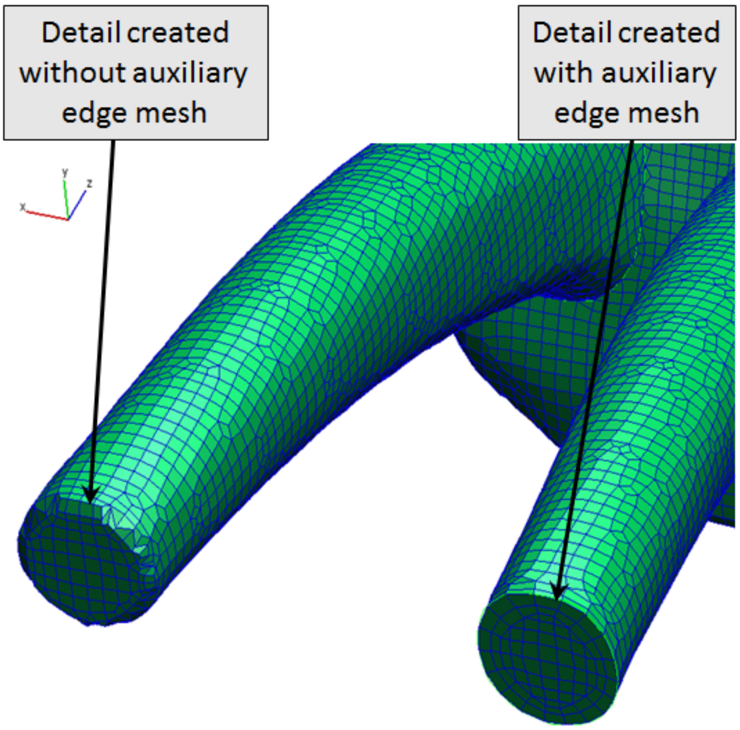

Figure 3.7.: Example for usage of an Edge Mesh, Source: own model

3.2.3. CFD - model

After the mesh generation process is finished the actual CFD model is build by applying all boundary and initial conditions to the volume mesh. It is basically the entire setup of the simulation prior to the launch. It consists of activities such as collecting boundary and initial conditions, input of material parameters and finally defining output quantities for the selected operating conditions.

3.2.4. CFD - simulation

After launching (starting) the simulation this involves all activities including the monitoring of the simulation run.

3.2.5. CFD - results

The term CFD - results is related to all activities starting from post-processing over reporting and finally it leads into the assessment of the results in terms of engineering outcome.

In case the assessment of the results is not satisfying, depending on the detected deficits the process hast to be repeated by

- Modification of CAD model,
- Repeat the meshing process,
- Update of boundary, initial conditions or modifying the material parameter.

3.3. Modelling of heat transfer problems

For advanced thermal analysis accurate boundary conditions are required. Especially the spatial distribution of heat transfer coefficients and fluid temperatures are important. In terms of modelling of conjugate heat transfer (CHT) problems which are related to CFD, FIRE offers three modelling approaches. An overview with the major features is provided in Figure 3.8. Considering the historical order of implementation into the FIRE code, the very first approach is named CFD-FEA interface or CFD-FEA coupling and it is an offline interface to any third party Finite Element Analysis (FEA) software.[82]
The second approach, which is capable of simulating multiple domains, is named *AVL Code Coupling Interface* (ACCI).[83] It allows to couple fluid-structure interaction by establishing a co-simulation among the participating domains. The third modelling approach uses a multi-material capability, establishing a close coupling of the participating domains within one single simulation setup. Since the new multi-material capability is scope within this thesis, it is described more detailed in Section 3.3.2.

[82] Cf. AVL List GmbH. (2014) Sept. 30, pp. 121-155
[83] Cf. AVL List GmbH. (2014) Sept. 30, pp. 47-120

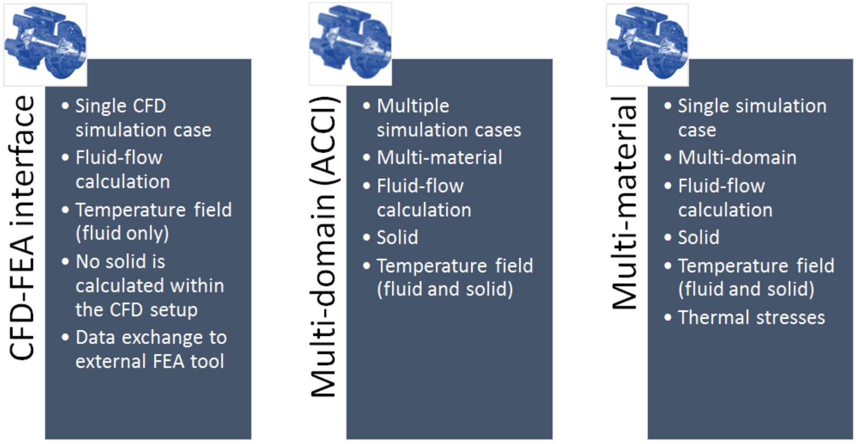

Figure 3.8.: Overview of heat transfer modelling approaches, Source: own chart

3.3.1. Classical modelling approaches

This subsection describes the two classical coupling approaches for heat transfer problems related to CFD. The CFD-FEA coupling and the ACCI coupling are briefly described and in addition application examples are given.

3.3.1.1. CFD-FEA coupling

The CFD-FEA coupling module allows the exchange of data between the CFD software FIRE and structural analysis tools based on the Finite Element Method (FEM), which are participating in CFD-FEA thermal coupling problems. The main features are[84]:

- Mapping result data from CFD boundaries on FE shell meshes, hence delivering boundary conditions to the FEA.
- Mapping FE wall temperatures on CFD, hence receiving wall boundary conditions from FEA (transient, steady, time-averaged).
- Averaging and mapping of several steady-state calculation results on FE shell meshes.
- Heat transfer coefficients and fluid temperature can be written in common FEA formats.
- FE shell meshes and CFD volume meshes do not require to reference to the same co-ordinate system, a transfer matrix can be applied.

The mapping process itself is an exchange of fluid-solid interface data between CFD and FEA and the exchange is accomplished via an external file exchange. Thus, this coupling is an offline coupling and to get a better understanding it is outlined in Figure 3.9.

After mapping the heat transfer coefficient and the near wall fluid temperature to the FE shell mesh, the data are used in the FEA tool for further processing. For instance, this simulation workflow is used for a fluid structure coupling of a head and block compound simulation in the thermal analysis of a cylinder head and block. As shown in Figure 3.10. for graphical representation, the entire thermal analysis is based on an

[84] AVL List GmbH. (2014) Sept. 30, p. 121

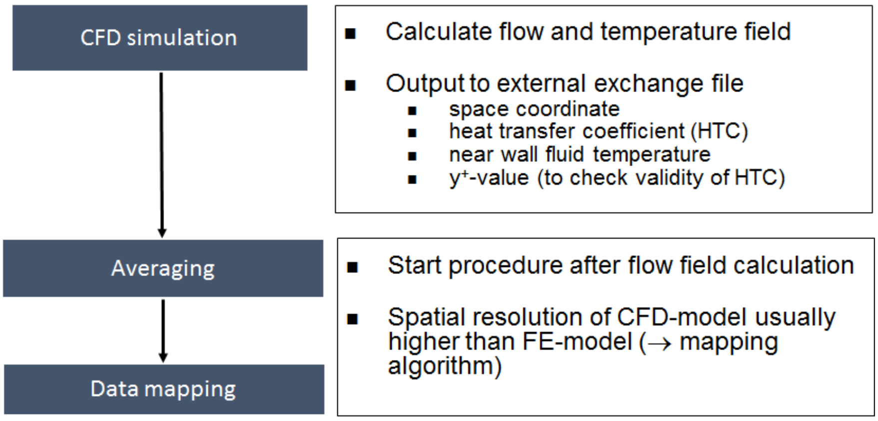

Figure 3.9.: Mapping procedure in CFD-FEA coupling, Source: own chart

iterative process.

The iteration loop starts with the simulation of the flow and temperature field in the water cooling jacket based

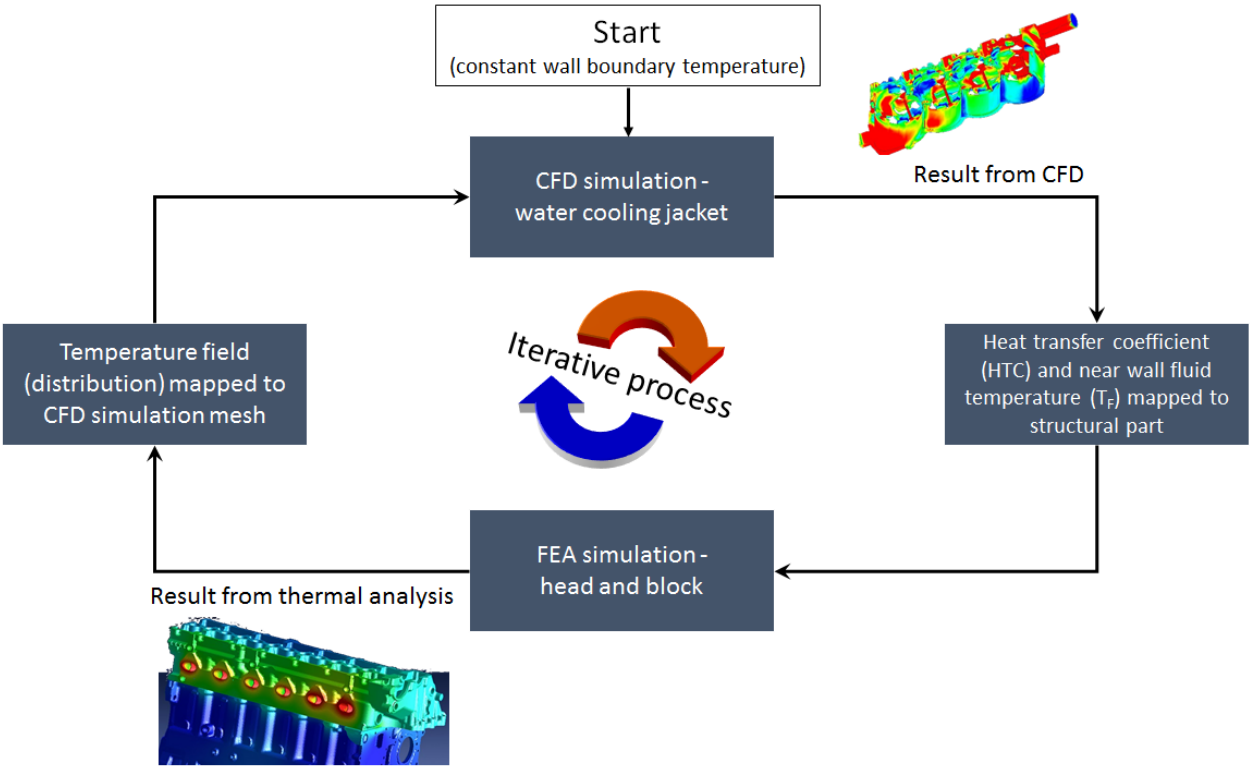

Figure 3.10.: Thermal analysis of an engine cylinder head and block, Source: own chart

on constant wall boundary temperatures. The simulated spatial distribution of the heat transfer coefficient and the fluid temperature near the wall is provided from CFD to the FEA tool. This procedure is called mapping and its basic principle was shown earlier in Figure 3.9.

Applying the CFD results as boundary conditions to the FEA, the FEA simulation calculates the temperature field in the entire structural part of the cylinder head and block. At the end of the first loop, the wall temperature distribution from FEA is further mapped back to the CFD and serves as boundary condition for the next iteration loop. Sufficient accuracy of the calculated heat fluxes and heat transfer coefficients is usually reached after one to two iteration cycles.

In a similar way the heat transfer coming from the gas-side (in-cylinder combustion simulation) is provided to the FEA tool.

The increasing demand for simplification of simulation workflows in order to make the component development process more efficient leads to the next level in simulation approaches. In particular to the thermal analysis of a cylinder head and block but also in general to a thermal analysis of components the trend goes towards co-simulation, as very often more than one simulation tool is involved, for instance here a CFD and a FEA tool. Following the need for a next level simulation tool, the features of a co-simulation interface is explained in the next subsection.

3.3.1.2. Multi-domain simulation via code coupling interface - ACCI

Coupling of simulation codes using the AVL Code Coupling Interface[85] (ACCI) allows to establish a co-simulation between two or more FIRE simulation cases or other simulation codes. A typical example is a conjugate heat transfer problem accomplished with the coupling of a CFD simulation and a solid heat transfer simulation.[86]
Both the CFD simulation and the solid simulation are set up as separate simulation cases. In general, the exchanged data are values from boundary conditions at the surface or at parts of the surface and source terms, such as mass, momentum and energy, in the volume or in parts of the volume of the respective simulation domains.[87]
The exchange of data is done:

- in steady mode at each iteration,
- in transient mode each coupling timestep, which may be larger than the timestep used in the coupled simulation cases.

In general, mesh related quantities, such as pressure or velocity at cell-centers or bounary face-centers as well as non-mesh related quantities can be exchanged. Non-mesh related quantities can be for example generalized material data or Lagrangean particles.[87]
The coupling itself in FIRE is performed by a separate software module. This is the actual AVL Code Coupling Interface. Basically it can also be integrated in any other simulation software. Therefore the module provides the following functionality:

- Data transfer and buffering between the different processes,
- Time control and synchronization of the processes,
- Mapping of data between different meshes, including moving mesh topologies.[88]

The data transfer is based on the TCP/IP protocol where the coupled simulation processes may all run on different clients, as long as they are in the same network. The FIRE solver simulations in particular fully support also Message Passing Interface (MPI) capability.
The ACCI module allows a coupled simulation of an arbitrary number of participating processes, the so-called clients, which exchange an arbitrary number of quantities, called attributes, at an arbitrary number of geometric locations, called interfaces. Hence, the basic concepts in ACCI are clients, interfaces and attributes, all identified by different names, called ID.
The exchange frequency of the clients that provide and request a specific attribute at a specific interface

[85] Cf. AVL List GmbH. (2014) Sept. 30, pp. 47-120
[86] Cf. Schaefer K. H. (2016)
[87] AVL List GmbH. (2014) Sept. 30, p. 47
[88] Cf. Edelbauer, W. , Suzzi, D. (2006)

have to match. However, ACCI allows to mediate between different time-step-increments in different clients in a way that it basically buffers any exchange-data sent by a client and delivers them when requested by another client.
The code coupling module in FIRE consists of three different software layers as shown in Figure 3.11. for better understanding:

- The Communication Layer (ACI) at the lowest level,
- The Application Layer (ACCI), which provides all the basic functionality for co-simulations,
- The FIRE-ACCI Interface.

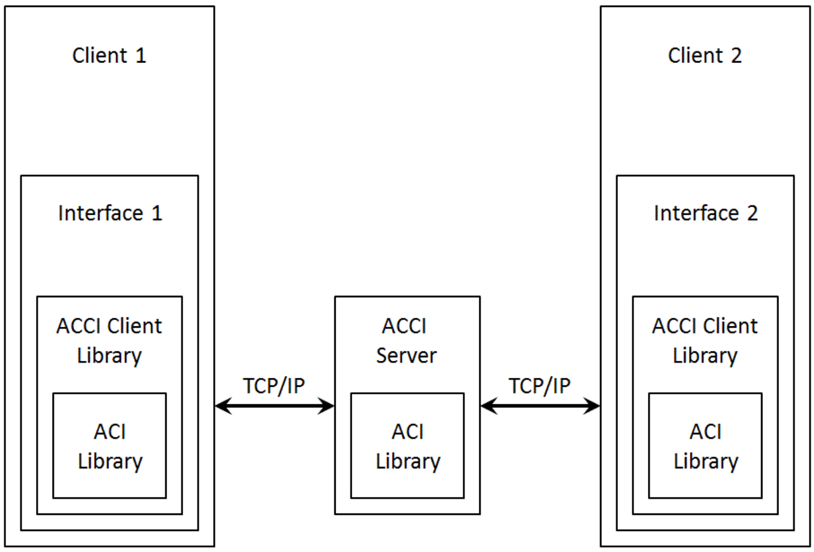

Figure 3.11.: ACCI coupling protocol, Source: own chart

Attributes can be any type of data such mixed strings, integer, real numbers, arrays etc., for instance pressure or temperature fields represented by values at the elements or nodes of a corresponding geometric mesh. A client may implement and support an arbitrary number of attributes, identified by their different names.

If clients exchange a specific attribute, they have to agree on a common meaning, e.g. treat both quantities as a temperature field or a velocity field. In case of non-mesh related data they must also agree on a common structure of these data, e.g. sending first a string-id, then a number of real values etc.

The technical realization of such data transfer via attributes is visualized in Figure 3.12., exemplary chosen for a CHT problem between fluid and solid. Due to requirement for numerical stability and to reach a good convergence behavior of the coupling, the solid domain starts with sending the attribute of the wall temperature. At the same time the fluid domain is sending the heat transfer coefficent to the solid domain. On the other hand the fluid receives the wall temperature and the solid receives the heat transfer coefficient. The common interface is build by the overlapping area between the two domains. The mesh resolution at the interface is different on either side of the interface as each of the domains is executing its simulation task on its own mesh. The fluid solves the mass, momentum and energy equation and the soldid solves the energy equation only.
ACCI was designed to provide a high degree of flexibility which allows to configure different coupling scenarios during run time, without having to change anything in the client code. It allows, for example, to specify

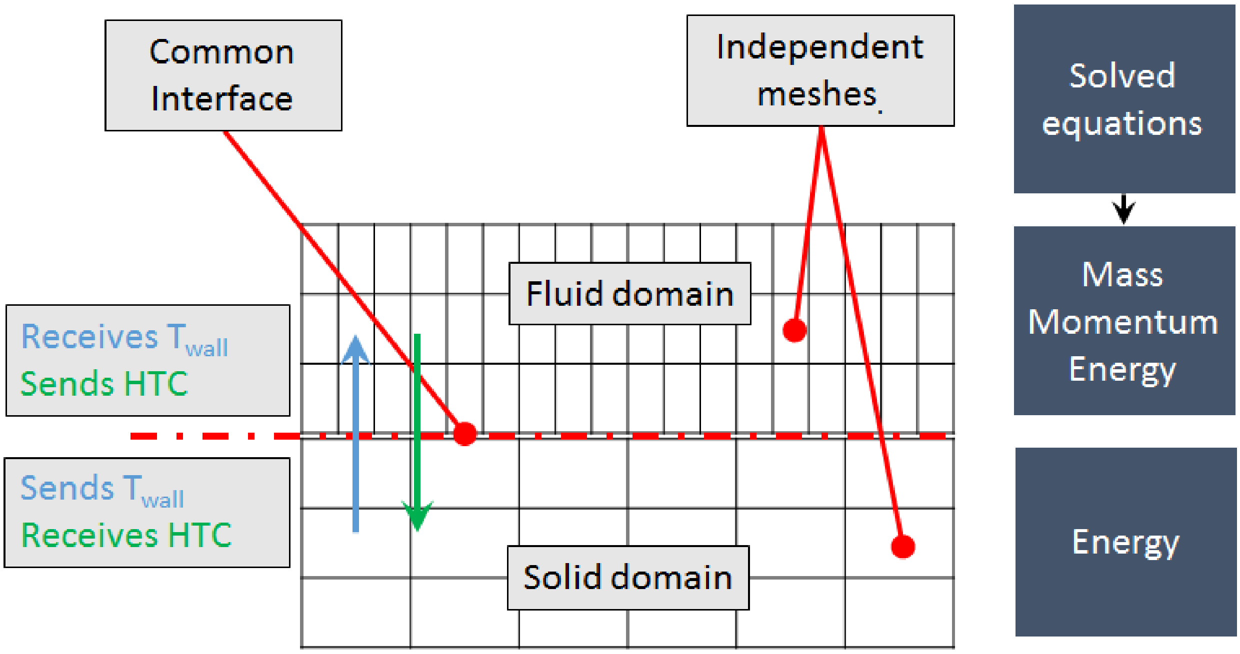

Figure 3.12.: ACCI coupling principle, Source: own chart

a thermal FIRE-FIRE-coupling at some surfaces for one simulation and to specify a flow-coupling in an overlapping volume-part for another, without having to change anything in the FIRE code. In this regard a fully coupled fluid-structure analysis was accomplished for the purpose of a quenching simulation[89]. Quenching is a common heat treatment technique used in the automotive or aerospace industries to minimize undesired thermal deformations which may lead to distortion or even to cracking of casted parts.
The Figure 3.13. provides a better understanding of the ACCI approach exemplary explained on the quencing process. It shows the simulation results of a quenching process which predicts the cool down-process of a casted cylinder head after dipping it into liquid oil (cooling fluid). In the left part of the picture, the oil vapor volume fraction during the quenching of a cylinder head is displayed. In the right part of the picture the corresponding coupling processes are shown. As shown, the ACCI coupling requires for a simulation problem that consists of two simulation cases (fluid and solid), in total three processes. The ACCI server (Process 2) manages the data exchange between the simulation cases (Process 1 and Process 3).
ACCI became also of relevance for the dynamics of the heat transfer in turbochargers as denoted by Schaefer[90]. With the availablity of the multi-material capability in the new simulation tool FIRE M, the opportunity arises now for a further optimization of the thermal analysis on the component level. This is discussed in the next subsection, exemplary demonstrated on the thermal analysis of turbocharger components.

3.3.2. Multi-material approach

As outlined in the previous section, a method to setup and analyse conjugate heat transfer problems (CHT) is either to perform an offline coupling via file exchange or calculate different computational domains separately by submitting one executable code for each calculation domain and exchanging the data via the so-called coupling server. Especially CHT, as part of the general multi-material or multi-physics tool chain, plays an important role in this field. Hence, a new sophisticated approach was developed and implemented in FIRE

[89] Kopun, R.; Skerget L.; Hribersek M.; Zhang D.; Edelbauer W. (2014)
[90] Schaefer K. H. (2016), p. 18

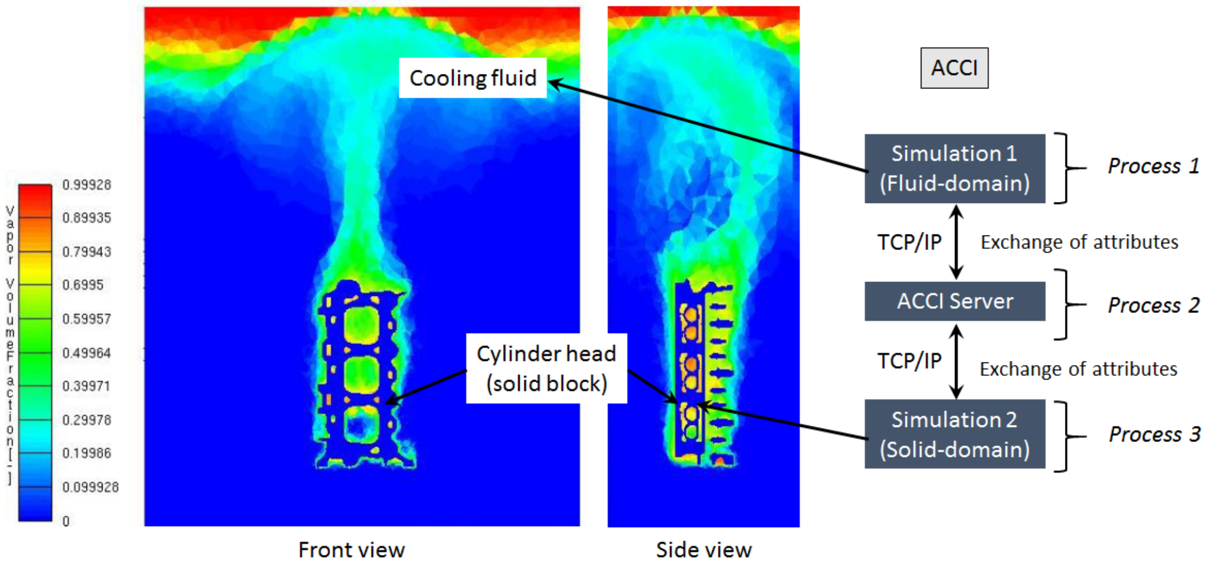

Figure 3.13.: Application example of ACCI coupling, Source: own chart

M, allowing the calculation of different domains within one simulation run by submitting only one executable code.

In other words, a multi-material simulation is only one calculation run with a computational mesh, consisting of conform connected domains. In Figure 3.14. one can see the basic coupling principle.

The solution method (numerical procedure) is based on the fully conservative finite volume approach as

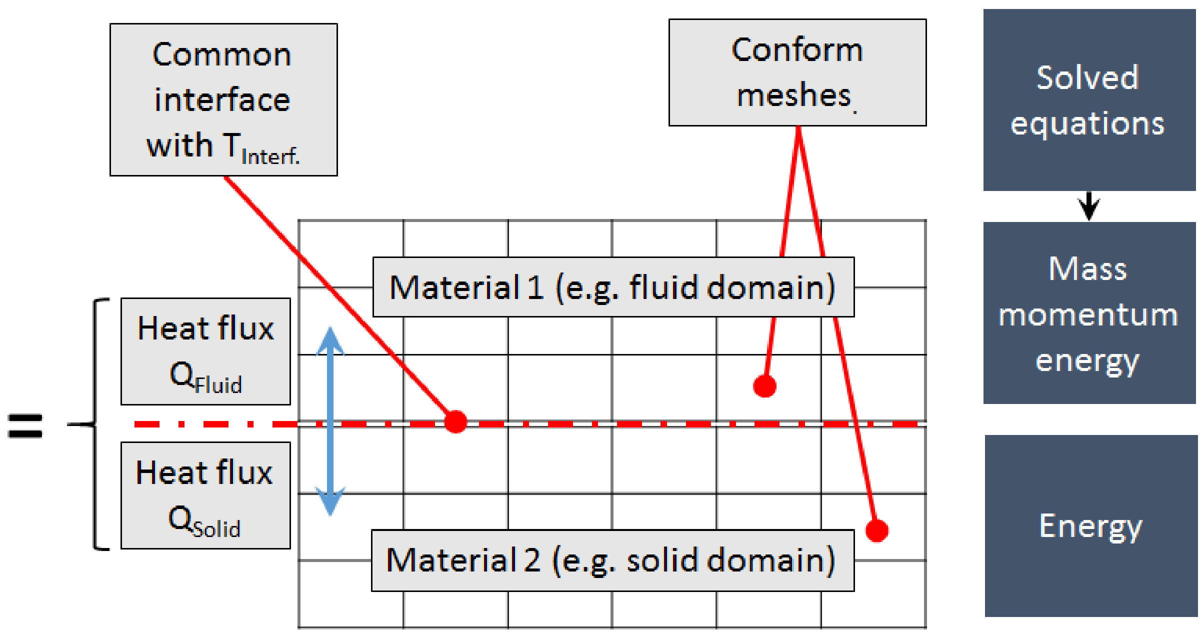

Figure 3.14.: Multi-material coupling principle, Source: own chart

described in section 2.3.2. All related variables, for instance momentum, pressure, density, turbulence quantities as well as enthalpy and temperature are calculated at the cell center. The interpolation schemes for the calculaton of the gradients and cell-face values and the cell-face based connectivity are implemented in such a way to handle an arbitrary number of cell faces which accomodates to polyhedral mesh structures provided by state of the art meshing techniques[91].

[91] Cf. Basara B. (2004), pp. 377-407

To develop a better understanding of Figure 3.14. it is necessary to look at the the mathematical modelling. It is based on a second-order midpoint rule for integral approximation and a second order linear approximation for any value at the cell-face. According to Basara[92] the cell-face gradient can be written as

$$\nabla\phi_j = \overline{\nabla\phi_j} + \frac{\overrightarrow{A}_j}{\overrightarrow{A}_j \cdot \overrightarrow{d}_j}\left[(\phi_{P_j} - \phi_P) - \overline{\nabla\phi_j} \cdot \overrightarrow{d}_j\right] \tag{3.1}$$

ϕ_j / kg^{-1}	Intensive transferable property
$\overrightarrow{A}_j$ / m	Surface normal vector of face element A_j
$\overrightarrow{d}_j$ / m	Vector between cell centers P, P_j

The face gradient $\overline{\nabla\phi_j}$ can be either calculated by linear interpolation or arithmetic averaging according to the solver manual[93]. The basic structure of a polyhedral mesh is displayed in Figure 3.15. showing two adjacent polyhedral cells P, P_j connected via a common face element A_j. Furthermore, a diffusion term has

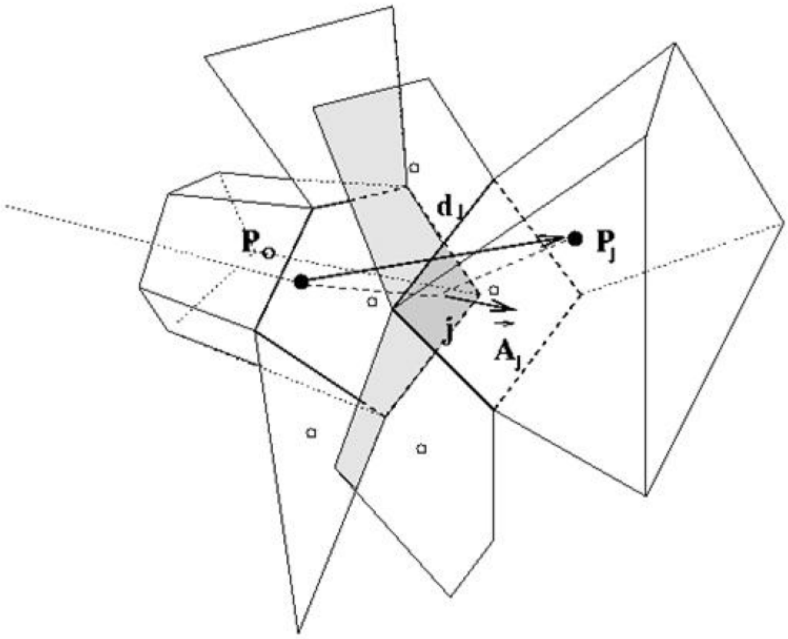

Figure 3.15.: Control volume of a polyhedral mesh, Source: external source[92]

to be incorporated into the surface integral source. The cell face diffusion flux at the computational face is given then by[94]

$$D_j = \bar{\Gamma}_{\phi j}\frac{A_j^2}{\vec{A}_j \cdot \vec{d}_j}\left(\phi_{P_j} - \phi_P\right) + \underline{\bar{\Gamma}_{\phi j}\overline{\nabla\phi}_j \cdot \left(\vec{A}_j - \frac{A_j^2}{\vec{A}_j \cdot \vec{d}_j}\vec{d}_j\right)} \tag{3.2}$$

Γ_{ϕ_j} / s^{-1} Diffusion flux

This diffusion flux is split into two main parts, were the left term denotes the normal-diffusion and the right term (underlined) denotes the cross-diffusion. The cross-diffusion (right term) part vanishes on orthogonal grids, which is also the case for polyhedral meshes. The remaining normal-diffusion is introduced as surface source term in the numerical procedure. This fact becomes vital in terms of multi-material calculations when for instance cell-center P, P_j belongs to the fluid domain and cell-center P_j belongs to the solid domain.

[92]Basara B. (2004), p. 384
[93]Cf. AVL List GmbH. (2014) Feb. 28, section 3.2.2.3.2
[94]Basara B. (2004), p. 384

Then the heat fluxes from either side become equal, $Q_{Fluid} = Q_{Solid}$, and one can recalculate the temperature T_{Interf} at the interface between fluid and solid domain. The overall solution procedure is finally based on the iterative *SIMPLE* algorithm as described in section 2.3.2.

The multi-material approach in general becomes relevant for applications dealing with conjugate heat transfer problems. The basic implementation was demonstrated by Basara et. al.[95]. Another example for a successful application is the quenching of cased aluminium parts[96].

3.4. Relevance for model setup of a turbocharger

The thermal simulation of turbocharger components in CFD is part of a bigger simulation tool chain. The typical targets for CFD simulation within the turbocharger development process are not only fluid flow problems. The thermal investigation specifically is providing accurate thermal boundary condition for thermo-mechanical fatigue analysis.[97]
Therefore, this section is divided into two subsections summarizing the input and setup data for the CFD part and the coupling to the structure analysis tool separately.

3.4.1. CFD - model input data

The procedure explained here starts with the actual generation of the mesh and it is accomplished with the automated meshing tool named *FAME Poly* which is part of the software package *AVL FIRE M* in the used version *R2017*. The preparatory work prior to meshing was explained in section 3.2.1.
The main topology of the mesh consists of polyhedral elements. In order to apply the appropriate treatment of the wall boundaries, the structure of the boundary layer is based on hexahedron elements. The complete mesh statistics is given in Table 3.1.

Avg. cell-size at the surface	1 mm
Avg. cell-size in the volume	3 mm
No. of solid domains	13
No. of fluid domains	2
Total no. of domains	15
No. of rotating domains	2
No. of hexahedron cells	200000
No. of polyhedral cells	7000000
Total number of elements	7200000

Table 3.1.: Mesh statistics of the created multi-material mesh

The meshing procedure was performed on a 2 x 8 core *Intel(R) Xeon(R) CPU E5-2640 v3 @ 2.60GHz* based workstation equipped with a memory of 64 GB RAM and running with the *Linux* operating system *version 2.6.32-642.11.1.el6.x86_64 (Red Hat 4.4.7-17)*. The CPU time for the meshing process on this particular platform is given with 2460 sec. In order to continue with the setup, no further manual mesh decomposition

[95] Basara B., v. d. Meer A. J., Diemath A. (2009)
[96] Kopun, R.; Skerget L.; Hribersek M.; Zhang D.; Edelbauer W. (2014)
[97] Cf. Bukovnik S., Diemath A., Offner G., Smolik L. (2017), pp. 1-11

in different domains is required as it is the case in the multi-domain (ACCI) approach. The final volume mesh is displayed in Figure 3.16.

After the mesh generation process is finished the actual CFD model is build by applying all boundary

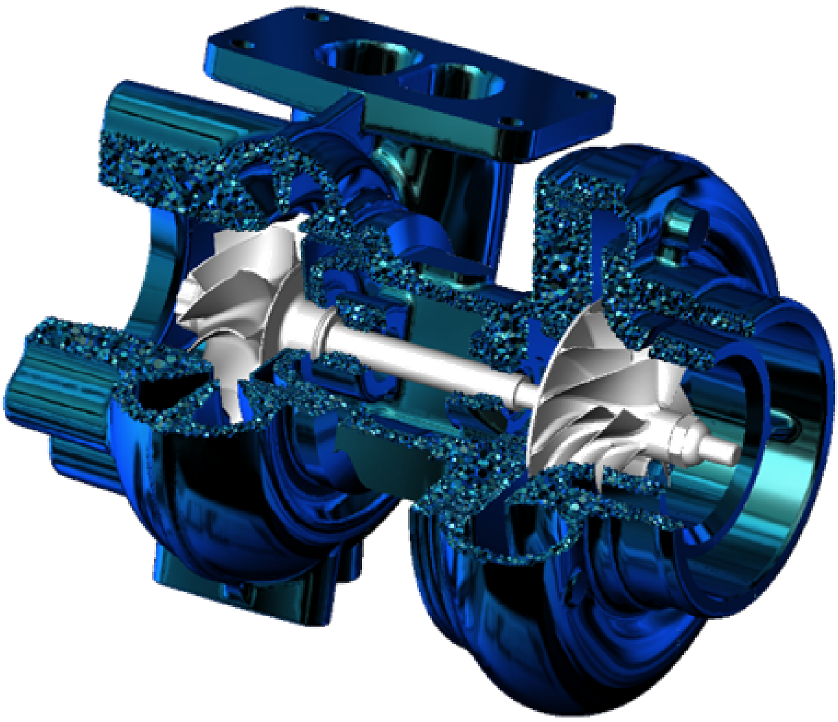

Figure 3.16.: Final volume mesh, Source: own model

and initial conditions to the volume mesh. Furthermore, the material and fluid properties for the relevant material are listed in Table 3.2. and are in accordance to the turbocharger manufacturer. All fluid and material properties are taken from the internal data base of *FIRE M*.

The fluid property of the exhaust gas (EGR) on the turbine side is represented by prescribing the composition of the EGR at the turbine inlet. EGR is initialized also in the entire turbine stage. The EGR produced by a Diesel engine is a composition represented in Table 3.3. by following species:

The following operating points have been considered in this study starting with the turbine side listed in Table 3.4. On the compressor side the flow conditions are listed in Table 3.5. A summary for all initial conditions is given in Table 3.6. The relevant material in FIRE M is adressed by their corresponding number.

And finally the wall boundary conditions are assigned to the relevant region of the simulation domain. In order to develop a better understanding of the situation the wall boundaries are displayed using the graphical representations of Figure 3.17. Those regions which are not related to a certain selection are assigned automatically to an adiabatic wall boundary condition in the FIRE code.

Since all external wall boundary conditions are exposed to the same environment, the convection and radiation boundary input data are summarized in Figure 3.18.

Material	Name	Property
Material 1	Turbine flow domain	EGR
Material 2	Turbine housing	GJS
Material 3	Bearing housing	GJL
Material 4	Heat shield	X6CrNiTi1810
Material 5	Turbine rotor	Inconel 718
Material 6	Compressor housing	GJS
Material 7	Compressor rotor	AlCu2Mg1.5Ni
Material 8	Shaft	GJS
Material 9	Compressor nut	GJS
Material 10	Axial bearing insert	GJS
Material 11	Axial bearing sealing	GJS
Material 12	Compressor fluid domain	Air
Material 13	Floating bushing compressor side	Bronce
Material 14	Floating bushing turbine side	Bronce
Material 15	Oil line	Shell 5W30

Table 3.2.: Material and fluid properties

Species	Mass fraction
CO2	0.2069 -
H2O	0.0749 -
N2	0.7182 -

Table 3.3.: EGR composition

Loadpoint	Inlet pressure	Inlet mass flow
40200 rpm	122630 Pa	0.1315 kg s^{1}
60500 rpm	153220 Pa	0.2120 kg s^{1}
80700 rpm	210950 Pa	0.3297 kg s^{1}
90700 rpm	254390 Pa	0.3995 kg s^{1}

Table 3.4.: Load conditions for CFD - turbine stage

Loadpoint	Outlet pressure	Outlet mass flow
40200 rpm	123400 Pa	0.1709 kg s^{1}
60500 rpm	167400 Pa	0.2392 kg s^{1}
80700 rpm	241800 Pa	0.3551 kg s^{1}
90700 rpm	298800 Pa	0.3957 kg s^{1}

Table 3.5.: Load conditions for CFD - compressor stage

Material	Temperature	Pressure	TKE	TLS
Material 1	600 °C	100000 Pa	1 m^2/s^2	0.001 m
Material 2	500 °C	-	-	-
Material 3	175 °C	-	-	-
Material 4	500 °C	-	-	-
Material 5	500 °C	-	-	-
Material 6	20 °C	-	-	-
Material 7	35 °C	-	-	-
Material 8	20 °C	-	-	-
Material 9	20 °C	-	-	-
Material 10	35 °C	-	-	-
Material 11	20 °C	-	-	-
Material 12	20 °C	123400 Pa	1 m^2/s^2	0.001 m
Material 13	20 °C	-	-	-
Material 14	20 °C	-	-	-
Material 15	20 °C	100000 Pa	0.375 m^2/s^2	0.001 m

Table 3.6.: Initial conditions

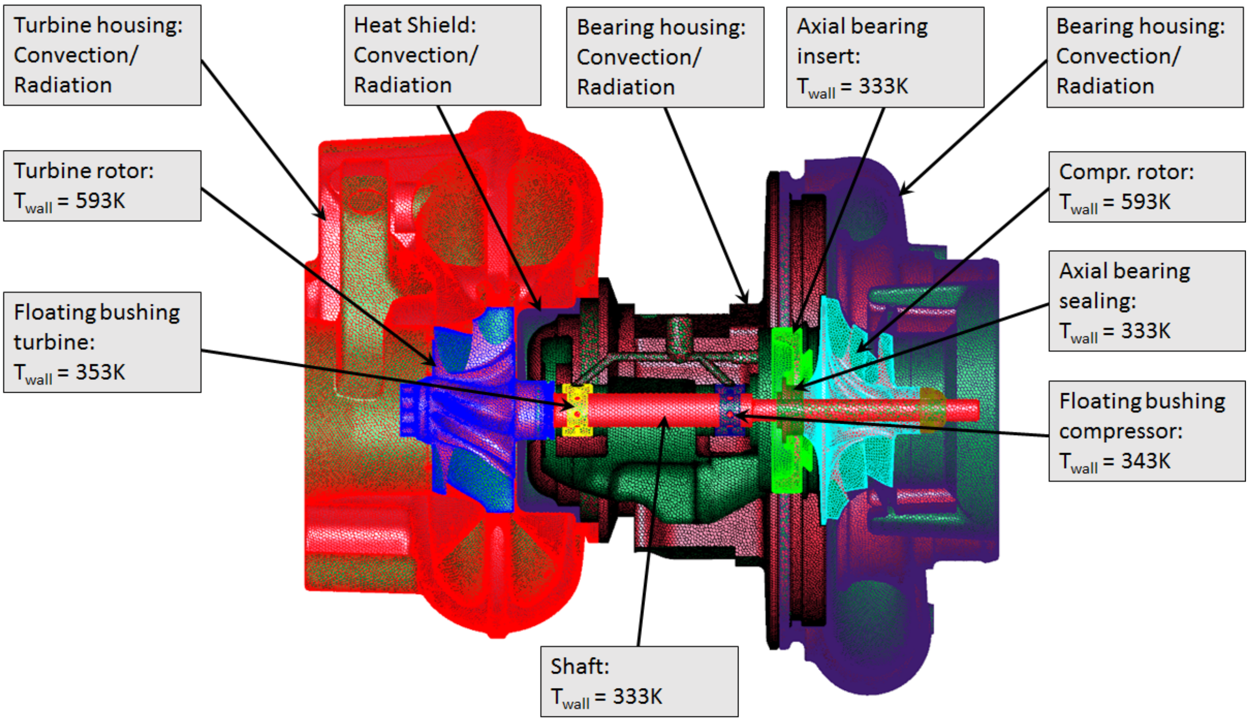

Figure 3.17.: Thermal wall boundary conditions overview, Source: own model

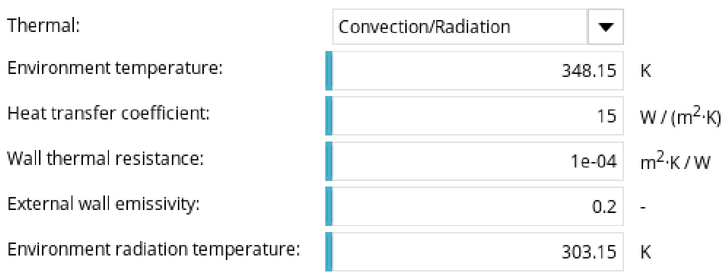

Figure 3.18.: Input data for convection and radiation boundary condition, Source: own model

3.4.2. Coupling data to FEA

Small changes of bearing surface temperature, clearance and bearing profile can change bearing stiffness and damping characteristics. This may influence the dynamics, especially the rotor radial deflection. NVH or durability issues like rotor colliding with housing may be generated as a consequence. In the referenced article[98] a new methodology for dynamic turbocharger investigation is described. It considers multi-body dynamics (MBD) of flexible rotor and housing structures coupled with elasto-hydrodynamics (EHD) of the inner and outer oil film. The energy equation for the calculation of the oil film temperature is considered in EHD using thermal boundary condition obtained from 3D CFD simulation. As earlier mentioned the CFD simulation within the turbocharger development process is related to flow and thermal investigation as well as specifically providing accurate thermal boundary condition for thermo-mechanical fatigue analysis. The bearing profile under thermal load is derived from Finite Element analysis and based on the same thermal boundary conditions as well, which were delivered from CFD. A short introduction into this methodology shall be given here.

Figure 3.19 shows a schematic representation of a typical turbocharger model, which is used also in the referenced article. The major components, which need to be considered, are the housing and the rotor, which itself is supported by two bearings. Each bearing consists of an inner and an outer oil film and a floating bushing. Inner and outer oil film are connected via six drillings in the bushing, respectively. Accordingly the mathematical sub-model need to be considered, which are interconnected, respectively. Since this kind of modelling is not scope within this thesis, details of the sub-models as well as their coupling are provided in the article which was also written by the author of this thesis.[99]

As turbocharger can operate at very high temperatures the heat that is spreading from the turbine side through the structure to the oil film might influence the temperature of the oil. In addition, due to the rotation of the rotor and floating bushing there will is heat generated in the oil film due to viscous friction. This heat is dissipated to the surrounding structure but it also heats up the oil. AVL EXCITE simulation tools offer the possibility to calculate energy equation of the oil film. With this approach it is possible to obtain the correct temperature distribution within the oil film and by this a correct oil viscosity. Boundary condition for the energy equation of the oil film is the structure temperature. This temperature is not uniform but it is strongly influenced by the heat coming from the turbine side and by cooling effect of the cold air at the compressor side.
The best approach for obtaining the structure temperature distribution is to use the results from 3D CFD calculation that is fully coupled fluid-structure interaction where both domains are modelled within the same tool. The temperature profile applied as boundary condition at both compressor and turbine side is shown in the Figure 3.20. The data exchange is provided from CFD via an external file.
Refering to Figure 3.20 right hand side a subgrid is created in order to specify data points for the transfer, the so-called mapping process. As this procedure is an offline coupling the temperature of the relevant grid point is written to a simple text file. The structure of the file can be seen in the left hand side of Figure 3.20.

The interacting surfaces of the turbocharger housing and floating bushing are typically assumed as perfect cylinder in the dynamic simulation. The clearance in the oil films is defined by the geometry of the parts. The clearance used in the simulation is a corrected clearance, a so-called hot clearance, depending on the operating temperatures of the parts. Under high temperature load, especially at the turbine side, the thermal deformation of the structure will not be uniform due to the asymmetrical geometry of the turbocharger

[98]Cf. Bukovnik S., Diemath A., Offner G., Smolik L. (2017), pp. 1-11
[99]Cf. Bukovnik S., Diemath A., Offner G., Smolik L. (2017), p. 3

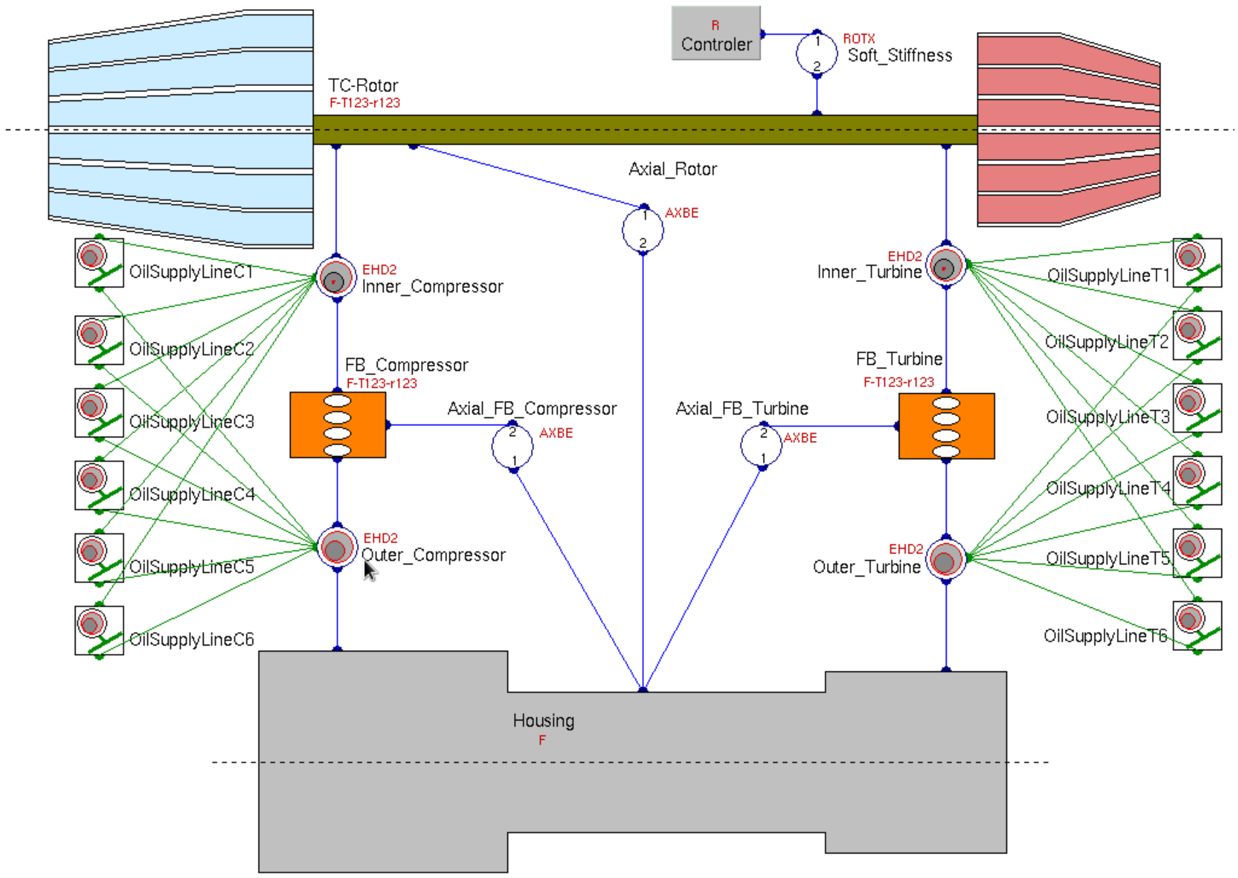

Figure 3.19.: Schematic turbocharger model in AVL EXCITE, Source: external reference[90]

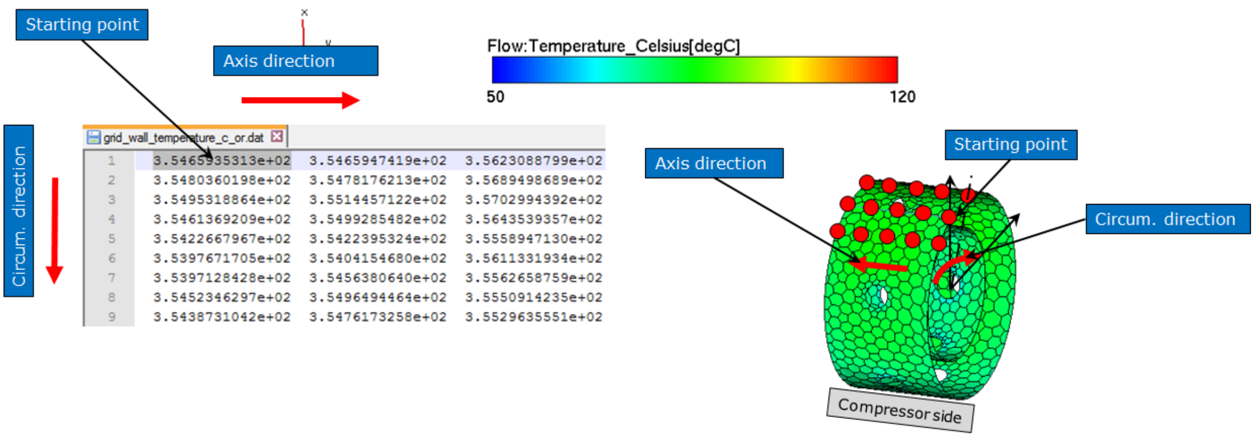

Figure 3.20.: Temperature transfer (CFD) to bushing shells of FEA, Source: own model

housing as well as asymmetrical temperature distribution in the housing structure. The deviation of the shape from the perfect cylinder can be several microns which is already a high percentage of the clearance and in some cases should not be neglected. This deviation can be defined in the dynamic simulation model as the boundary condition using a surface map. Such map is obtained as a result of thermal structure analysis performed in FEA tool. The thermal boundary conditions for the FEA calculations are structure temperatures obtained from 3D CFD calculation. The deformed shape of the structure under the thermal load is then also calculated in the FEA. Results are shown in the practical part of this thesis in chapter 4.

3.5. Summary

In this chapter the entire simulation approach for steady heat transfer in a turbocharger was described with the main focus to the CFD part in this tool chain. It is seen as a transition between the theoretical part and the practical part of this thesis, as it provides also vital information to the engineering target of such kind of simulation. The engineering focus is here the supply of accurate temperature boundary conditions for the turbocharger's rotor dynamics. The proposed approach represents the simulation of heat transfer within the turbocharger structure and its parts by considering the solid and fluid parts of the turbocharger as a multi-material simulation model.

The difference between the mulit-domain and multi-material based simulation was also outlined, indicating a preference for the multi-material approach in future as it is easier to setup and to apply to a heat transfer task in general.

Finally, the entire tool chain is shown in Figure 3.21 presenting the two major information paths in order to provide most accurate boundary conditions for the MBD simulation.

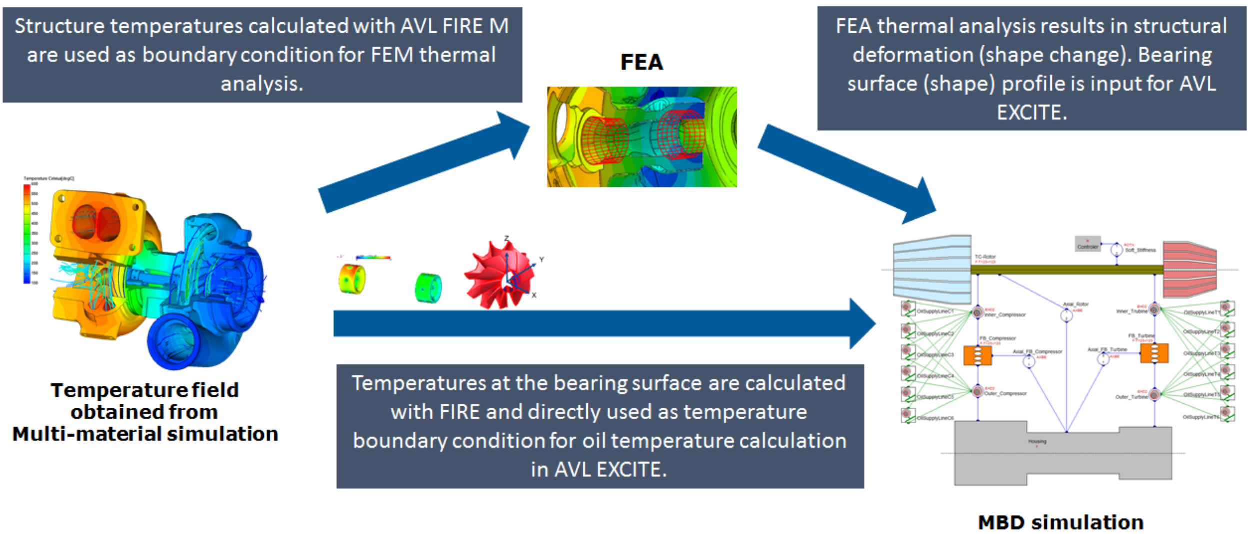

Figure 3.21.: Engineering focus, Source: own model

4. Results and Evaluation

This chapter outlines the effort that was taken in order to evaluate the results of the previously described simulation workflow. Furthermore, the intention is to use the terms *Model* and *Workflow* (which were explained in section 3.2) in a much wider sense as they are in close relation to each other.

4.1. Introduction

In many publications only the contribution to the engineering result provided by a simulation was considered in the investigation process.[100] Only little attention was payed to look also into the acceptance and usability of a simulation workflow from the perspective of a simulation engineer.[101] In terms of verification and validation of CFD simulations much more literature can be found. These exemplary chosen report[102] is seen as subsidiary for many other publications which typically use a rather mathematical approach such as the investigation of convergence criteria, applied algorithm and error estimation.

The terms validation and verification are voluntarily briefly described in the following few lines, as it is crucial to distinguish between them. According to the American Institute of *Aeronautics and Astronautics (AIAA)*,

Validation is defined as:

"The process of determining the degree to which a model is an accurate representation of the real world from the perspective of the intended uses of the model."[103]

and

Verification is defined as:

"The process of determining that a model implementation accurately represents the developer's conceptual description of the model and the solution to the model."[104]

Since the terms validation and verification are very often used in a wide sense when describing evaluation processes a more precise distinction between the validation and verification (V&V) of the software and the V&V of a simulation workflow is made as they are fundamentally different. The validation and verification of the software itself is not scope within this thesis, but a few lines shall be written in order provide a better overview and separate them clearly from other terms used in this work.

[100] Cf. Bergqvist, S. (2014)
[101] Cf. Barth, P. (2011)
[102] Cf. Oberkampf, W. L., Trucano, T. G. (2002)
[103] AIAA G-077-1998. (1998)
[104] AIAA G-077-1998. (1998)

Software Validation checks that the software meets the user's requirements. This is typically done by the software vendor for instance by applying dynamic testing[105] in order to study the dynamic behavior of a program. Therfore, the software has to be compiled and run with variables which are not constant and change over time. This can also be accomplished automatically, e.g. within AVL's software division *Advanced Simulation Technologies (AST)*, automated overnight builts are created with additional automated tests in order to find problems in the code immediately.

Software Verification ensures that the software has been built according to the requirements and specifications, but this implies also that the specifications were initially correct.[106] Further information related to software validation and software verification can be provided by the *IEEE Standards Association*[107].

The entire methodology of *Model verification and validation* is primary used for quantifying the results and building credibility in numerical simulation models.[108]

Validation in terms of *validating a simulation model* means building the right model or workflow and make sure that the model is an accurate representation of the source system.[109]
If one applies this statement to a simulation problem, e.g. when a physical problem has to be represented by a certain model, the user has to ensure that his/her model reflects as accurately as possible this particular physical problem. Usually, this is accomplished by quantitative measures, for instance by comparing numerical solutions to experimental data.[110]

The meaning of verification applied to the simulation model itself is seen here in the following sense: the model should meet the set of design specifications. Another formulation states that *"Model verification deals with building the model right and it is used to ensure that the model is developed correctly according to the modeling method and it functions properly without error."*[111]
According to *Thacker* the verification is related to the identification and removal of errors in the model itself. The suggested method therefore is to compare the numerical solution to analytical or highly accurate benchmark solutions.[112]
A simulation engineer who is applying the model in a simulation workflow contributes in the following way to the verification process:
"The most common type of calculation-verification problem is a grid convergence study to provide evidence that a sufficiently accurate solution is being computed."[113]

4.2. Evaluation process

A certain sequence is followed in this section in order to evaluate and assess the thermal analysis workflow, as described earlier in chapter 3. The evaluation process is split into to two main pillars as shown in Figure

105 Myers, G. J. (2004) p. 113
106 Myers, G. J. (2004) pp. 90-94
107 Cf. IEEE Std 1012-2012. (2012)
108 Thacker B .H. et al (2008) p. 2
109 Çetinkaya D. (2013) p. 8
110 Thacker B .H. et al (2008) p. 2
111 Çetinkaya D. (2013) p. 8
112 Thacker B .H. et al (2008) p. 2
113 Thacker B .H. et al (2008) p. 2

4.1. The main points are described briefly below:

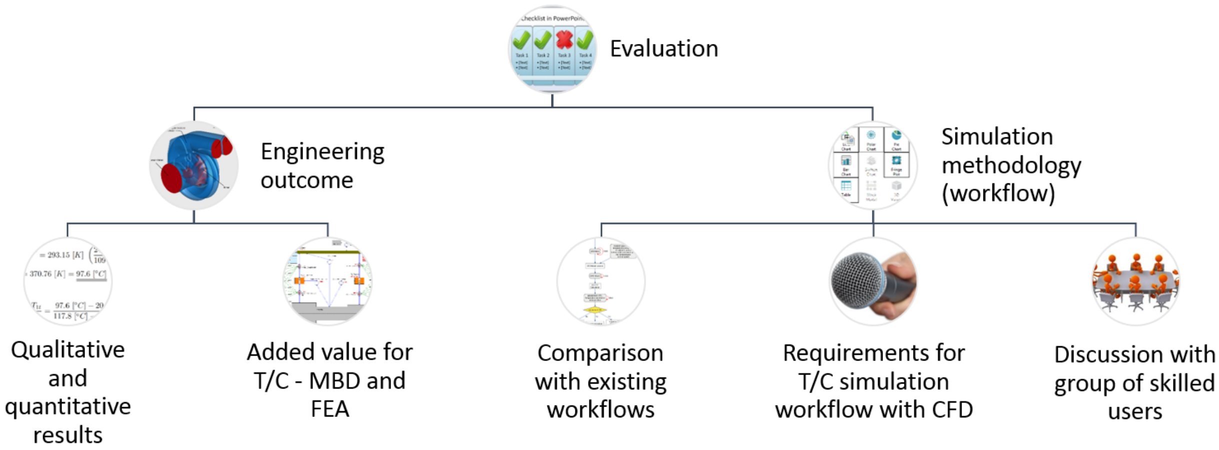

Figure 4.1.: Evaluation process - overview, Source: own chart

Engineering outcome

The first pillar in the evaluation process consists of the check of the engineering outcome. It is seen as a prerequisite here as it is necessary to check whether the gathered results meet the expectations or not. Qualitative and quantitative results are typically used to make an engineering statement. Furthermore the contribution to other simulation tools, in particular the delivery of boundary conditions for MBD and FEA is investigated.

Qualitative and quantitative results

In the case of a turbocharger, the quantification is done by comparing turbine and compressor (T/C) efficiencies with measurement data.

Added value for T/C - MBD and FEA

Since the thermal analysis of a turbocharger is part of a bigger simulation tool chain, the added value for other tools has to be evaluated. In particular the obtained results from the 3D-CFD simulation are used to provide more accurate thermal boundary conditions for the multi-body dynamics in order to study flexible rotor and housing structures with elasto-hydrodynamics (EHD) of the inner and outer oil films.

Simulation methodology

The second pillar in the evaluation process is the consideration of the simulation methodology. It consists of three topics:

Comparison with existing workflows

The new multi-material approach is compared with the ACCI-based (multi-domain) coupling methodolgy. Advantages and disadvantages of both workflows are outlined.

Requirements for a T/C simulation workflow using CFD
Interviews with people from the simulation management were done in order to collect a list of requirements to get a view from the perspective of simulation management. The interviews were done face to face and were following an interview-technique called semi-structured or guided interview. Usually this interview is scheduled and the interviewer is prepared with a set of questions. These questions may or may not have to be shared in advance.[114]

Dicussion with group of skilled users
Additional interviews were done with a group of users of different skill levels with the purpose to reflect existing workflows and the new simulation approach. Further intention was also to gather information for potential improvement of a CFD simulation workflow in general. Participants of this interview were analysis engineers for CFD as well as for FEA.

4.3. Engineering outcome

In this section the qualitative as well as the quantitive results of the multi-material simulations are discussed. Furthermore, the added value for other tools in the tool chain are outlined.

4.3.1. Qualitative and quantitative results

The obtained results presented in this section are split into two separate parts. The first part discusses the flow results related to the turbine stage and the second one deals with those from the compressor stage.

4.3.1.1. Turbine stage

According to the fundamentals of the turbocharger thermodynamics introduced in chapter 2.2.2.1, the thermodynamic assessment is applied at significant positions in the domain. Refering to Figure 2.6. (chapter 2.2.2.1) the flow conditions are gathered at the main turbine inlet and outlet, which corresponds to the positions 3 and 4 in Figure 2.6. The corresponding position is also shown here in Figure 4.2. in order to get a better overview. The EGR enters the main inlet of the turbine (position 3), is guided through the volute and expands in the blade channels of the rotor and leaving the turbine at the main outlet (position 4). The obtained results for the significant positions as well as the calculated quantities in order to compare measurement with simulation are summarized in Table 4.1. All presented results are averaged and area weighted values at the relevant position. The isentropic turbine efficiency η_T, calculated based on equation (2.3), is calculated once based on the simulated data and then based on the measurement data. Afterwards they are compared in Table 4.1. for all four operating points.
There is a deviation observed between the simulated and the measurement based turbine efficiency. This deviation is related to measurement based efficiency η_T and is found in the most right column of Table 4.1.

One big uncertainty in this setup is the physical property of EGR used in simulation and measurement. In fact, the composition in the simulation is based on an assumption for a typical combusted Diesel fuel, whereas the composition of EGR on the testbed is not known here. Another explanation for the lower turbine

[114] Cf. Marshal C., Rossman G.B. (2011) p. 144

efficieny in the simulation might be a possible deviation of the measurement points compared to the testrig.

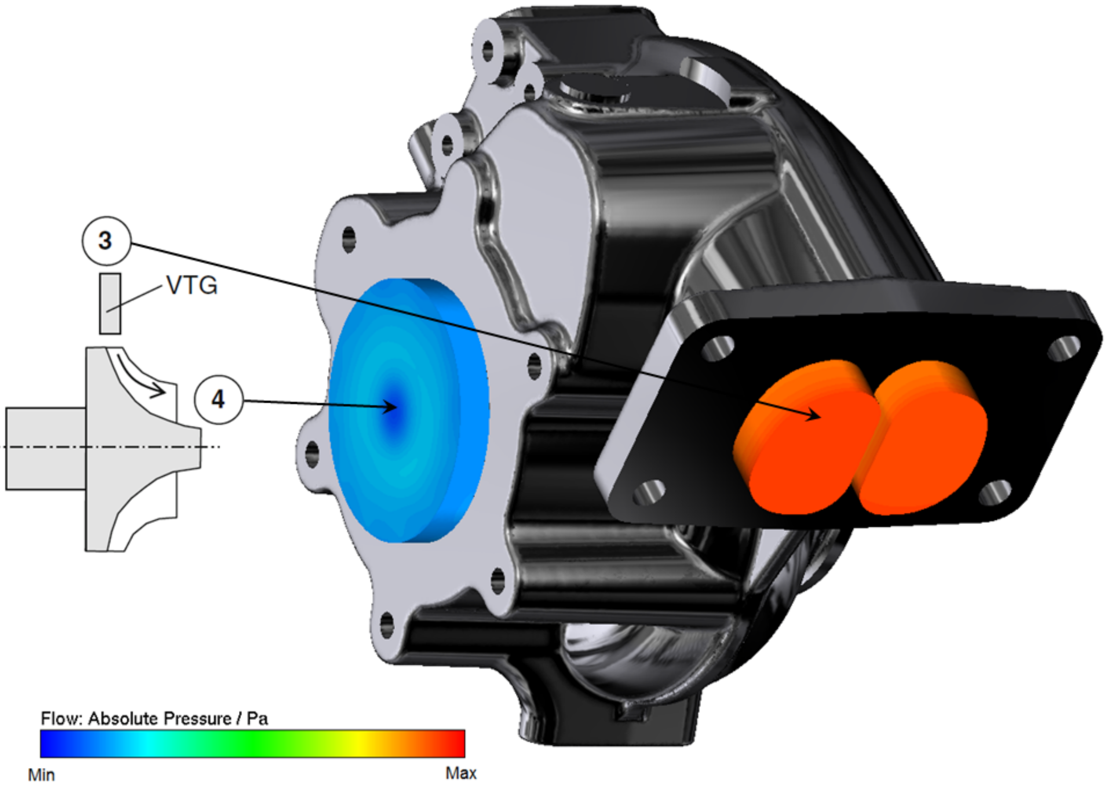

Figure 4.2.: Turbine stage - overview, Source: own model

OP	Sim. T_{4s}	Sim. T_{4t}	Sim. η_T	Meas. T_{4s}	Meas. T_{4t}	Meas. η_T	Dev. to meas. η_T
40200 rpm	556.3 °C	555.4 °C	0.97	524.5 °C	523.9 °C	0.99	-1.2$\%$
60500 rpm	527.3 °C	518.4 °C	0.89	505.2 °C	503.4 °C	0.98	-9.2$\%$
80700 rpm	482.4 °C	466.8 °C	0.88	470.6 °C	466.7 °C	0.97	-9.0$\%$
90700 rpm	457.5 °C	439.7 °C	0.89	456.9 °C	452.1 °C	0.96	-8.1$\%$

Table 4.1.: Comparison of simulated and measured results - turbine stage

4.3.1.2. Compressor stage

The thermodynamic assessment of the compressor stage is done in an analog way. The air enters at the main compressor inlet (position 1) and is compressed in the channels of the compressor blades. Afterward it is guided through the compressor volute to the main outlet (position 2) as shown in Figure 4.3. The isentropic compressor efficiency η_C according to equation (2.7) is calculated on simulation based and measurement based quantities for comparison.

As summarized in Table 4.2 the simulated compressor efficiency has an acceptable deviation compared to the measured one on the testbed. The deviation might be related to slightly different boundary conditions in the simulation than on the testbed.

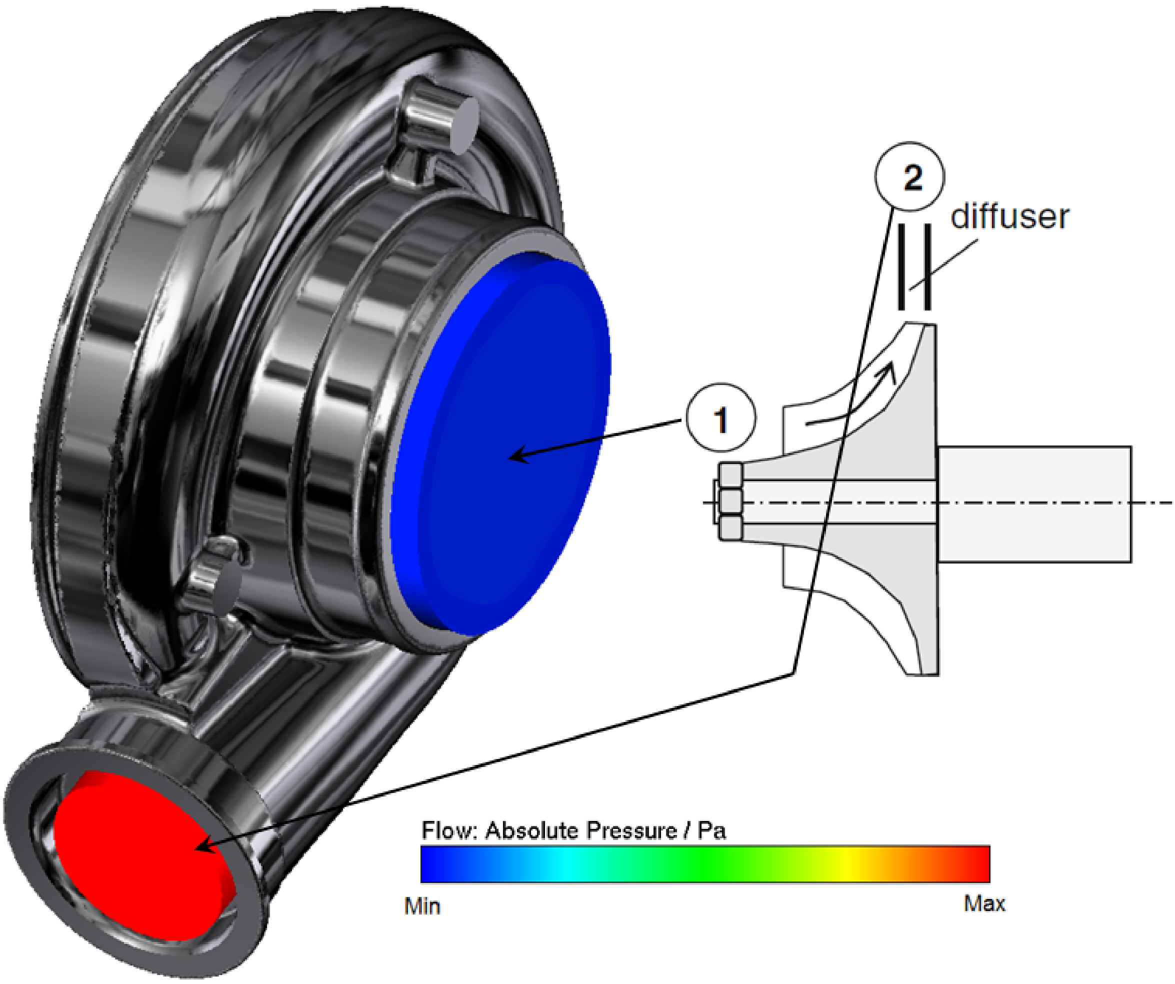

Figure 4.3.: Compressor stage - overview, Source: own model

OP	Sim. T_{2st}	Sim. T_{2t}	Sim. η_C	Meas. η_C	Dev. to meas. η_C
40200 rpm	37.0 $°C$	44.7 $°C$	0.69	0.71	-2.8$\%$
60500 rpm	64.4 $°C$	76.5 $°C$	0.78	0.78	4.8$\%$
80700 rpm	99.8 $°C$	122.0 $°C$	0.78	0.78	4.3$\%$
90700 rpm	122.3 $°C$	154.5 $°C$	0.76	0.76	0.5$\%$

Table 4.2.: Comparison of simulated and measured results - compressor stage

4.3.2. Added value for T/C - MBD and FEA

The boundary condition for the energy equation of the oil film, as already mentioned in section 3.4.2 , is the structure temperature. This temperature is not uniform but it is strongly influenced by the heat coming from the turbine side and by cooling effect of the cold air at the compressor side. The temperature profile applied as boundary condition at both compressor and turbine side is shown in the Figure 4.4 exemplary for the loadpoint of 80700 rpm.

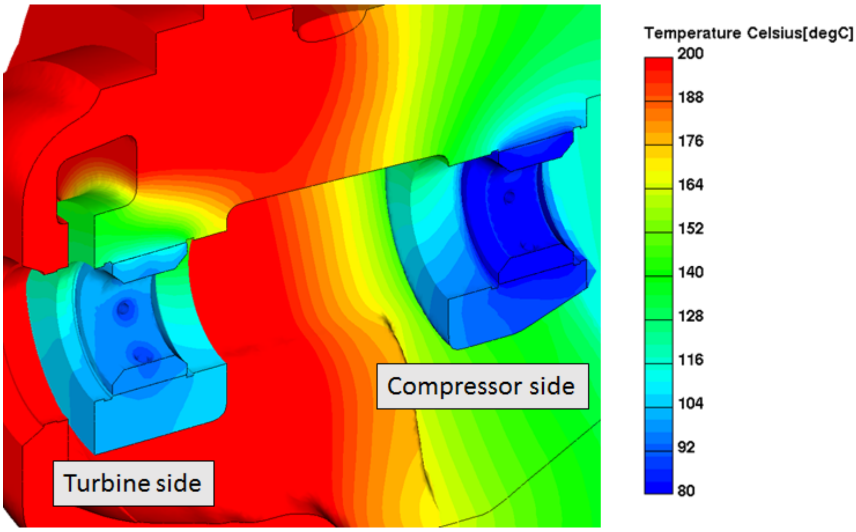

Figure 4.4.: Temperature distribution around the bushing bearings, Source: own model

The bore shape under thermal deformation of the structure can influence the clearance of the oil film. Under high temperature load, especially at the turbine side, the thermal deformation of the structure will not be uniform due to the asymmetrical geometry of the turbocharger housing as well as asymmetrical temperature distribution in the housing structure. The deviation of the shape from the perfect cylinder can be several microns which is already a high percentage of the clearance and in some cases should not be neglected. This deviation can be defined in the dynamic simulation model as the boundary condition using a surface map. The deformed shape of the structure under the thermal load calculated in FEA is displayed in Figure 4.5[115].

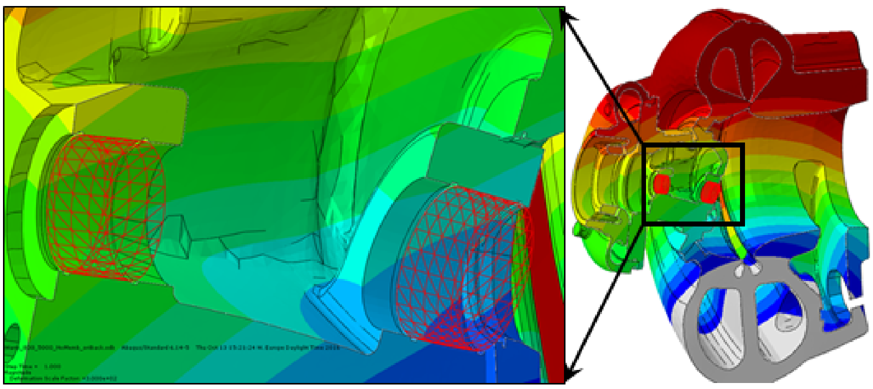

Figure 4.5.: Turbocharger housing under thermal deformation, Source: external reference[115]

[115]Bukovnik S., Diemath A., Offner G., Smolik L. (2017), p.6

Additonal information for the rotor dynamics is also obtained from the flow field data. Pre-calculated boundary conditions from CFD, such as rotor forces, are also provided to the MBD in order to calculate the displacement at the compressor nut or provide information on the bearing forces. Figure 4.6. shows exemplarily the calculation of the radial and axial forces in CFD. The aerodynamic phenomena contributing to this forces are listed in the following:

- Pressure and shear forces act on the rotating parts (blades and shafts),
- Rotating mechanism transmits these forces and torque is acting on these rotating parts,
- Superposition of torques created by the forces acting on every single boundary face,
- Pressure force on face results from wall boundary pressure,
- Shear force on face results from local velocity gradient and is determined by the logarithmic wall law.

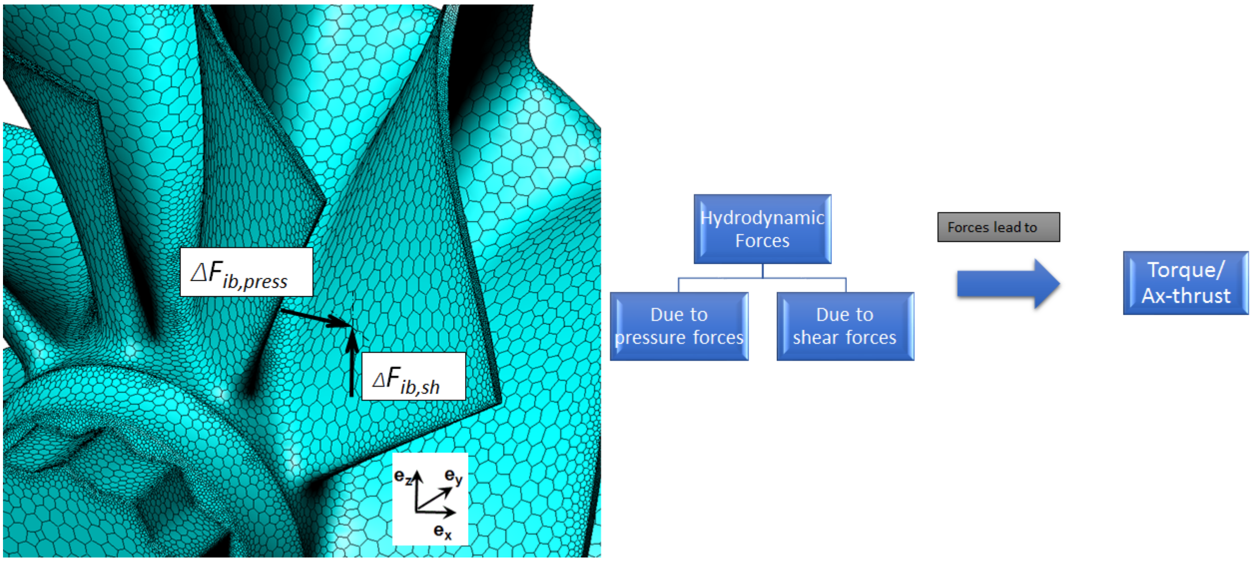

Figure 4.6.: Forces acting on impeller, Source: own model and chart

The article from Bukovnik et al.[116] furthermore concludes that the simulation results showed that there can be a significant difference in the assumed and real temperature of the oil film. For instance, the assumption of the oil film temperature for the nominal case is 90°C for both, the inner and outer oil film. Looking at the compressor side, the assumption of 90°C for the outer oil film is good as the temperature range is between 85°C and 95°C. On the turbine side the temperatures vary in the range of 105°C to 115°C. Hence, is not possible to have a good temperature assumption for all oil films and for the complete speed range of the turbocharger. This incorrect temperature has a strong influence on the dynamic behavior of the turbocharger and underlines capabilities of the modern simulation tools for the turbocharger application.

[116]Bukovnik S., Diemath A., Offner G., Smolik L. (2017), p. 7

4.4. Simulation methodology

In this section the simulation methodology is investigated which was outlined earlier in the right part of Figure 4.1.

4.4.1. Comparison to other simulation workflow

In the framework of the investigation done on the turbocharger *S410 Euro4* by *Schaefer*[117], the thermal analysis was performed applying the so-called *ACCI-method*, a multi-domain simulation capability of *FIRE v2014.2*[118].
The work from *Schaefer* offers a unique opportunity to compare two different simulation methodologies under similar engineering conditions and on a level of complexity which is very typical for simulation tasks performed in industry.

Starting with the pre-processing and in particular with the surface preparation work, the both workflows are similar as in both cases a watertight surface representation is required for the meshing process.
The meshing process itself is the same as in both cases the polyhedral meshing approach from AVL FIRE M was used. The differences occur after the automatic meshgeneration, as in case of the multi-material setup no further manual mesh decomposition in different domains is required. For the multi-domain (ACCI) approach a mesh has to be available for each single simulation case (component of the assembly).
The simulation setup for multi-domain simulation in general requires for each component a separate simulation case. All the boundary and initial conditions as well as the numerical setup has to be repeated for each individual case. The multi-material setup allows to setup the simulation in one single environment. In fact, the concept of having several different simulation cases does not exist anymore, the settings are applied directly to the relevant material. Numerical settings and output quantities are defined in a more generalized way in the multi-material setup. Furthermore, the availability and accessability to the material parameters and fluid properties is more convenient for the user.
The comparison in simulation time show no major difference as both cases are of similar mesh size given with approximately 24 hours on 50 cores.
Comparing the results of the temperature field in the structural parts as shown in Figure 4.7, the temperature field in the turbine housing is very similar. There are deviations in the temperature field in the bearing housing observed, as there are two major differences in the geometry between the two cases. The multi-domain[119] setup does not contain the floating bushings modelled as well as the oil line.
In general the quality of results is comparable in both cases.
The biggest advantage of the multi-material setup is the simultaneously consideration of fluid and structure problems, starting from the pre-processing over simulation setup to the post-processing.
Although the simulation time per operating point is similar, the multi-material simulation provides more robustness in terms of stability as only one simulation run by submitting only one executable code is required. There is no co-simulation necessary requiring additionial processes running in order to manage the data exchange between the domains.

[117]Schaefer K. H. (2016) p. 30
[118]Cf. AVL List GmbH. (2014) Feb. 28)
[119]Schaefer K. H. (2016) p. 84

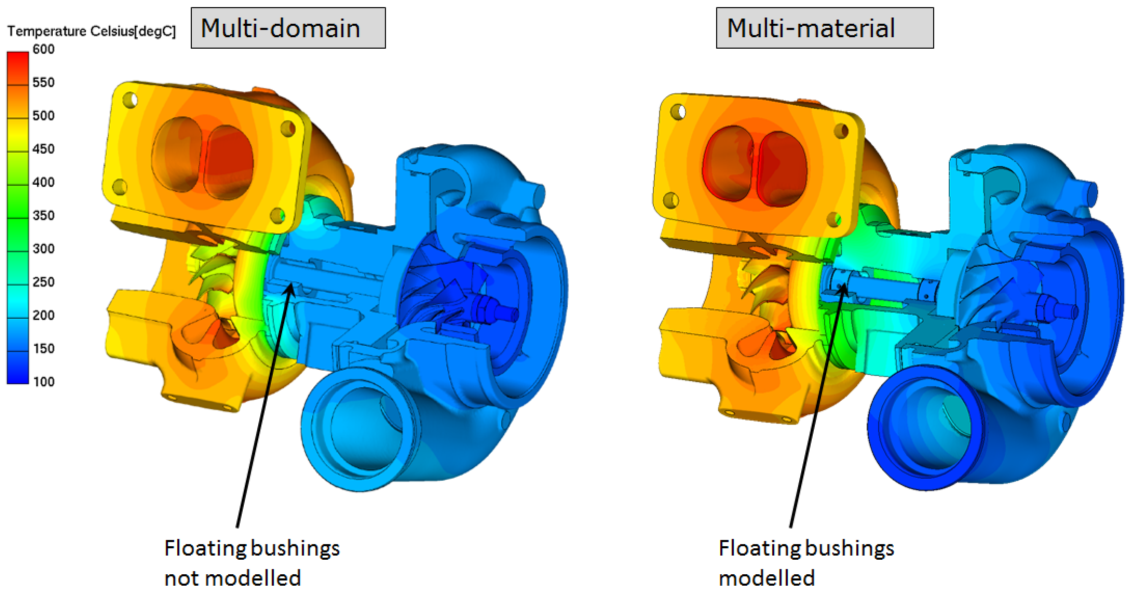

Figure 4.7.: Comparison multi-material vs. multi-domain, Source: left model external source by Schaefer[119], right part - own model

4.4.2. Requirements for T/C simulation workflow with CFD

This section describes the preparatory work for the interview and the outcome for the people from simulation management. For the detailled list of participants in the interview, please refer to Appendix A. These interviews were done in German language only.

4.4.2.1. Preparation for the interview

A list of questions was prepared in advance for the interviews of the people from simulation management. The interviewed person did not receive the list prior to the interview.

1) How important is it to use a multi-material simulation approach in the T/C development?

2) How do you see the future of CFD in particular in the simulation of a T/C?

3) How much time is required to train a new simulation engineer of being able to perform a simulation task by himself?

4) How much time do you allow a new simulation engineer for the training to be able to perform a simulation task by himself?

5) Does a new simulation engineer (freshman) typically start with *easier* (meaning less complex) tasks compared to an experienced analyst?

6) From the engineering perspective, under which conditions would you see a rather *easy* to use and stable workflow as acceptable, although it produces less accurate absolut results, for instance when comparing the results with available measurement data (keywords: error estimation and known errors of a methodology or an entire workflow)?

7) Under which circumstances would you accept that a high sophisticated workflow results in a more accurate solution than the previous one, but may fail completely under certain conditions?

8) Where do you see potential for improvement in the current workflow? What is seen as a bottleneck? Keywords: Preparatory work (geometry preparation), meshing, simulation (runtime?), post-processing, reporting etc...

9) Considering the tool chain in the development process of a component, should a design engineer use a simulation tool? Under which conditions do you see that happen?

4.4.2.2. Interview of simulation management

In this subsection, the anwers are presented in a summarized form over all the participants. There is no dedicated assignment to the relevant person forseen. The number of the relevant answers corresponds to those of the question list in subsection 4.4.2.1. Before starting with the actual interview, the relevant person received a short introduction related to thermal analysis of a turbocharger. Then the question list was handed over and the interview was started. The interviews lasted between 30 to 50 minutes.

Question 1: How important is it to use a multi-material simulation approach in the T/C development?
Answers:
A fluid-solid coupling during simulation runtime is seen in general beneficial in the capability of providing more accurate boundary conditions to the FEA compared to an offline coupling. In particular, the multi-material workflow shows more potential in terms of overall handling and stability compared to the multi-domain approach using ACCI. Another positive effect of this workflow related to the interaction with MBD is the possibility to reduce the number of interactions among the tools as shown in the Figure 4.7 below which was created during the interview. It states that in order to provide a *final temperature field* as a boundary condition to the MBD, the path via the FEA tool is not mandatory. Thus, this complex task can be accomplished by one analyst instead of involving two people. One restriction is given to this kind of fluid-structure coupling. It can only be applied as long as the problem deals with isotropic (linear) material parameters.

Question 2: How do you see the future of CFD in particular in the simulation of a T/C?
Answers:
In general, the usage of CFD is seen as raising in the T/C development as the downsizing of the ICE is becoming more important. Concerning the scope of the relevant simulation task a certain diversification is required: Calculating the temperature field of a T/C within the CFD simulation will become a so-called standard application with a clearly specified task list. Looking into direction of TMF simulation on T/C housing the CFD is also forseen to become a standard application. The simulation of acoustic problems for instance, is seen as an on demand simulation task. As a future outlook, transient T/C simulations will possibly provide

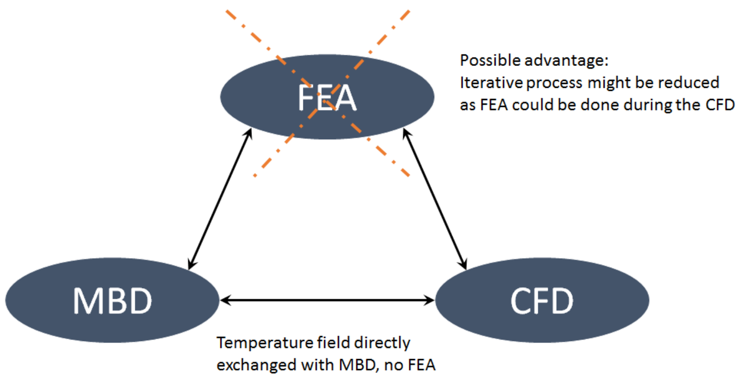

Figure 4.8.: Interaction CFD - FEA - MBD, Source: transcipt from own interview notes

statements about the blade passing frequency. Another transient problem to be solved is the filling level of the oil in the bearings in order to provide sufficient lubrication. This is also rather seen as non-standard application which should be performed on demand.

Question 3: How much time is required to train a new simulation engineer of being able to perform a simulation task by himself?
Answers:
AVL provides a certain standarization for recurring simulation tasks in the simulation departments. A new simulation engineer receives a basic software training between three to five days usually immediately after starting in the company. This helps to get an overview of the software. This introcuction is done in a standarized way and does not consider the engineering capability of the beginner. Within AVL, standarized CFD simulation tasks require between two and six weeks lead time to be completed. An average simulation engineer requires between three to six month of the same task execution to be able to bring down the execution time frame to the standard. After six month the person has developed the understanding for the handling of the numerics and the software. During this period, the simulation engineer is guided by an experienced engineer at the level of senior or lead engineer. To become a skilled user on an expert level, it typically takes one to one and a half years to develop the required skills of being able to deliver also the requested engineering contribution to the task. Then the analysis engineer is able to take over responsibility for the engineering outcome of the simulation.

Question 4: How much time do you allow a new simulation engineer for the training to be able to perform a simulation task by himself?
Answers:
The given time frame corresponds to the mentioned numbers stated in *answers to 3*, which are based on many years of experience within AVL. In case the analysis engineer exceeds the given time frame the person is not considered as suitable for the position of an analysis engineer.

Question 5: Does a new simulation engineer (freshman) typically start with easier *(meaning less complex) tasks compared to an experienced analyst?*
Answers:
The strategy within AVL is that a freshman starts with a basic software training to get an overview of the software. Additional material is provided via example tutorials which have to be executed. In case of CFD

simulations, a task with lower level of complexitiy is for example a steady simulation of an air flow problem. This is typically what a new user starts with. Also depending on the complexity of the task the work in a team where the new engineer is guided by an experienced senior or lead engineer is common. Since AVL-AST offers also the CFD software to customers for sale the experience within the software support process gives sometimes a complete different picture. In some cases a new simulation engineer starts immediately with a very complex simulation task and this is seen as very counterproductive for a good progress of a simulation project. In such cases the time required to become a skilled expert in simulation exceeds even the numbers stated in *Answers to 3*.

Question 6: From the engineering perspective, under which conditions would you see a rather easy to use and stable workflow as acceptable, although it produces less accurate absolut results, for instance when comparing the results with available measurement data (keywords: error estimation and known errors of a methodology or an entire workflow)?
Answers:
Many customers in the industry prefer a simulation workflow to be robust in terms of lead time, costs and reliability. Under such conditions it is accepted by customers if the simulation provides less accurate results as long as a relative comparison between different design variants is guaranteed. In the concept phase of a new component this kind of simulations allow to investigate many different concepts in a short period of time. This happens typically in the first three month of the development process of the component.

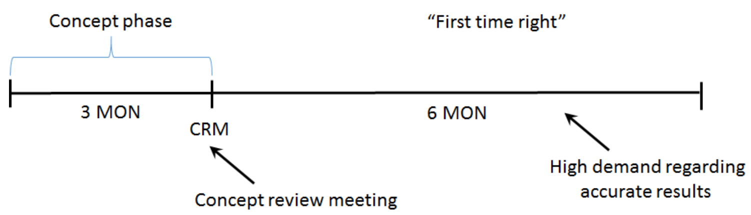

Figure 4.9.: Phases in component development process, Source: transcript own interview notes

Question 7: Under which circumstances would you accept that a high sophisticated workflow results in a more accurate solution than the previous one, but may fail completely under certain conditions?
Answers:
Accurate solutions are typically required after the Concept Review Meeting (CRM) in the development process. For instance durability simulations of a component are only possible with a more comprehensive workflow. In case of a turbocharger, this would mean that the calculated heat transfer has to be correct because the workflow has to ensure the virtual approval of the relevant component. Concerning the workflow itself it has to be considered that the numerical model applied has to be as accurate as necessary to improve the design. A too sophisticated numerical model appears to be also useless if the boundary conditions are based on the wrong assumptions.

Question 8: Where do you see potential for improvement in the current workflow? What is seen as a bottle-neck? Keywords: Preparatory work (geometry preparation), meshing, simulation (runtime?), post-processing, reporting etc...
Answers:
From simulation management point of view, the answers are provided rather in a global way than in a specific way as it is expected in the case of a user. For preparatory work and surface preparation the

amount of manual work a user has to handle is still seen as too high, as the current workflow still counts approximately two weeks for such kind of work. Although the meshing process itself using the polyhedral mesh structure is quite fast, the general request for mesh-less techniques is vital. About the simulation run in terms of stability and duration no statement was given. The interface between CFD and MBD requires some automatism as currently it is still done via file exchange. For the post-processing and reporting also the wish for more automation is requested. There is also the request to establish a link between the major simulation parameters and performance attributes of the component. Currently, the choice of the right simulation parameters is very much related to the experience of the relevant simulation engineer. This means that the trends which are carried out during the simulation of several design variants are strongly influenced by simulation parameters, for instance numerical settings the user has chosen. The user's influence on that has to be reduced by creating a database and standarized workflows.

Question 9: Considering the tool chain in the development process of a component, should a design engineer use a simulation tool? Under which conditions do you see that happen?
Answers:
This should be only done for simple tasks, e.g. the calculation of the pressure drop of a simple pipe in steady mode without heat transfer problematic. In AVL, for the majority of the tasks the level of complexity is too high to allow that a single person is working on design and analysis at the same time.

4.4.3. Dicussion with group of skilled users

Additional interviews were done with a group of users of different skill levels with the purpose to reflect existing workflows and the new simulation approach. Further intention was also to gather information for potential improvement of a CFD simulation workflow in general. Participants of this interview were analysis engineers for CFD as well as for FEA.

4.4.3.1. Preparation for the interview

The list of questions for the group of skilled users is given as follows:

1) How important is a multi-material simulation approach in the T/C development?

2) How do you see the future of CFD in particular in the simulation of a T/C?

3) How much time is required to train a new simulation engineer of being able to perform a simulation task by himself?

4) Does a new simulation engineer (freshman) typically start with *easier* (meaning less complex) tasks compared to an experienced analyst?

5) From the engineering perspective, under which conditions would you see a rather *easy* to use and stable workflow as acceptable, although it produces less accurate absolut results, for instance when comparing the results with available measurement data (keywords: error estimation of predictable and known errors of a methodology or an entire workflow)?

6) On the other hand a high sophisticated workflow results in a more accurate solution than the previous one, but may fail completely under certain conditions. Under which circumstances would you accept that?

7) Where do you see potential for improvement in the current workflow? What is seen as a bottleneck? Keywords: Preparatory work (geometry preparation), meshing, simulation (runtime?), post-processing, reporting etc...

8) Should a design engineer use a simulation tool? Under which conditions do you see that happen?

9) Do you see this new workflow as a competition to the existing tasks of a typical FEA simulation engineer? (keywords: temperature-field calculation in a solid)

4.4.3.2. Interviews with analysis engineers

As described in subsection 4.4.2.2 the anwers are also presented in a summarized form over all the participants. There is no dedicated assignment to the relevant person forseen. The number of the relevant answers corresponds to those in the question list in subsection 4.4.3.1. Before starting with the actual interview the relevant person received a short introduction and an overview of the new workflow. Then the question list was handed over and the interview was started. The interviewed engineers represent a variety in available simulations within AVL. Not every engineer has the same application background and knowledge. Therefore, in some cases it was also allowed to them to answer in a rather global way than exactly related to the topic of the turbocharger. Due to the variety of nationalities of the participating people the interviews were either done in German or English language. The range for the duration of the interviews was between 20 and 40 minutes.

Question 1: How important is a multi-material simulation approach in the T/C development?
Answers:
For the T/C component this new workflow is seen as very important as it allows now to provide more accurate boundary conditions for the MBS. Since in general the simulation of fluid-flow is already well established and is seen as standardized, the multi-material and multi-domain simulation is the next logical step. The interviewed engineers are aware of the fact that this task is part of a tool chain of simulation tools and therefore they see this workflow in a bigger context. Some of the engineers expect to take over this methodology with some kind of modification and apply it to the simulation of other components dealing with heat transfer problems. They definitely believe that this is the right way in future to provide more accurate results.

Question 2: How do you see the future of CFD in particular in the simulation of a T/C?
Answers:
Five out of the seven engineers propose a raise of CFD in the T/C development as the tendency in reducing testing is increasing. One engineer is even more specific and was quantifying the raise for the next five years. This person expects afterwards a saturation of applying T/C in vehicles and maybe a decrease due to upcoming electrification of vehicles. The biggest potential for a survival of a T/C this engineer expects only in heavy-duty and marine powertrain application. Two engineers see the future of CFD in T/C development from a different perspective. In their opinion the simulation workflow still provides too less automation and in terms of T/C performance simulation too many parameter are still required as boundary conditions and not received as a simulation result. In particular the rotational speed of a T/C was mentioned because in the current methodology the speed is still an input parameter. There is the request that the speed has to be actually a simulation result when calculating T/C performance maps.

Question 3: How much time is required to train a new simulation engineer of being able to perform a simulation task by himself?
Answers:
Among the engineers the opinion about the required time to be able to fulfill an engineering task is very much aligned. Compared to the answers from simulation management the participants are able to provide even more precise information. If one considers standardized workflows within the AVL working environment, for a steady simulation task a freshmen requires typically two to three month of being able to understand the software and the workflow. A fact, which does not include of being able to provide already proper engineering statements. In case of transient simulation problems this period is extended upto six month. To become a skilled user on an expert level it typically takes one to one and a half year to develop the requred skills of being able to deliver also the requested engineering contribution to the task. After this period they see themselves of being able to take also over responsibility for the engineering outcome of the simulation.

Question 4: Does a new simulation engineer (freshman) typically start with easier *(meaning less complex) tasks compared to an experienced analyst?*
Answers:
All participants were aligned in this cases. As the used tools are very complex, a step by step learning is required. In AVL's CFD departments this starts typically with steady state simulation problems. Especially the younger engineers were mentioning that there is a major influence to the personal progress they made depending on relevant senior or lead engineer in the way of guiding them in the early phase of their career.

Question 5: From the engineering perspective, under which conditions would you see a rather easy *to use and stable workflow as acceptable, although it produces less accurate absolut results, for instance when comparing the results with available measurement data (keywords: error estimation of predictable and known errors of a methodology or an entire workflow)?*
Answers:
An engineer who is executing a task is also exposed to a certain level of pressure within a project. From the user's perspective a stable workflow is preferred as long as the engineering targets are accomplished. Especially in the early stage of the design phase when many variants have to be investigated, the absolut accuracy of results is less important as long as general trends are well captured.

Question 6: On the other hand a high sophisticated workflow results in a more accurate solution than the previous one, but may fail completely under certain conditions. Under which circumstances would you accept that?

Answers:

The common answer is that a more comprehensive workflow should be used only in the detailled development phase. One engineer suggested further the use in case of trouble shooting only. For instance, a detailled analysis is used as an additional investigation in case results from testing provide contradicting trends to the ones proposed in the specification. Another engineer recommends sophisticated simulation methods rather for research purpose at universities, e.g. PHD. Non of the engineers accepts workflows which show a high degree of uncertainty in terms of stability. A workflow which fails under certain circumstances, what ever those reasons might be, is not acceptable in productive engineering environment, as there must always be an engineering statement possible at the end of the tool chain. Seeing this from the user's perspective, one engineer suggested that the tool should already provide the possibility during the setup of the problem to chose between a basic and an expert level. This would improve standardization in the tool chain and avoid further problems.

Question 7: Where do you see potential for improvement in the current workflow? What is seen as a bottleneck? Keywords: Preparatory work (geometry preparation), meshing, simulation (runtime?), post-processing, reporting etc...

This answers are given by engineers who are executing tasks by themselves, therefore, the answers are dedicated to certain stages of the workflow:

- *CAD data preparation* is still seen as on of the biggest bottlenecks in the workflow, even for very skilled users. The new surface repair capability implemented in FIRE M is appreciated by the users because it is a big step forward. Especially for one engineer among the participants, who has background in design, the surface preparation needs to be improved. A person with skills in at least one CAD software program has clear advantages as there is always the possibility to compensate the deficits of one tool by using another one.
- The *meshing procedure* using polyhedral meshes is seen as no problem as long as the input surface is provided in an appropriate quality. For engineers with skills in a CAD software the meshing process should become closer to the geometry preparation. Especially the transition of using the STL format between the CAD and the CFD meshing tool is seen as a disturbing factor for the smoothness of the workflow. These users would prefer having a solution without this intermediate format.
- Regarding *simulation and runtime* the engineers consider this as a matter of computational resources. One engineer got more precisely and stated that a simulation time below three days for a task is acceptable. This would allow to make corrections in the simulation setup in case of numerical problems and still being able to deliver an engineering statement within the requested time frame for the task.
- For the *post-processing* which goes for the engineers together with the *reporting* it is very important to have some automation. Users want to have an automatic generation of figures and charts always in the same style. Their scope is to solve an engineering problem and not the development of the software. FIRE M offers therefore a template based post-processing, allowing the user to prepare a set of figures and charts and apply them to different variants of the same simulation model. This is seen as an important step forward in the usabiliy. But the interview revealed that performance of this new post-processing requires improvement as it is seen as too slow in terms of user interaction.

Question 8: Should a design engineer use a simulation tool? Under which conditions do you see that happen?
Answers:
The majority of the engineers stated clearly that a design engineer should not use an analysis tool in general. In their opinion a design engineer should have the best overview of the considered component and therefore stay focused on design related matters. The CFD engineer deals with problems on another level of detailling than the design engineer. Physical modelling should be done by an analysis engineer (CFD and FEA). Two engineers were suggesting that the design engineer should receive a basic introduction in modelling of physical problems and also a basic software training in order to get a better understanding for the work of an analysis engineer. In their opinion this would improve the communication between the two teams, simulation and design. Only one of the engineers could see a design engineer using a CFD tool in order to perform simple tasks. For instance this would be the calculation of a simple pressure drop in a pipe system.

Question 9: Do you see this new workflow as a competition to the existing tasks of a typical FEA simulation engineer? (keywords: temperature-field calculation in a solid)
Answers:
For none of the engineers this is seen as a competition, because the calculation of the final temperature field in CFD is only possible as long as the problem deals with isotropic (linear) material parameters.

4.5. Summary

In this chapter the evaluation of the simulation workflow which was outlined in chapter 3 was performed. In the introduction the terms validation and verification are voluntarily briefly described to build up the transition to the evaluation process. In the main part of this chapter the engineering outcome and the simulation method itself were assessed. Therefore, the evaluation process was split into two main pillars.
The first pillar in the evaluation process consists of the check of the engineering outcome. It is seen as a prerequisite here as it is necessary to check whether the gathered results meet the expectations or not.
In particular, validating a simulation model, as outlined in section 4.1, was accomplished as quantitative results were compared with measurement data and qualitative results were used to provide an engineering statement. It can be concluded that the model reflects this physical problem in a sufficient way.

Furthermore the contribution to other simulation tools, in particular the delivery of boundary conditions for MBD and FEA was investigated showing a strong indication that this novel approach providing suitable results for the thermal analysis of turbochargers.

The second pillar in the evaluation process, which is related to the simulation methodology, was split into three parts.
The comparison to other simulation workflows, which is outline in section 4.4.1., is the first part. The multi-material setup is the prefered solution for future considerations as it allows a simultaneously consideration of the fluid and structure interaction. It provides similar quality of result with enhanced stability compared to other workflows.
Part two and part three in the evaluation process are related to the requirements for a turbine and compressor simulation workflow using CFD from a management point of view and user's perspectives. This section

contains the interviews with people from the simulation management and a group of skilled users in order to receive information about importance, potential for improvements and future considerations for such kind of workflow. From a managment point of view the complex task of a combined temperature and flow field calculation is seen as beneficial as it reduces the simulation effort. The iterative interaction between fluid and solid, which has to be applied in older simulation workflows, can be reduced by performing the temperature field calculation within CFD. Hence, this task can be performed by one analyst instead of involving two people.

From user's perspective, some of the participating engineers in the survey expect to adapt this methodology for other simulation problems. At the time the interviews were performed, not many engineers had the occation to perform this workflow by themselves. Six month after the interviews, the situation has changed and this simulation methodology is already in use for other applications than turbocharger components only. Especially in cooling problems, such as cooling of electrical engines, battery and fuel cells, the multi-material simulation is already state of the art simulation technique.

The improvement of the workflow is strongly related to the capabilties of the software. It is a continous process as customer's demand is permanently evaluated. For instance, the requirement for standardization in the framework of the user's interview is taken into account in two ways. The first step towards standardization is seen in the software training. In particular to the turbocharger simulation, a standardized training example for that topic is currently in preparation and will be available for the next major software release. As part of the continous software improvement process, the need for a higher degree of automation in the software is also taken into account. Template based simulation setup as well as template based post-processing is provided by the software[120]. Furthermore, the offline and script based capabilities of the software are continously improved which allow further automation of the existing workflow in the future.

[120] Cf. AVL List GmbH. (2016)

5. Summary and Conclusions

This work describes the fluid dynamics and conjugate heat transfer, as part of the general multi-physics approach, which is implemented in the commercial CFD code AVL FIRE M. The methodology is known as the AVL FIRE M multi-material approach, where the temperatures and local heat transfer coefficients on the domain interfaces are exchanged after each iteration step and fluid- and structure-domains are modelled within the same tool. Hence, the temperature distribution within the structural part of the turbocharger is also obtained from the CFD steady simulation. The solution is based on the fully conservative finite-volume method adopted for unstructured meshes which can contain computational cells of any shape. All dependent variables, such as momentum, pressure, density, turbulence kinetic energy, dissipation rate, and total enthalpy / temperature are calculated at the cell center. For the fluid part, such as the gas flow in the turbine and compressor domains, the Reynolds-Averaged Navier-Stokes (RANS) are used for numerical simulations. The rotational motion of the compressor and turbine is modelled via the method of moving reference frame (MRF) which is well known in computational fluid dynamics. The simulation grid for the multi-material simulation in FIRE M counts in total 7.17 million polyhedral cells and the structural part of that mesh is displayed in Figure 3.16. The entire mesh consists of 15 domains, whereas 13 domains are solid material of various material properties and the remaining two domains contain the calculated gas flow for exhaust gas residual (EGR) from the turbine side and air from the compressor side.

5.1. Summary

3D CFD simulations are typically done for a flow and thermal investigation as well as specifically providing accurate thermal boundary condition for thermo-mechanical fatigue analysis. In the investigation shown in this thesis the condition with the hottest structure observed during 3D CFD analysis is used as a boundary condition for the dynamic investigation.
Figure 5.1 shows the simulation results of the temperature field in a compact way for the operating point 80700 rpm. The hot EGR (600°C) enters the turbine housing and the temperature field reveals that a high amount of heat is transported to the bearing housing induced by the large temperature gradient. In fact, the large temperature gradient induces heat fluxes in the entire assembly. The temperature hot spot of the assembly is located in the inlet flange of the turbine stage and reaches a peak temperature of 575°C. The high local velocities and temperatures in the contact area with the twin-flow volute lead to a temperature decrease of more than 50°C downstream towards the impeller. This is mainly caused by convective heat transfer. Looking at the bushing bearing on the turbine side, the material temperature can increase up to 120°C in the outer oil ring[121]. Temperature measurement data on the structural part were not available, hence no comparison between simulated and measured results is possible.

The modelling of rotating parts using the steady MRF method is an efficient alternative to the comprehensive transient methods available in commercial codes. This is a reasonable approach as the turbine's and compressor's rotational speed reaches up to 200000 revolutions per minute. Summarizing, the multi-material simulation approach provides reliable results compared to turbocharger measurement data.

[121] Cf. Bukovnik S., Diemath A., Offner G., Smolik L. (2017), p.7

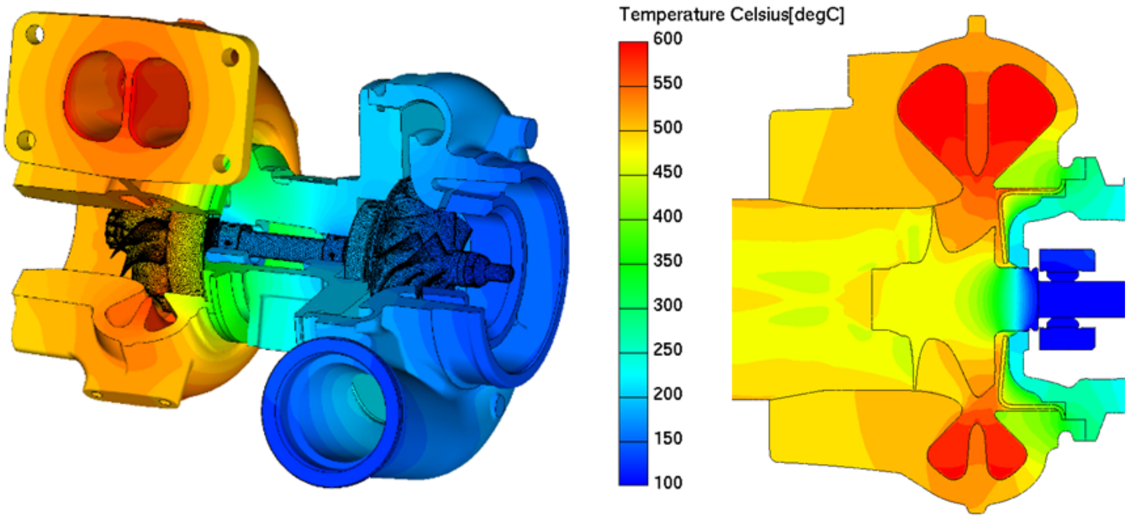

Figure 5.1.: Simulation Results in FIRE M, Temperature field in entire structure (left) and fluid/structure for turbine section (right), Source: own model

5.2. Conclusions

Beside the application on a turbocharger the multi-material simulation is getting more and more popular due to higher accuracy and decreasing turn-around time of the simulation task.

Especially in cooling problems, such as the cooling of electrical engines, battery and fuel cells, the multi-material simulation is already state of the art simulation technique. Increased user acceptance of the methodology is already observed within AVL as more users started to use this methodology by applying it to other components. Hence, the presented methodology proves to be a next level approach in prediction of turbocharger simulation in the development process.

6. Outlook

Referring to the interviews, which were done in section 4.4.2., AVL provides a certain standardization for recurring simulation tasks. As a future outlook, one of the first steps towards standardization is seen in the software training for new engineers. In particular to the turbocharger simulation, a standardized training example for that topic is currently in preparation and will be available for the next major software release.

The improvement of the workflow is strongly related to the capabilties of the software. It is a continous process as customer's demand is permanently evaluated. As part of the continous software improvement process, the need for a higher degree of automation in the software is also taken into account. Template based simulation setup as well as template based post-processing is provided by the software. Furthermore, the offline and script based capabilities of the software are continously improved which allow further automation of the existing workflow in the future.

From the engineering perspective the consideration of radiation within the turbine stage should be considered in the simulation. For instance, the following article[122] on gas turbine engines denotes an error in the local temperature of approx. 60°C due to reflected radiation in the turbine stage.

Furthermore transient turbine and compressor simulations can possibly provide vital information to acoustic problems and give statements about the blade passing frequency. Blade vibrations caused by unsteady fluid-structure interactions is known to cause severe damage of the components. The reliable prediction of the alternating blade stresses caused by blade induced responce may improve the technical maturity during the design phase.
Finally, the consideration of the lubrication system as a multiphase simulation may also give better information on the situation around the bearings.

Future work should be concentrated also on expanding the capability of the code to simulate fluid-structure interaction with special focus on calculation of the material stresses.

[122]Cf. Atkinson H.W., Guenard, R.N. (1978)

Bibliography

Editorial resources

Aghaali, H. (2013): *On Engine Turbocharger Performance Considering Heat Transfer*, Academic thesis, Royal Institute of Technology, Stockholm, Sweden, 2013

AIAA G0771998 (1998): *AIAA Guide for the Verification and Validation of Computational Fluid Dynamics*, The American Institute of Aeronautics and Astronautics, Virginia, USA, 1998

Ansorge, R. (2003): *Mathematical Models of Fluid Dynamics*. WILEY-VCH GmbH Co.KGaA., Hamburg, Germany, 2003

Atkinson H.W., Guenard, R.N. (1978): *Turbine Pyrometry in Aircraft Engines*, IEEE Electronic Show and Convention Electro '78, Paper No. 33/3, Boston, USA, 1978

Barth P. (2011): *Entwicklung einer transienten Turboladerstroemungssimulation anhand des 3D-CFD-Simulationsprogramms AVL FIRE*, Diplomarbeit, Ruhr Univ. Bochum, Bochum, Germany, 2011

Basara B. (2004): *Employment of the second-moment closure on arbitrary unstructured grids*, International Journal for Numerical Methods in Fluids, 44: pp. 377-407, WILEY SONS, Hoboken, New Jersey, USA, 2004

Basara B., v. d. Meer A. J., Diemath A. (2009): *Numerical simulation of fluid flow and conjugate heat transfer in a matrix of surface-mounted cubes: Evaluation of different modeling approaches*, Turbulence, Heat and Mass Transfer 6, Begell House Inc., 2009

van Basshuysen, R. ; Schaeffer, F. (2014): *Handbuch Verbrennungskraftmaschine*, 7th Edition, Springer Vieweg, Wiesbaden, 2013

Bender K. (2005): *Embedded Systems qualitaetsorientierte Entwicklung*, Springer, Heidelberg, 2005

Bergman T. L., Incopera F. P. (2011): *Fundamentals of Heat and Masstransfer*, 7th Edition. WILEY and SONS, Hoboken, New Jersey, USA, 2011

Bergqvist S. (2014): *Prediction of Turbo Compressor Maps using CFD*, Master's thesis in Applied Mechanics, CHALMERS UNIVERSITY OF TECHNOLOGY, Stockholm, Sweden, 2014

Braess H. H., Seiffert U. (2013): *Vieweg Handbuch Kraftfahrzeugtechnik,7th Revised Edition*, Springer Vieweg, Wiesbaden, 2013

Bukovnik S., Diemath A., Offner G., Smolik L. (2017): *Turbocharger dynamic analysis: Part II Advanced design simulation in time domain using CFD predicted thermal boundary conditions*, SIRM 2017, 12th International Conference on Vibrations in Rotating Machines, Graz, Austria, 15. to 17. February 2017

Cetinkaya, D. (2010): *Applying a Model Driven Approach to Component Bases Modeling and Simulation*, Proceedings of the 2010 Winter Simulation Conference. Baltimore, Maryland, USA, 2010

Charlesworth D. J. (2003): *Solution of the Incompressible Navier-Stokes Equations on Unstructured Meshes*, Doctoral thesis, Dept. of Mechanical Engineering, University College London, UK, 2003

Edelbauer W., Suzzi, D. (2006): *New Concept for On-line Coupling of 3D-Eulerian and Lagrangian Spray Approaches in Engine Simulations.*, Proc. of ICLASS 2006. Kyoto, Japan, 2006

Eissler W. (2011): *Optimierung des Abgasturboladers für den 6-Zylinder Diesel von Mercedes-Benz*, Aufladetechnische Konferenz. Tagungsband Dresden, 2011

Ferziger J. H. (2002): *Computational Methods for Fluid Dynamics*, Third Revised Edition. Heidelberg: Springer Verlag Berlin, 2002

Fritz J. (2013): *Integriertes Vorgehensmodel zur Evaluierung von Systems-engineering-IT-Werkzeugen*, Masterarbeit, CAMPUS 02, Fachhochschule der Wirtschaft, Graz, 2013

Garimella R. V., Kim J., Berndt M. (2013): *Polyhedral Mesh Generation and Optimization for Non-manifold Domains*, Los Alamos National Laboratory, Los Alamos, NM, USA, 2013

Gausemaier J. (2008): *Domänenübergreifende Vorgehensmodelle*, In: TransMechantronik, pp. 1-17. 2008

Gsenger C. (2015): *Untersuchung des numerischen Verhaltens neuer Vernetzungsmethoden in AVL FIRE*, Bachelorthesis, FH Joanneum GmbH, Graz, 2015

Hanjalic K., Popovac M., Hadiabdic M. (2004): *A robust near-wall elliptic relaxation eddy-viscosity turbulence model for CFD*, Int. J. Heat Fluid Flow 25, 2004

Hanjalic K., Launder B. (2011): *Modelling Turbulence in Engineering and the Environment Second-Moment Routes to Closure*, Cambridge University Press, Cambridge, UK, 2011

Hommel M. (2006): *Parallelisierte Simulationsprozesse für virtuelles Prototyping in der Automobilindustrie*, Fakultät Elektrotechnik und Informationstechnik, Technische Universität Carolo Wilhelmina zu Braunschweig, 2006

Kossiakoff A., Sweet W. N., Seymour S. J., Biemer S. M. (2011): *Systems Engineering: Principles and Practice*, Second Edition, WILEY SONS, Hoboken, New Jersey, USA, 2011

Kopun R., Skerget L., Hribersek M., Zhang D., Edelbauer W. (2014): *Numerical Investigation of Quenching Cooling Processes for Different Cast Aluminium Parts*, Journal of Mechanical Engineering 60, 2014

Laurien E., Oertel H. (2013): *Numerische Strömungsmechanik: Grundgleichungen und Modelle - Lösungsmethoden - Qualitaet und Genauigkeit*, Springer, Stuttgart und Göttingen, 2013

Lesieur M. (1996): *Turbulence in Fluids*, Third Revised and Enlarged Edition, Fluid Mechanics and its Applications, Volume 40, Kluwer Academic Publishers, London, UK, 1996

Marshal C., Rossman G.B. (2011): *Designing Qualitative Research*, Fith Edition, Sage Publications, Inc., Los Angeles, California USA, 2011

Merker G. P., Teichmann, R. (2014): *Grundlagen der Verbrennungskraftmaschine. Funktion, Simulation und Messtechnik*, 7. Auflage, Springer Vieweg, Wiesbaden, Germany, 2014

Myers G. J. (2004): *The Art of Software Testing*, Second Edition, WILEY and SONS, Hoboken New Jersey, USA, 2004

Nguyen-Schäfer Hung (2015): *Rotordynamics of Automotive Turbochargers*, Second Edition. Cham: Springer International Publishing, (Springer Tracts in Mechanical Engineering), 2015

Oberkampf W. L., Trucano, T. G. (2002): *Verification and Validation in Computational Fluid Dynamics*, Sandia Report SAND2002-0529, Albuquerque, New Mexico, USA, 2002

Patankar S. V. (1980): *Numerical Heat Transfer and Fluid Flow*, Washington: Hemisphere Publishing Corporation, USA, 1980

Otero C., D J. A., Togores R., Manchado C. (2006): *Chordal Space Structures, Shaped from Voronoi Diagrams*, ICCCBE, Montr, Canada, June 14-16, 2006

Peric M., Ferziger J. H. (2002): *computational Fluid Dynamics*, Third Edition, Springer Verlag Berlin, Germany, 2002

Peric M. (2004): *Flow Simulation using Control Volumes of arbitrary Polyhedral shape*, ERCOFTAC Bulletin 62, September 2004

Potinecke T. W. (2009): *Methode zur Systematisierung von Teilprozessen in der Produktentwicklung beim Einsatz von CAx-Technologien*, Jost Jetter Verlag, Heimsheim, Germany, 2009

Roach P. (2007): *The Role of CFD in Turbocharger Performance Improvement*, Paper No.: 51, CIMAC Congress, Vienna, 2007

Saric S., Basara B., Zunic Z. (2016), *Advanced near-wall modeling for engine heat transfer*, International Journal of Heat and Fluid Flow, Elsevier Inc., Science Direct, 2016

Schaefer K. H. (2016): *Dynamics of Heat Transfer in Turbochargers*, Master Thesis, University of Leoben, Austria, 2016

Schaefer M. (1999): *Numerik im Maschinenbau*, Springer Darmstadt, Germany, 1999

Schulze G., Fritz A. H. (2008): *Fertigungstechnik*, 8. neubearbeitete Auflage, Springer-Verlag, Berlin, Heidelberg, 2008

Thomke S., Fujimoto T. (2000): *The effect of front-loading problem solving on product development performance*. The Journal of Product Innovation Management. Elsevier 17(2): 128-142, 2000

Thompson J. F., Soni B. K., Weatherill N. P. (1999): *Handbook of Grid Generation*, CRC Press, Boca Raton, London, New York, Washington D.C., USA, 1999

VDI-Heat Atlas (2010): *Second International Edition of VDI-Wärmeatlas, with 539 tables*, Berlin and Heidelberg: Springer, (Springerreference), Germany 2010

VDI 2206 (2004): *Entwicklungsmethodik für mechatronische Systeme*, Beuth-Verlag, Berlin, Germany, 2004

Versteeg H. M. (1995): *An Introduction to Computational Fluid Dynamics - The Finite Volume Methode*, Essex: Pearson Education Limited, UK, 1995

White F. M. (1979): *Fluid Mechanics*, McGraw-Hill, Inc., New York, USA, 1979

Online resources

Thacker B. H. et al (2008): *Concepts of Model Verification and Validation*, Report LA-14167-MS, Los Alamos National Laboratories, New Mexico, USA, 2008

http://www.ltas-vis.ulg.ac.be/cmsms/uploads/File/LosAlamos_VerificationValidation.pdf retrieved at 2nd February 2017 from secondary source, since the primary source as statet in the report is not available anymore.

Technical Manuals

AVL List GmbH. (2010): *AVL Single Cylinder Engines*, Graz, Austria, 2010

AVL List GmbH. (2014): *AVL EXCITE Power Unit - Turbo Charger Analysis*, Graz, Austria, 2014

AVL List GmbH. (2014) Feb. 28: *AVL FIRE - CFD Solver Users Guide*, Graz, Austria, 2014

AVL List GmbH. (2014) Sept. 30: *AVL FIRE Coupling Module CAE*, Graz, Austria, 2014

AVL List GmbH. (2016): *AVL FIRE M R2017 - Users Guide*, Graz, Austria, 2016

List of Figures

List of Tables

List of Abbreviations

	Abbreviation	Explanation
A	AIAA	The American Institute of Aeronautics and Astronautics
	ACCI	AVL Code Coupling Interface
B	BWTS	Borg Warner Turbo Systems
C	CAC	Charge Air Cooler
	CAE	Computer Aided Engineering
	CFD	Computational Fluid Dynamics
	CHT	Conjugate Heat Transfer
E	EGR	Exhaust Gas Residual
F	FEA	Finite Element Analysis
	FEM	Finite Element Method
	FIRE	Commercial Code for CFD - Flow In Reciprocating Engines
	FIRE M	Commercial Code for CFD with focus on multi-material problems
G	GUI	Graphical User Interface
I	ICE	Internal Combustion Engine
M	MBD	Multi-Body Dynamics
	MEP	Mean Effective Pressure
	MPI	Message Passing Interface
	MRF	Multiple Reference Frame
N	NA	Naturally Aspirated (Engine)
S	STL	Standard Tessellation Language
T	T/C	Turbine and Compressor
	THA	Thermal Analysis
	TMF	Thermal Mechanical Fatigue
V	VDI	Verein Deutscher Ingenieure
	VFT	Virtual Functional Test
	VTG	Variable Turbine Geometry
	V&V	Verification and Validation

Appendix A.

List of interviewed engineers

Position	Experience in simulation since	Education (background)	Software application	Main engineering application
Senior Analysis Engineer	21 years	Mechanical engineering (university degree)	AVL FIRE	general purpose CFD, T/C flow, aerodynamics, cooling, battery, fuel cells
Senior Analysis Engineer	15 years	Mechanical engineering (university degree)	AVL EXCITE	MBS, structural mechanics
Lead Engineer	12 years	Thermal engineering (university degree)	AVL FIRE, STAR CD, CCM+, FLUENT, GT-Power, AVL Boost	In-cylinder, general purpose CFD, cooling, battery and thermochemistry, aftertreatment
Analysis Engineer	6 years	Mechanical engineering (university degree)	AVL FIRE, AVL Cruise, Cruise M, Flowmaster, CATIA v5	General purpose CFD, aftertreatment, turbocharger, multi-domain simulations
Analysis Engineer	5 years	Mechanical engineering (university degree)	AVL FIRE, CFX, CATIA v5, Rhinoceros	In-cylinder flow (diesel, gasoline, dual fuel), background as design-engineer
Analysis Engineer	5 years	Mechanical engineering (university degree)	AVL FIRE	General purpose CFD, gear splashing, cooling
Analysis Engineer	3 years	Mechanical engineering (university degree)	AVL FIRE	General purpose CFD, in-cylinder flow, cooling, torque converter

Table A.1.: List of interviewed engineers

Position	Experience in simulation since	Education (background)	Software application	Main engineering application
Skill Area Manager - Customer Services AST/CC	25 years	Mechanical engineering (university degree)	AVL EXCITE	MBS, structural mechanics
Skill Team Leader - CFD Simulation Management PTE/DAC	29 years	Mechanical engineering (university degree)	AVL FIRE	General purpose CFD, in-cylinder flow, software development of FIRE
Team Leader - CFD Simulation Group AST/CCAF	21 years	Mechanical engineering (university degree)	AVL FIRE	General purpose CFD, rotating machinery, pumps, aerodynamics, cooling

Table A.2.: Interviewed participants from simulation managment